Doctorate Course in Chemistry – Cycle XXX

Facoltà di Scienze e Tecnologie

Università degli Studi di Milano

Academic Year 2017-2018

Biocatalytic Strategies for Selective Organic Synthesis

Candidate: Ivan Bassanini, N° R11038

Tutor: prof. Daniele Passarella

Co-tutor: dr. Sergio Riva (ICRM-CNR)

1. Table of Contents

2. Preface

2.1 Biocatalysis in Organic Synthesis

The term 'biocatalysis' delineates the family of catalytic processes operating in a living biological system to perform chemical transformations on organic compounds. The main 'actors' of these processes are the biological systems enzymes, globular proteins possessing the ability of promoting chemical transformation with peculiar characteristics and outstanding performances. For instance, a narrow group of biocatalysts (*i.e.* acetylcholinesterase, β-lactamase, catalase …), defined as 'diffusion-limited enzymes', can accelerate a chemical reaction so efficiently that the rate determining step becomes the diffusional limits of the reactants and/or products in the reacting media itself; reaching the so-called 'catalytic perfection' with values of kinetic constants estimated to be between 10^8 $M^{-1} s^{-1}$ and $10^9 M^{-1} s^{-1}$.

Even if most of the known enzymes operate by accelerating a reaction speed to a rate that is 1000 – 10000 times slower than a diffusion-controlled reaction, biocatalysts possess a broad range of features that makes them an appealing resource for an organic chemist. Proteins are in fact macromolecules constituted by a network of chiral (L)-α-amino acids linked by amide bonds that, thanks to their extensive chirality and 3D-folding, can catalyze highly selective transformations. Thus, enzymes can discriminate between two enantiomers (*ndr* kinetic resolution), interact with a pro-chiral group leading to the stereoselective formation of a new stereocenter (*ndr* asymmetric synthesis) or can guide the chemical bonds formation or breaking in a specific direction as well as toward a specific functional group (*ndr* regio- and chemo-selective processes).

In this thesis work different enzymatic activities have been exploited to promote selective transformations to assess synthetic problems in organic chemistry. The results that will be presented have been collected in six different papers published ISI journals and one submitted manuscript.

Paper I: 'Dicarboxylic esters: Useful tools for the biocatalyzed synthesis of hybrid compounds and polymers'

Bassanini, Ivan; Hult, Karl; Riva, Sergio*

Beilstein J. Org. Chem., **2015**, 11, 1583–1595. doi:10.3762/bjoc.11.174

Paper II: 'Self-assembled 4-(1,2-diphenylbut-1-en-1-yl) aniline based nanoparticles: podophyllotoxin and aloin as building blocks'

Fumagalli, Gaia; Christodoulou, Michael S.; Riva, Benedetta; Revuelta, Inigo; Marucci, Cristina; Collico, Veronica; Prosperi, Davide; Riva, Sergio; Perdicchia, Dario; **Bassanini, Ivan**; García-Argáez, Aida; Via, Lisa Dalla; Passarella, Daniele*

Org. Biomol. Chem., **2017**, 15, 1106

Contribution: enzymatic modification of aloin

Paper III: 'A sustainable one-pot two-enzymes synthesis of naturally occurring arylalkyl glucosides'

Bassanini, Ivan; Krejzová, Jana; Panzeri, Walter; Monti, Daniela; Křen, Vladimír; Riva, Sergio*

ChemSusChem., **2017**, 10, 2040 –2045

Major Contribution

Paper IV: 'Novel thermostable amine transferases from hot spring metagenomes'

Ferrandi, Erica Elisa; Previdi, Alessandra; **Bassanini, Ivan**; Riva, Sergio; Peng, Xu; Monti, Daniela*

Appl. Microbiol. Biotechnol., **2017**, 101, 4963–4979

Contribution: screening of the amino/donor acceptor scope of these new enzymes

Paper V: 'Peroxygenase-catalyzed enantioselective sulfoxidations'

Bassanini, Ivan; Ferrandi, Erica Elisa; Vanoni, Marta; Riva, Sergio; Crotti, Michele; Brenna, Elisabetta; Monti, Daniela*

Major contribution

Paper VI: **'Laccase-catalyzed dimerization of glycosylated lignols'**

Bassanini, Ivan; Gavezzotti, Paolo; Monti, Daniela; Krejzová, Jana; Křen, Vladimír; Riva, Sergio*

Major contribution

Submitted Manuscript I: **'Facile chemo-enzymatic synthesis of substituted (*E*)-2,3-diaryl-5-styryl-*trans*-2,3-dihydrobenzofurans, a novel family of potential allosteric modulators of the 90 kDa heat shock protein (Hsp90)'**

Bassanini, Ivan; Costa, Massimo; D'Annessa, Ilda; Colombo, Giorgio; Monti, Daniela; Riva, Sergio*

Major contribution

In chapter three, the regioselectivity of lipase-mediated *trans*-acylations (**Paper I**) will be discussed to introduce the enzymatic strategy exploited to produce aloin conjugates to be tested for their ability to self-assembly into nanoparticles (**Paper II**).

A novel highly stereo- and regio-selective enzymatic synthesis of naturally occurring bioactive arylalkyl glucosides will be presented in chapter four (**Paper III**).

The discovery of novel thermostable aminotransferases from hot-spring metagenomes and, more importantly for this thesis, their potential synthetic exploitation to produce enantiomerically enriched amines will be discussed in chapter five (**Paper IV**).

The *Aae*UPO-catalyzed enantioselective sulfoxidation of arylalkyl sulfides to the correspondent (*R*)-sulfoxides will be the focus of chapter six (**Paper V**).

Finally, chapter seven will be dedicated to the description of laccases as selective activators of Csp^2-H bond. The oxidation of glycosylated lignols (**Paper VI**) and the chemo- and regio-selective oxidative coupling of (4)-*E*-styrylphenols to produce a family of potential allosteric modulators of the 90 kDa heat-shock protein (Hsp90) will be extensively discussed (**Submitted Manuscript I**)

2.2   General information

a) Materials, chemicals, and equipment

NMR spectra were recorded with a Bruker AC spectrometer (400 or 500 MHz) in $[D_4]MeOH$, $[D_6]DMSO$, $[D_1]CHCl_3$ or D_2O. Mass spectra were recorded with Bruker Esquire 3000 Plus spectrometer.

Biotransformations were performed with a G24 Environmental Incubator New Brunswick Scientific Shaker (Edison, USA) or a Thermomixer Comfort (Eppendorf, DE).

Reactions were monitored by thin-layer chromatography (TLC) [precoated silica gel 60 F254 plates (Merck, DE)]; development with UV lamp, Komarovsky reagent (1 mL 50% ethanolic H_2SO_4 with 10 mL 2% methanolic 4-hydroxybenzaldehyde), a 20% solution of H_2SO_4 in ethanol or a molybdate reagent $((NH_4)6Mo_7O_{24}\cdot4\ H2O$, 42 g; $Ce(SO_4)_2$, 2 g; H_2SO_4 conc., 62 mL; made up to 1 L of deionized water). Flash chromatography: silica gel 60 (70–230 mesh, Merck, DE).

All reagents were of the highest purity grade from commercial suppliers: Sigma-Aldrich (St Louis, MO, USA) or VWR (Radnor, PA, USA).

GC-MS analyses were performed using a HP-5MS column (30 m × 0.25 mm × 0.25 µm, Agilent) on a Finnigan TRACE DSQ GC/MS instrument (ThermoQuest, San Jose, CA).

HPLC analyses were conducted using a Jasco 880-PU pump equipped with a Jasco 875-UV/Vis detector and.

Uv-spectra were recorded on a nitrogen flushed Jasco J-1100 spectrophotometer (Easton, MD, USA) interfaced with a thermostatically controlled cell holder.

b) List of abbreviations

MeOH = methanol;

DMSO = dimethyl sulfoxide;

AcOEt = ethyl acetate;

ETP = petroleum ether;

THF = tetrahydrofuran;

DMAP = *N,N*-dimethylamino pyridine;

DBU = 1,5-diazabiciclo(5.4.0)undec-5-ene;

TMSOTf = trimethylsilyl trifluoromethanesulfonate;

DCM = dichloromethane;

TBAF = Tetra-*n*-butylammonium fluoride;

TBDMS = *tert*-butyldimethylsilyl

3. Lipases: regioselective biocatalyzed *trans*-acylations

Since the discovery that enzymes can operate in organic solvents, the scope of preparative scale biocatalyzed transformations has dramatically increased over the past four decades.[1, 2, 3, 4]

Moreover, enzymatic reactions in organic solvents are nowadays emerging as a fruitful and promising research investment for the industrial preparation of bulk and fine chemicals, to reduce the cost of the biocatalytic process and improve its economics. In fact, due to water's high boiling point and low vapor pressure, the isolation of products from an aqueous-media is very often expansive and difficult.[5]

The outstanding impact that this new synthetic tool had and has on biocatalyzed organic synthesis is attested by the uncountable number of scientific reports published on the topic since the eighties of the last century, most of them dealing with the exploitation of hydrolases in organic solvents.[6, 7]

When used in an organic media, lipases and proteases, two of the best characterized hydrolases, were found to be able to efficiently catalyze reactions that are thermodynamically unfavorable in water. In fact, stereo and regio-selective esterification, amidation and *trans*-acylation (*trans*-esterification) reactions are successfully catalyzed by a lipase or an esterase suspended in an anhydrous organic solvent: the biocatalytic formation of a novel carbon-hetero atom bond instead of its hydrolytic breaking, is the favored catalyzed process in an organic media. The proposed mechanisms for lipase-catalyzed hydrolysis and *trans*-acylation are reported in **Figure 3.1**.[8] As it can be seen, the need of an anhydrous media appears fundamental to guarantee the nucleophilic attack to the acyl-enzyme intermediate by a nucleophile different from water, whose action would promote a 'classical' hydrolytic reaction.

The use of organic media had also significantly expanded both the substrates and the acylating agents' scope. Lipases, whose natural substrates are fatty acid triglycerides, were found to be able to catalyze the esterifications of a plethora of natural and un-natural compounds, including sugars and steroids, using both simple aliphatic acylating agents and more complex and sterically demanding acyl-donors.[9, 10, 11]
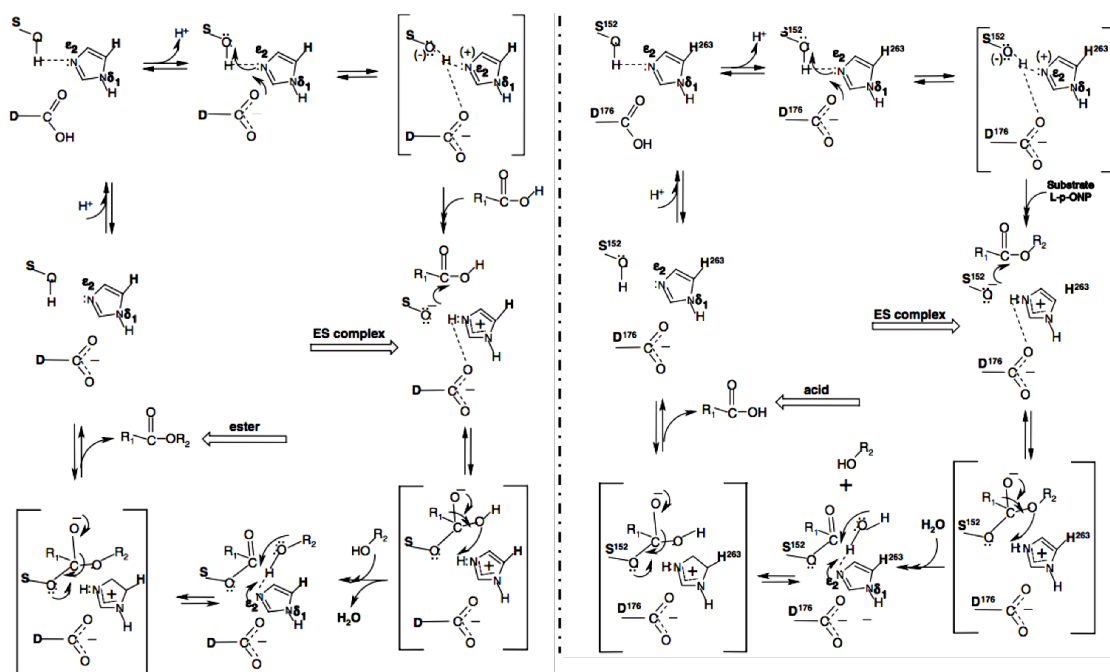

Figure 3.1: Lipase catalyzed *trans*-acylation (**left**) and lipase-mediated hydrolysis (**right**).

In this context, among the number of acyl donors, 'activated esters' of dicarboxylic acids proved to be promising and versatile tools to produce bifunctionalized compounds.

In **Paper I**, a review on the use of dicarboxylic esters as acyl donors in lipase-mediated acylations, we have shown that the synthetic employment of vinyl and/or trifluoro esters to make biocatalytic *trans*-acylations irreversible processes is a well-described strategy, thanks to their ability of releasing poor-nucleophilic alcohols. Along with the remarkable number of examples dealing with the biocatalytic synthesis of polymers, the development of these biotransformations resulted in a versatile and, more important, regioselective entry to

'hybrid compounds'. In fact, the combination of an activated di-ester and a proper lipase allowed the regioselective formation of symmetrical and un-symmetrical conjugates starting from polyhydroxylated substrates, without the need of protective group chemistry or activating coupling agents. The efficiency and potency of these biocatalytic *trans*-acylations led Dordick and coworkers to propose the so-called 'combinatorial biocatalysis' as an approach to easily produce small libraries of derivatives of bioactive natural compounds, using a panel of different acylating-agents and hydrolases.[12, 13, 14]

Bifunctional hybrid conjugates, very interesting molecular scaffold in the field of medicinal and pharmaceutical chemistry, were easily prepared by exploiting the two extremities of the activated dicarboxylates to connect two different molecules, generally via a two-step approach (**Scheme 3.1**).

$R = CH_2CF_3; CH=CH_2$
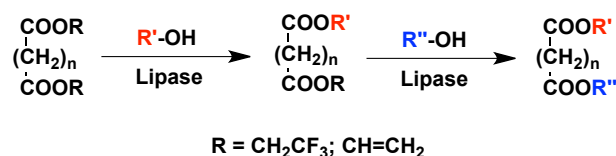
Scheme 3.1: Two-step entry to hybrid compounds.

A quick overview over the regioselective production of symmetrical and, most important, un-symmetrical conjugates of polyhydroxylated natural compounds, will be proposed therein through the selection of notable examples from **Paper I**.

(3.1a): n = 10
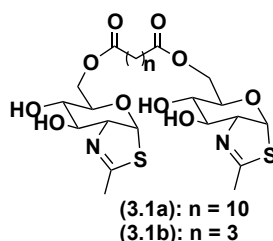**(3.1b): n = 3**

Figure 3.2: C6-dicarboxylic acid diesters derivatives of NAG-thiazoline.

Dicarboxylic acid diesters derivatives of the thiazoline of *N*-acetylglucosamine (NAG-thiazoline, **Figure 3.2**) were prepared by Křen and co-workers, starting from the 'nude' NAG-thiazoline using an immobilized *Candida antarctica* preparation from Novozyme®

(Novozym435) in dry acetone. Their inhibitor activities towards fungal β-*N*-acetylhexosaminidase was evaluated as well.[15]

According to the simple synthetic entry proposed in **Scheme 3.1**, a sugar-conjugate of paclitaxel (**3.2**) was obtained in a pretty straightforward synthetic pathway (**Scheme 3.2**) involving the regioselective acylation of its side chain to give the key-intermediate 2'-vinyl adipate (**3.3**) in 60% isolated yields. The following Novozym435-catalyzed elaboration of **3.3** allowed the linkage to glucose, producing the water-soluble hybrid compound **3.5**.[16]

As a second example, **Scheme 3.3** shows the biocatalytic entry to the hybrid conjugates **3.9** and **3.10**, obtained by our group linking together a bioactive alkaloid (colchicoside, **3.7**; thiocolchicoside, **3.8**) and the steroid cortisone (**3.6**), to merge their analgesic and anti-inflammatory and effects. Worth of notice is the use of activated esters of dithio-dicarboxylic acids, in **3.10**.[17]
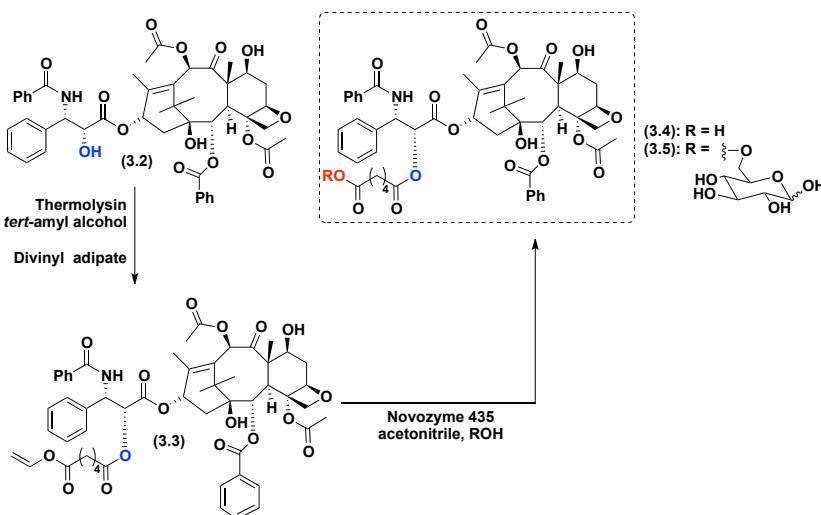
Scheme 3.2: Biocatalyzed synthesis of a paclitaxel sugar-conjugate (**3.5**)

Symmetrical dimers of lignols (phytochemicals acting as source materials for biosynthesis of both lignans and lignin) and phenolic stilbenes, were also synthetized using Novozym435 in combination with different activated diesters (**Figure 7.11**, chapter 7.3, results unpublished)

to be used as substrate to study the possibility of conducing laccase-mediated oxidative macrocylizations, as described in chapter 7 on '*Laccases*'.[18]
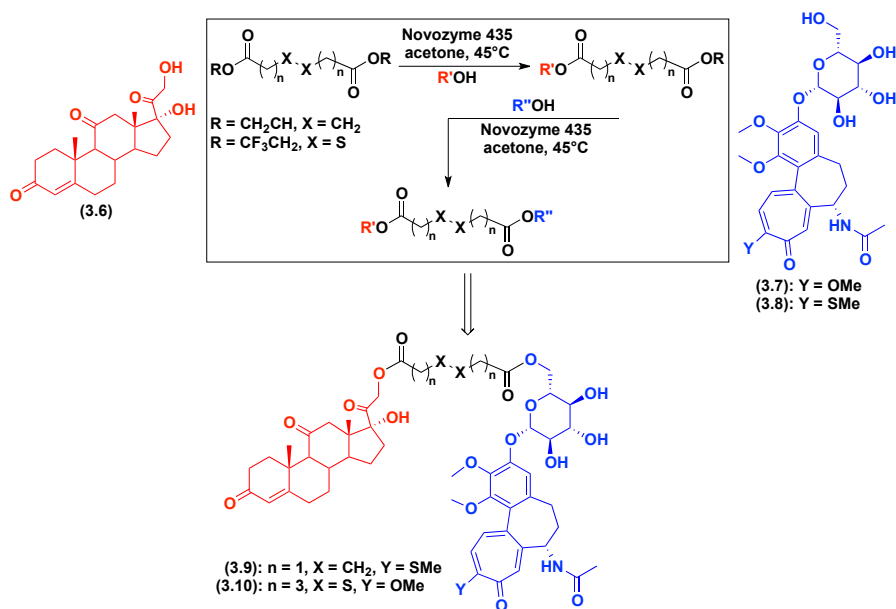
Scheme 3.3: Biocatalyzed synthesis of hybrid diesters **3.9** and **3.10**.

In general, these classes of compounds can be synthesized by (sometimes troublesome) chemical protocols that require an accurate control over the reaction conditions and, in most of the cases, several protection/deprotection steps.

As it has been shown, these drawbacks are totally avoided using a biocatalyzed approach, exploiting, once again, the well-known efficiency, selectivity and versatility of lipase-mediated *trans*-acylations in organic solvents.

Thrilled by this elegant biocatalytic approach, able to solve issues of regioselectivity, we developed a chemo-enzymatic entry to aloin-based drug conjugates suitable for applications in the field of cancer nanotherapy, as it will be discussed in paragraph **3.1**.

3.1   Lipase-mediated synthesis of aloin conjugates

The self-assembling of drug conjugates and the consequent spontaneous formation of nanoparticles (NPs) in aqueous media is emerging as a promising research niche in the field of cancer nanotechnology.[19, 20, 21]

Specifically, the use of drugs conjugates obtained by a covalent bonding with biocompatible lipid moieties, has gained considerable attention.[22, 23]

The spontaneous self-assembly into NPs is mediated by an ordered structural organization of building blocks, as a consequence of specific local interactions. In this scenario, to promote self-assembly under controlled experimental conditions, the role of the amphiphilicity has been largely established.

In **Paper II**, the use of 4-(1,2-diphenylbut-1-en-1-yl)aniline (**3.11**, **Figure 3.3**), a tamoxifen analog possessing antiproliferative properties, as new self-assembly inducer was investigated. In fact, the establishment of π-stacking interactions among the aromatic rings of the adjacent molecules of **3.11** could promote the formation of a hydrophobic core, forcing the exposure of the polar moieties toward the aqueous environment.[24, 25]
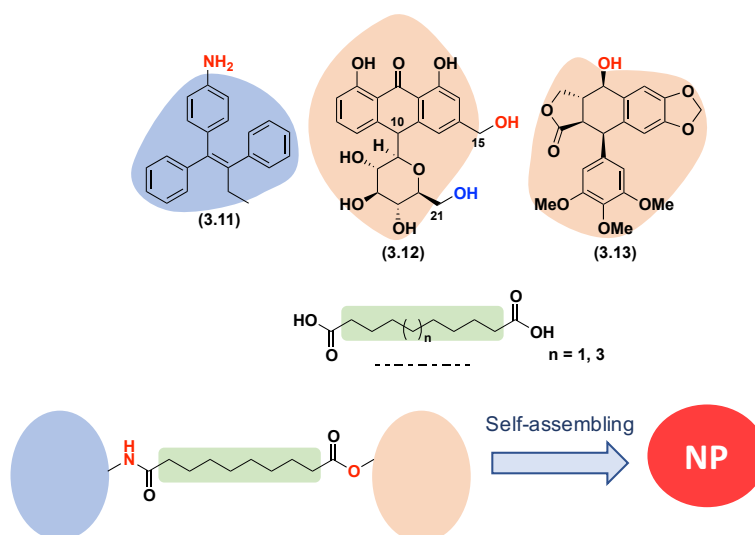

Figure 3.3: Building blocks and schematic composition of the designed drug conjugates.

Aloin (**3.12**) and podophyllotoxin (**3.13**) were also selected as building blocks for the drug conjugates (**Figure 3.3**). The former, a natural polyhydroxylated bioactive compound, was chosen because of its hydrophilic structure to test the self-assembly properties of amphiphilic conjugates; the latter, a lipophilic antiproliferative compound, was used to prove the ability of **3.11** to induce self-assembly also in a totally lipophilic conjugate. To this purpose, four different conjugates were prepared (**Figure 3.4**).

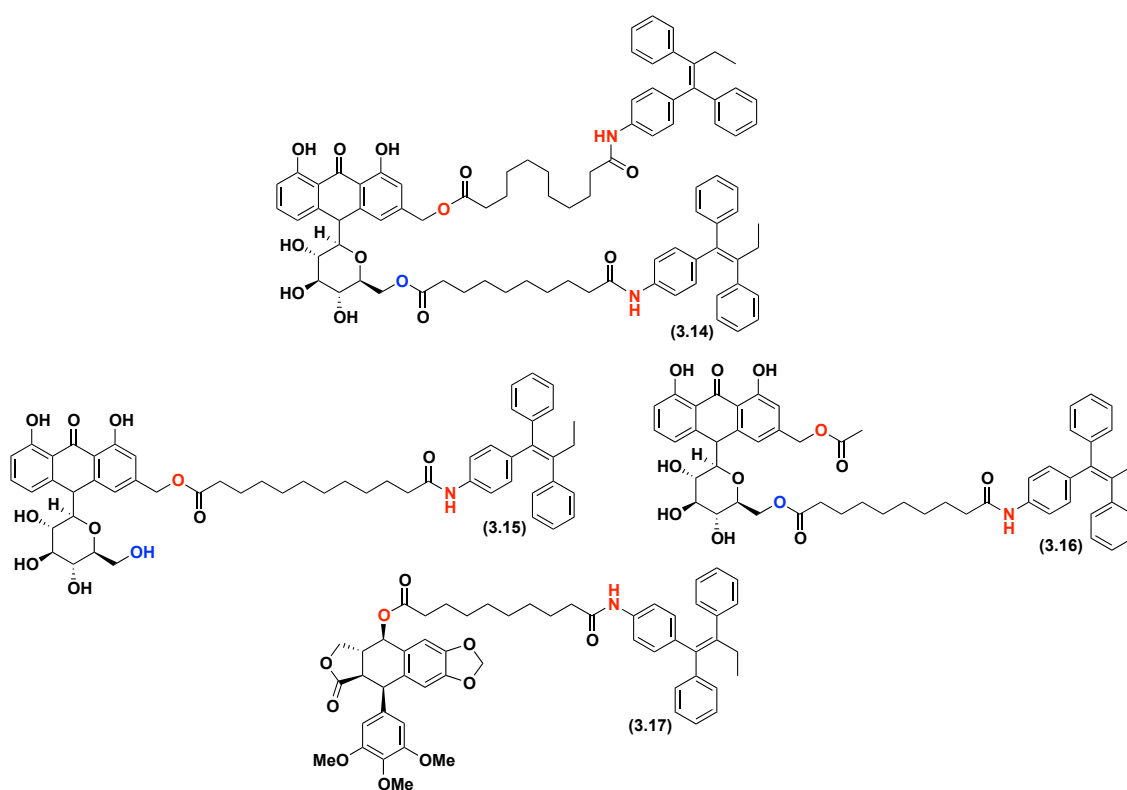**Figure 3.4**: Structure of the drug conjugates **3.14** – **3.17**.

The synthesis of the molecular conjugate **3.14** and **3.17** was easily achieved following classical chemical coupling protocols starting from aloin, sebacid acid and aniline **3.11** (**Scheme 3.4**).

To synthetize conjugates **3.15** and **3.16**, a selective single acylation of one of the two primary hydroxyl groups of aloin was strictly needed.
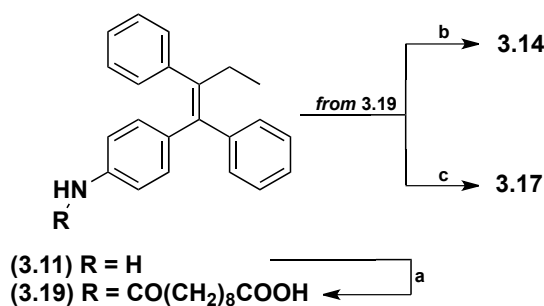
Scheme *3.4*: Chemical synthesis of compounds **3.14** and **3.17**
Reagents and conditions: sebacic acid, DIPEA, HATU, 42 %; (b) aloin, EDC, DMAP, 8 %; (c) podophyllotoxin, EDC, DMAP, 80 %.

This task resulted very tricky by classical chemicals means, but, given the nature of the compounds involved, it appeared to us as a promising field for the exploitation of the previously described lipase-controlled regioselective *trans*-acylations. In fact, aloin is a polyhydroxylated natural compound possessing two primary hydroxyl groups in two different regions of the its molecular skeleton (one on the aglycone and the other on the sugar moiety) on which a lipase may operate selectively. Indeed, the target hybrid compounds (**3.15** and **3.16**) could be easily obtained using an activated diester as acyl donor, *via* a sequence of biocatalyzed and chemical acylations, as it will be described in the following.

A small library of lipases, different in nature, formulation and origin was tested on aloin, using both vinyl acetate (**a**) and divinyl dodecanoate (**b**) as acyl donors, to study the regiochemical outcome of the biocatalyzed *trans*-acylation. The results obtained are reported in **Table 3.1**. From this screening, as shown by ^{1}H NMR analysis, it appeared clear that almost all the tested lipases showed a marked preference for the benzylic C_{15}-OH. Lipase AK, CE and PS on Celite$^{®}$ (1 % w/w lipase/celite) allowed the regioselective production of compound **3.20** (**Scheme 3.5**) while **3.22** was obtained easily by the action of Novozyme435 and, again, lipase AK and CE (**Scheme 3.6**). Specifically, when Novozym435 was used as catalyst, product **3.20** was obtained in a 1:1 mixture with the corresponding acid **3.21** (**Scheme 3.5**).

Thus, acid **3.21** was easily synthesized from aloin in the presence of Novozyme435 *via* a one-pot process in which the cleavage of the second vinyl moiety of **3.20** was triggered *in situ* by

adding a controlled amount of water. **3.21** was then transformed into the target conjugate **3.15**, as an inseparable mixture of diastereoimers at position 10, by condensation with the aniline derivative **3.11** in the presence of HBTU (**Scheme 3.5**).

| Lipase	Vinyl Acetate		Divinyl Dodecanoate	
	C_{15}-OH	C_{21}-OH	C_{15}-OH	C_{21}-OH
Porcine Pancreatic Lipase	n.r.	n.r.	n.r.	n.r.
Lipase AK	X	n.r.	X	n.r.
Lipase CE	X	n.r.	X	n.r.
Candida rugosa Lipase	n.r.	n.r.	n.r.	n.r.
Lipozyme IM20	X	X	n.r.	n.r.
Lipase PS on Celite®	X	n.r.	n.r.	n.r.
Novozym435	X	X	X[a]	n.r.
Lipase N	n.r.	n.r.	n.r.	n.r.

Table 3.1: Lipase regioselectivity in the acylation of aloin.
Reagents and conditions: aloin (0.05 M, 1.0 eq), acyl donor (2.0 eq), dry acetone, 45 °C, 250 rpm, 48 h.
n.r. = no reaction; [a]1:1 mixture of **3.20** and **3.21**

For the preparation of conjugate **3.16**, aloin was at first acetylated on the aglycone primary OH exploiting, again, a lipase-based strategy. In fact, a combination of lipase PS on celite® (1 % w/w lipase/celite) and vinyl acetate gave intermediate **3.22** with complete control over the regioselection of the C-O bond formation. Isolated was yield up to the 80 %.

The synthesis of **3.16**, as an inseparable mixture of diastereoimers at position 10, was then accomplished by condensation of **3.22** and acid **3.19** in the presence of EDC (**Scheme 3.6**).
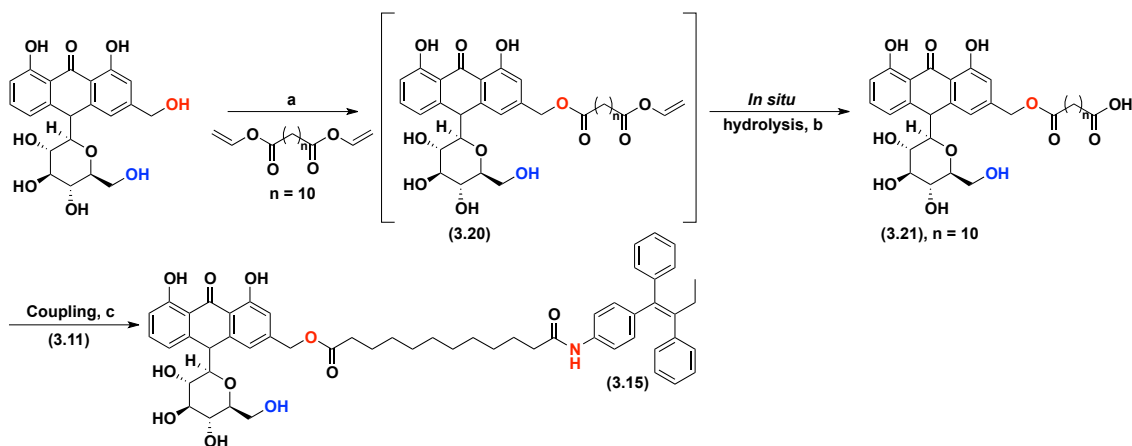
Scheme 3.5: Chemo-enzymatic synthesis of **3.15**.
Reagents and conditions: **a, b**) Aloin, Novozym435 then water, 40 %; **c**) DIPEA, HATU, 65 %.
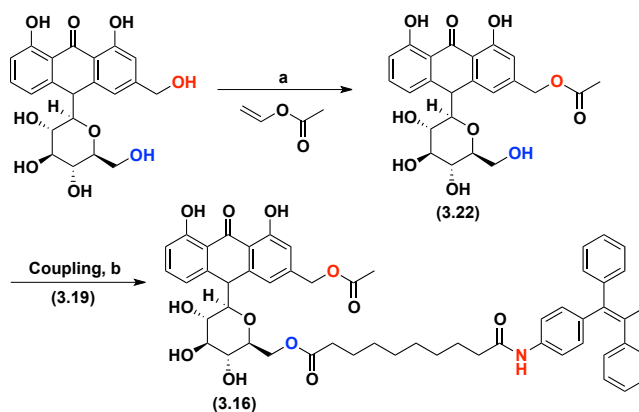
Scheme 3.6: Chemo-enzymatic synthesis of **3.16**.
Reagents and conditions: **a**) Aloin, lipase PS on Celite® (1 % w/w lipase/celite). then water, 80 %;
b) DMAP, EDC, 65%.

The ability of the obtained compounds (**3.14** - **3.17**) to form NPs was finally investigated: all the conjugates, except **3.15**, seemed to self-assemble, and the resulting homogeneous suspensions were characterized by dynamic light scattering (DLS), transmission electron microscopy (TEM, **Figure 3.5**) and nanoparticle tracking analysis (NanoSight).
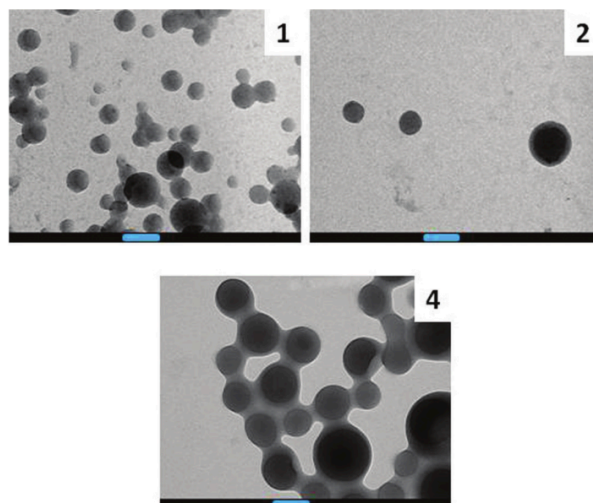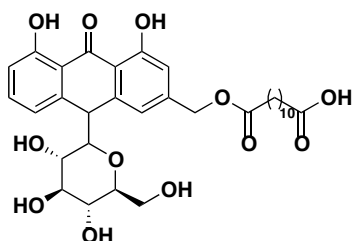
Figure *3.5*: TEM micrographs of nanoparticles formed by self-assembly of (**1**) compound **3.14**, (**2**) compound **3.16** and (**4**) compound **3.17**. All samples were stained with uranyl acetate solution. In all the panels scale bar represents 100 nm. All rights reserved to ©The Royal Society of Chemistry.

3.2 Experimental

3.2.1 Lipase-catalyzed synthesis of compound 3.21

To a solution of aloin (100 mg, 0.24 mmol) in dry acetone (15 mL) divinyl dodecanedioate (101 mg, 0.36 mmol) and Novozym435 (30 mg) were added. The resulting heterogeneous mixture was incubated at 45 °C and 210 rpm for 48h. After that, 5 µL water were added to the mixture which was incubated again for additional 2 h, checking the formation of the target acid by TLC (CHCl$_3$/MeOH/HCOOH = 8:2:0.1, UV). The crude mixture was then filtered, concentrated *in vacuo* and purified by flash column chromatography on silica gel (AcOEt/MeOH/H$_2$O = 9.5:0.5:0.1) affording the purified product as a yellow oil (60 mg, 40%). **^{1}H-NMR (CD$_3$OD, 400 MHz; mixture of diastereoisomers, 25 °C)**: δ 7.50 (1H, ddd, *J* = 8.3, 7.5, 6.3 Hz), 7.06 (2H, q, *J* = 6.0 Hz), 6.89-6.84 (2H, m), 5.16 (2H, d, *J* = 3.7 Hz), 4.59 (1H, d, *J* = 1.5 Hz), 3.58 (1H, dd, *J* = 11.7, 1.9 Hz), 3.43-3.39 (2H, m), 3.33 (2H, dt, *J* = 3.3, 1.6 Hz), 3.28 (1H, t, *J* = 8.6 Hz), 3.03-2.97 (1H, m), 2.94-2.89 (2H, m), 2.47-2.37 (4H, m), 1.70-1.58 (4H, m), 1.29 (12H, bs). **^{13}C-NMR (CD$_3$OD, 100 MHz; mixture of diastereoisomers, 25 °C):** δ 194.1, 173.68, 173.60, 170.9, 161.84, 161.75, 161.62, 161.59, 145.5, 145.08, 145.04, 144.4, 142.1, 135.8, 135.0, 119.9, 118.60, 118.59, 117.5, 117.24, 117.22, 116.88, 116.70, 115.8, 115.5, 114.1, 113.9, 85.0, 80.30, 80.20, 78.55, 78.53, 70.62, 70.53, 70.46, 64.74, 64.71, 61.89, 61.85, 44.5, 33.6, 33.2, 29.08, 29.03, 28.91, 28.88, 28.74, 28.65, 24.7, 24.3. **MS (ESI)** = 653.3 [(M+Na)$^+$].

3.2.1 Lipase-catalyzed synthesis of compound 3.22
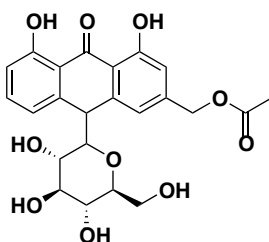
Aloin (100 mg, 0.24 mmol) and vinyl acetate (33 µL, 0.36 mmol) were dissolved in 15 mL of dry acetone under nitrogen atmosphere. Molecular sieves 4Å (30 mg) and lipase PS supported on Celite® (80 mg, 1 % w/w lipase/celite) were then added to the resulting solution

which was incubated at 45 °C and 210 rpm for 48 h. After that, the formation of the desired product was observed by TLC (CHCl$_3$/MeOH/HCOOH = 8:2:0.1, UV) and the crude mixture filtered, concentrated *in vacuo* and purified by flash column chromatography on silica gel (AcOEt/MeOH/H$_2$O = 9.5:0.5:0.1), affording the purified product as a yellow solid (85 mg, 80%). **^{1}H-NMR (CD$_3$OD, 400 MHz; mixture of diastereoisomers, 25 °C):** δ 7.47 (1H, ddd, *J* = 8.3, 7.6, 5.8 Hz), 7.04-7.00 (2H, m), 6.86-6.81 (2H, m), 5.16 (2H, d, *J* = 3.6 Hz), 4.50 (1H, d, *J* = 1.9 Hz), 3.59-3.55 (1H, m), 3.42-3.37 (2H, m), 3.29-3.25 (1H, m), 3.00-2.88 (3H, m), 2.17 (1H, s), 2.15 (2H, s). **^{13}C-NMR (CD$_3$OD, 100 MHz; mixture of diastereoisomers, 25 °C):** δ 194.0, 171.6, 171.13, 171.03, 161.77, 161.69, 161.55, 161.51, 145.4, 145.01, 144.88, 144.2, 142.0, 141.6, 135.7, 135.0, 119.9, 118.58, 118.51, 117.4, 117.2, 116.82, 116.63, 115.7, 115.5, 114.1, 113.8, 85.18, 85.01, 80.26, 80.17, 78.53, 78.50, 70.60, 70.58, 70.50, 70.46, 64.96, 64.91, 61.88, 61.83, 60.2, 44.45, 44.38, 19.50, 19.44, 13.1. **MS (ESI)** = 483.1 [(M+Na)$^+$].

4. Glycosidases: a stereo- and regio-selective synthesis of naturally occurring arylalkyl glucosides

Substituted benzyl, phenethyl and phenylpropenyl glucosides (**Figure 4.1**) are bioactive natural compounds largely occurring in plants.[26, 27, 28, 29, 30, 31] As an example, salidroside (**4.2a**) is associated with a wide number of pharmacological effects, including antioxidant, anti-inflammatory and anticancer activities. Furthermore, isoconiferin (**4.7a**) and triandrin (**4.5a**) are respectively studied for their potential antidepressant and hypotensive effects. Those biological effects are primary related to the structures of the aglycone. However, the physicochemical, the pharmacological and the toxicity profiles of these chemicals are strongly influenced by the conjugation with the sugar.

(4.1)   R = OH
(4.1a) R = β-Glc

(4.2) R_1 = OH, R_2 = H
(4.2a) R_1 = β-Glc, R_2 = H
(4.4) R_1 = OH, R_2 = OH
(4.4a) R_1 = β-Glc, R_2 = OH

(4.3) R_1 = OH, R_2 = R_3 = R_4 = H
(4.3a) R_1 = β-Glc, R_2 = R_3 = R_4 = H
(4.5) R_1 = OH, R_3 = OH, R_2 = R_4 = H
(4.5a) R_1 = β-Glc, R_3 = OH, R_2 = R_4 = H
(4.6) R_1 = OH, R_3 = OMe, R_2 = R_4 = H
(4.6a) R_1 = β-Glc, R_3 = OMe, R_2 = R_4 = H
(4.7) R_1 = OH, R_2 = H, R_3 = OH, R_4 = OMe
(4.7a) R_1 = β-Glc, R_2 = H, R_3 = OH, R_4 = OMe
(4.8) R_1 = OH, R_3 = OH, R_2 = R_4 = OMe
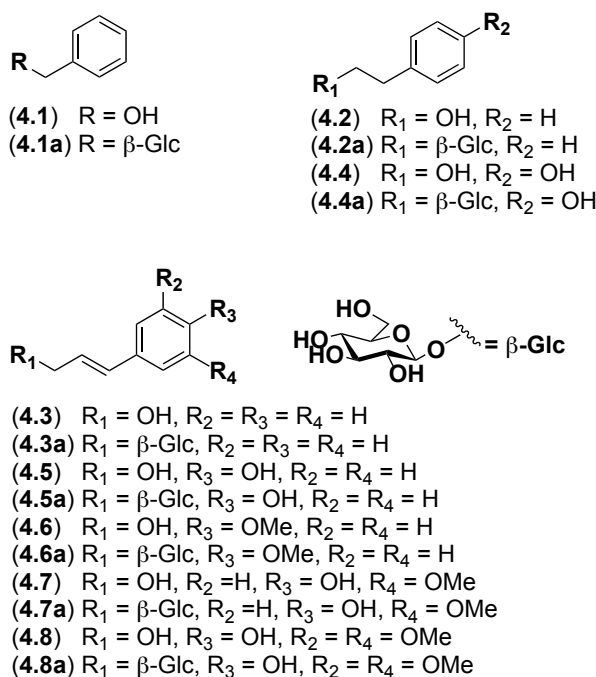**(4.8a)** R_1 = β-Glc, R_3 = OH, R_2 = R_4 = OMe

Figure 4.1: Compounds **4.1**-**4.8** and natural bioactive products **4.1a**-**4.8a**.

These bioactive glucosides have been either isolated in low amounts from natural sources or synthesized using classical glycosylation protocols. As an example, we have recently synthetized the (D)-glucoside **4.7a**. The selected synthetic pathway (**Scheme 4.1**, for details see **Paper VI**) was based on well-defined and reliable protocols; nevertheless, the sequence of protective and deprotective reactions consisted of seven steps. Moreover, two chromatographic purifications were required when glucose and the respective primary alcohol were used as starting materials. Such procedures were time-consuming and resulted in mediocre overall yields, also requiring the use large amounts of solvents, silica gel, and various toxic chemicals.
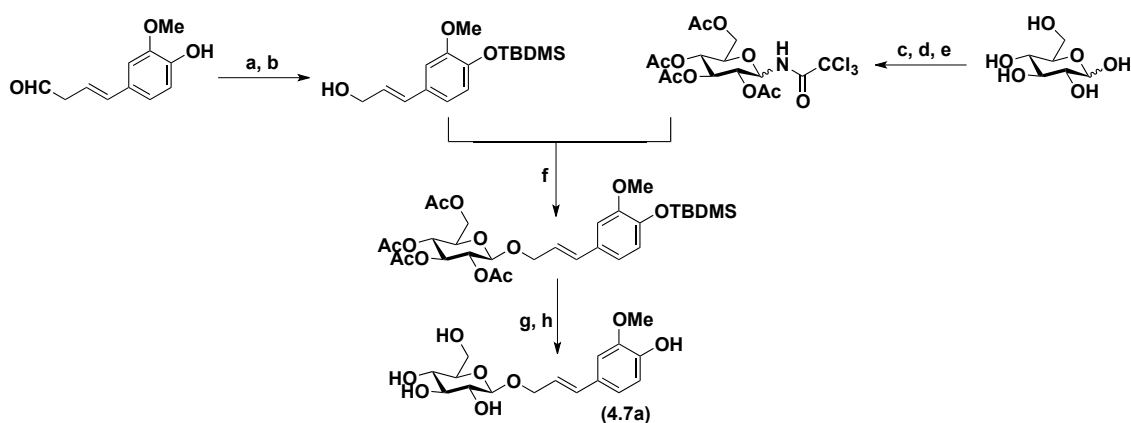
Scheme 4.1: Multi-step chemical synthesis of compound (**4.7a**).
Reagents and conditions: a. N$_2$, TBDMSiCl, imidazole, THF dry, 0 °C, 2h; **b.** N$_2$, NaBH$_4$, MeOH, 0 °C to r.t., 5h; **c.** Py, Ac$_2$O, DMAP, r.t., 24 h; **d.** AcOH glacial, NH$_2$(CH$_2$)$_2$NH$_2$, THF, r.t., 3 h; **e.** N$_2$, DBU, CCl$_3$CN, DCM dry, r.t.; **f.** TMSOTf, powdered sieves 4 Å, DCM dry, −15°C, 30 min, **30 %** **g.** TBAF, THF dry, 0 °C, 2 h; **h.** MeONa/MeOH, r.t., 3 h.

Therefore, an alternative and greener approach to synthetize arylalkyl glucosides was investigated, aiming at improving the overall efficiency and ensuring regio- and stereo-selectivity by exploiting the inherent selectivity properties of enzymes.

4.1   Biocatalytic entries to glycosides

As a general concept, the formation of stereoselective glycosidic bonds in Nature is mainly operated by glycosyltransferases (EC 2.4, GTFs). These enzymes catalyze the transfer of saccharide moieties from an activated glycosyl donor to a nucleophilic glycosyl acceptor building a new bond between the sugar moiety and a nucleophilic oxygen, carbon, nitrogen or sulfur atom.[32]
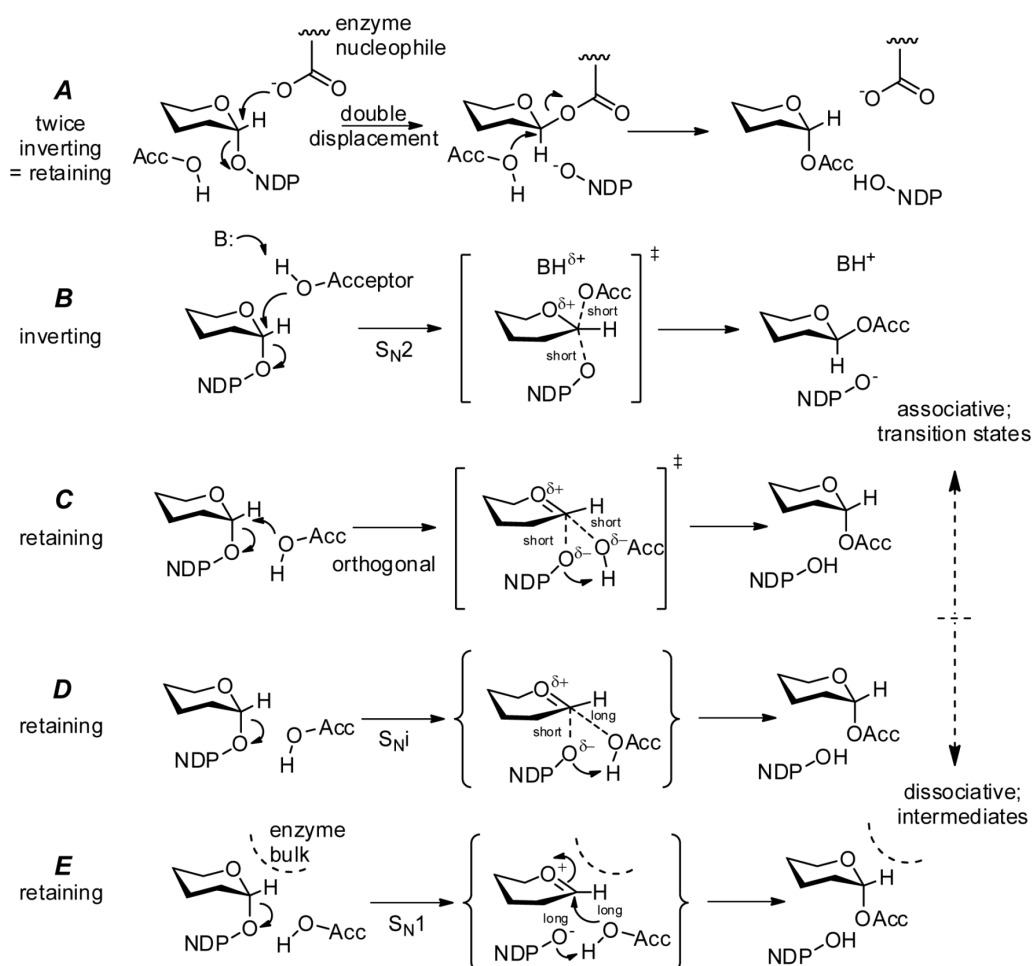

Figure 4.2: Proposed glycosyltransferase mechanisms. HOAcc = glycosyl acceptor.
(**A**) Double displacement mechanism: two inversions, via (**B**) an SN2 process, with net retention of stereochemistry involving a covalent glycosyl-enzyme intermediate. (**C**) Orthogonal mechanism: nucleophilic attack on C_1 concurrent with leaving group loss from a position approximately at right angles to the C_1-leaving group axis; (**D**) SN$_i$ mechanism: oxocarbenium-like intermediate character followed by rapid internal nucleophilic attach. (**E**) SN1 mechanism: discreet oxocarbenium intermediate.

GTFs can be classified in two main groups, depending on the stereochemical outcome of the glycosyl bond formation: 'retaining GTFs' preserve the stereochemistry of the donor's anomeric bond (*i.e.* α→α) while 'inverting GTFs' invert the absolute configuration at the anomeric position (*i.e.* α→β). In **Figure 4.2**, an overview about the possible mechanisms occurring for the two groups of GTFs' is reported.[33]

While, the inverting mechanism (**A**) appears as straightforward, requiring just a single nucleophilic attack from the accepting atom to invert stereochemistry, the nature of the retentive mechanism has been widely debated. Eventually, the 'orthogonal associative mechanism' (**E**), in which a single nucleophilic attack from a non-linear angle (as observed in many crystal structures) is postulated, was proposed and accepted.
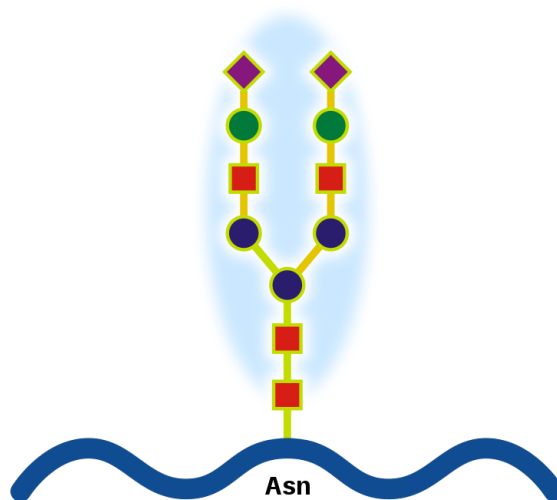

Figure 4.3: Schematic representation of a *N*-glycosylated asparagine residue of a protein backbone.[34]

The glycosyl transfer operated by GTFs occurs in biological systems on a plethora of compounds, from small molecules, with the production of glycosylated metabolites, to macromolecular structures. As an example, GTFs can glycosylate proteins by transferring a glycosyl moiety to nucleophilic protein residues, leading to the formation of *O*-linked or *N*-linked glycoproteins (**Figure 4.3**), depending on the nature of the residues involved in the reaction (serine, tyrosine and threonine or asparagine). GTFs can also use lipids as acceptors, thus promoting the formation of glycolipids.[32]

Regardless the synthetic potential of this class of biocatalysts to produce glycosides, the application of GTFs in organic synthesis is mainly affected by their need of activated glycosyl donors. They are expansive sugar nucleotides whose stereoselective synthesis can often be tricky (*i.e.* UDP-glucose or other nucleosides, glycosyl phosphate, **Figure 4.4**).[35, 36, 37]
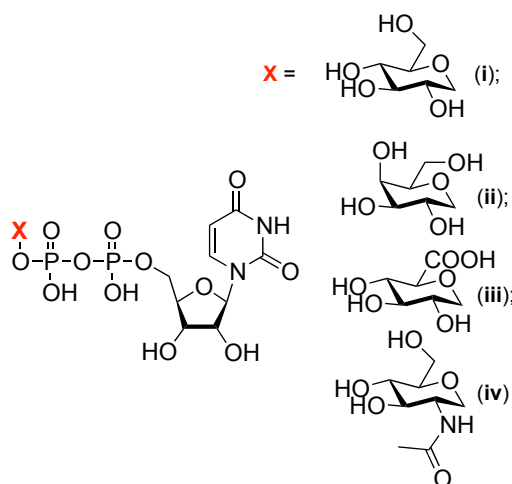

Figure 4.4: Examples of activated sugar donor. (**i**) uracil-diphosphate glucose, UDP-glucose; (**i**) uridine diphosphate galactose, UDP-galactose; (**iii**) uridine diphosphate glucuronic acid; uridine diphosphate *N*-acetylglucosamine (**iv**) .

The biocatalytic formation of stereoselective glycosidic bonds can also be accomplished by means of the promiscuous transglycosylation activity of the hydrolytic enzymes glycosidases, or by the action of the so-called glycosynthases, artificial mutants of natural glycosidases.[38, 39]
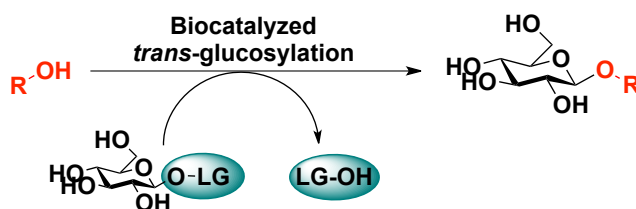
Scheme 4.2: Transglycosylation reaction

Promiscuous glycosidases are a group of enzymes widely used in organic chemistry as catalysts to synthetize glycosides. The synthesis of a new glycosidic bond can occur through either reverse hydrolysis (thermodynamic approach), where the equilibrium position is

reversed, or by transglycosylation (kinetic approach) whereby a glycosyl moiety is transferred from a glycoside to an acceptor alcohol to afford a new glycoside, as shown in **Scheme 4.2**.[40] As described for glycosyltransferases, also glycosidases can be either 'retentive' or 'inverting', depending on the stereochemical configuration of the new installed bond with the respect to the starting glycosyl donor.

Glycosynthases, enzymes generated by site-directed mutagenesis to eliminate the hydrolytic attitude of natural glycosidases, can catalyze the formation of a glycosidic bond, but they are no longer able to hydrolyze it, owing to their mutated active sites. Traditionally, glycosynthases (**Figure 4.5**) were formed from glycosidase by mutating the nucleophilic amino acids in the active site (usually an aspartate or a glutamate) to a small, non-nucleophilic amino acid such as alanine or glycine).
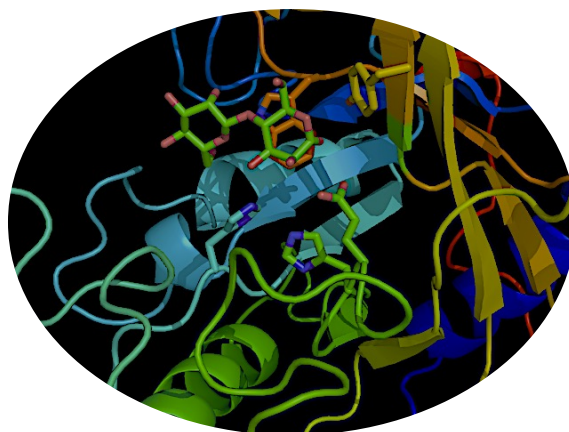

Figure 4.5*: A glycosynthase: mutant endomannase with bounded mannodiose.[41]

The development of modern approaches to directed evolution for the screening of amino acid substitutions, allowed to obtain glycosynthases with more and more enhanced synthase activity, able to successfully catalyze elegant glycoside syntheses.[42] However, to properly promote the formation of glycosidic bonds, glycosynthases usually need activated sugar donors, such as fluorides or azides, and, generally speaking, require considerable workload, affecting, as in the case of glycosyltransferases, their synthetic exploitation. In fact, biotransformations carried out in the presence of 'nude' sugars and nucleophilic alcohols typically occur with low conversions.[43]

In the quest of a novel and convenient biocatalytic strategy to produce naturally occurring glucosides (**Figure 4.1**), in **Paper III** we have exploited the action of a promiscuous, stereo- and regio-selective glycoside hydrolase to build a one-pot, two-enzymes strategy to synthetize glycosidic bonds between glucose and primary arylalkyl alcohols.

4.2   Two-enzymes approach

Rutin (**4.8**), a glycosyl derivative of the flavonoid quercetin (**4.9**) (glycon: rutinose, α-L-rhamnopyranosyl-β-D-glucopyranoside, **4.10**), is an important phytochemical contained in various plants and fruits (*i.e.* buckwheat, apples, tobacco, tomatoes, citrus, and grapes), that was named after one of its primary natural sources, the common rue *Ruta graveolens*.[44, 45] In Nature, among all the metabolic pathways related to this compound, rutin conversion into quercetin occurs *via* the action of a specific diglycosidase, the enzyme called rutinosidase. Rutinosidase, whose systematic name is α-L-rhamnopyranosyl-β-D-glucosidase, is a fugal biocatalyst that selectively hydrolyses the glycosidic bond between the disaccharide moiety (rutinose) and the aglycone (quercetin), as shown in **Scheme 4.3**.
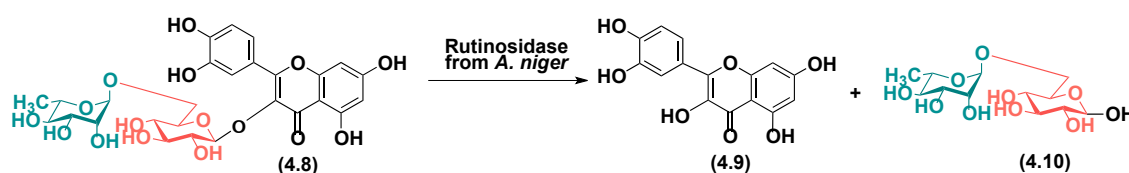
Scheme 4.3: Rutinosidase-mediated hydrolysis of ruin.

It has been recently shown by the group headed by professor Vladimir Křen that the diglycosidase rutinosidase from *Aspergillus niger*, cloned and expressed in *Pichia pastoris,* possesses such a strong promiscuous transglycosylation activity both for aliphatic alcohols and phenols, that can be regarded as much more efficient in these kind of biotransformations than other commonly used (mono)glycosidases. Moreover, thanks to its 'retentive' nature, the products obtained from the transfer of a rutinose moiety to a primary alcohol or phenol are formed stereospecifically as β-glycosides (**Figure 4.6**).[46] Nevertheless, this specific reaction has another advantage: both the reactant and the by-product(s) are nontoxic (natural) flavonoids and, thus, they do not compromise the potential pharmaceutical and/or nutraceutical applications of the obtained glycosyl products.

Regardless its complex structure, rutin (**4.8**) appears as a cheap and convenient glycosyl donor. It is in fact produced as a multiton commodity chemical from the brazilian tree Fava d'anta (*Dimorphandra mollis*) along with being accumulated as a waste by-product in different

manufacturing processes (*e.g.* the production of fruit juices). Also, it possesses a GRAS status (www.hcsc.gc.ca) and it's used in a plethora of nutraceuticals and pharmaceutical preparations as a capillary/blood vessel protectant and as an antiviral agent.
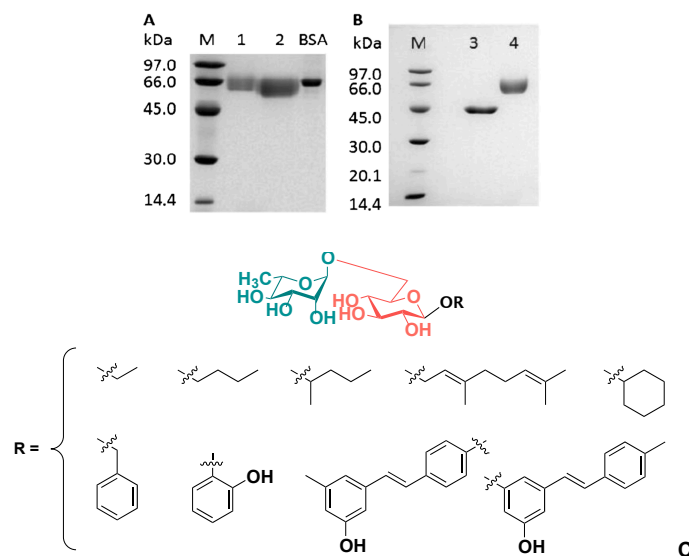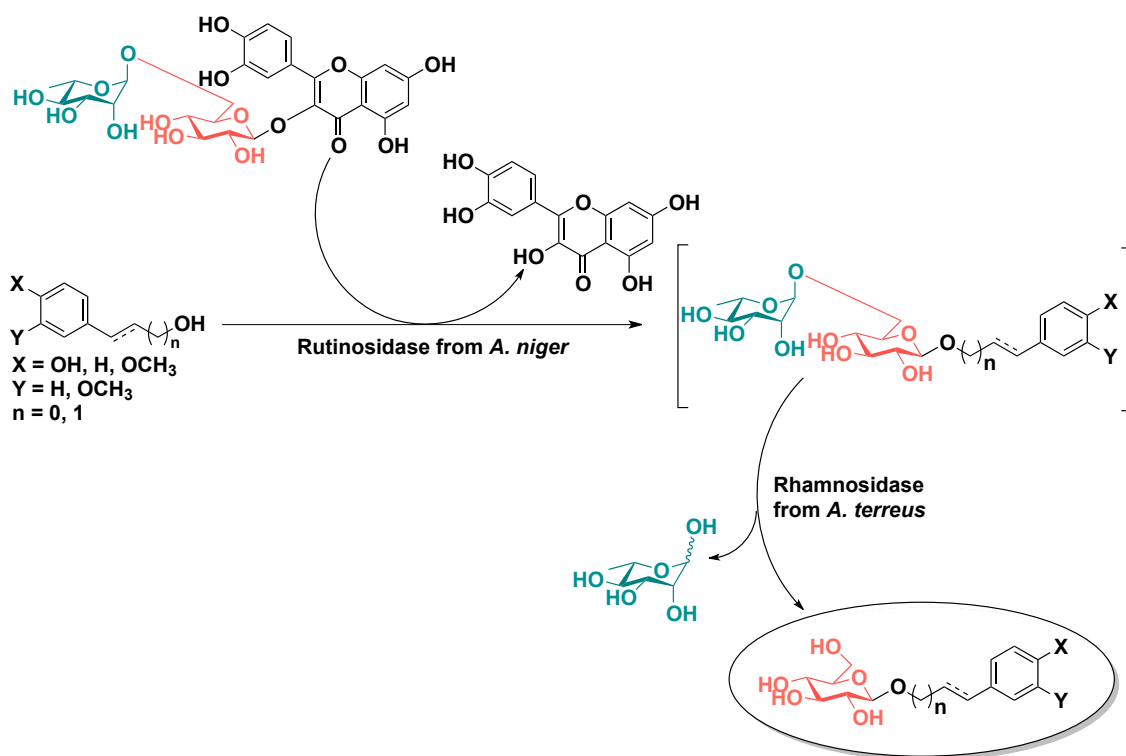

Figure 4.6: SDS-PAGE, 10% gel: **A.** 1 – crude secreted recombinant rutinosidase (after dialysis), 2 – purified recombinant rutinosidase; **B.** 3 – Endo Hf-deglycosylated purified recombinant rutinosidase; 4 – untreated purified recombinant rutinosidase. **C.** Synthetized β-rutinosides. © Wiley-VCH Verlag.

Given all the listed advantages, the combination of rutinosidase and rutin, as an inexpensive (presently it costs less than 50 € kg^{-1}) and nontoxic activated sugar donor, for the regio- and stereo-selective synthesis of rutinosylated conjugates appeared to us as highly versatile and promising. Therefore, a one-pot, two-enzymes entry to arylalkyl glucosides was built by exploiting the activity of the mentioned diglycosidase in combination with a proper glycoside hydrolase to selectively remove the unwanted rhamnose moiety, converting the rutinosylated substances into the desired β-glucosides.

The hydrolase that was selected for this purpose was a robust α-L-rhamnosidase from *Aspergillus terreus* (cloned and expressed in *Pichia Pastoris*) characterized by a significant selectivity and high activity in the trimming of the α(6→1)rhamnosyl unit of rutin to yield isoquercetrin (**4.11**, **Scheme 4.6**).[47, 48] The one-pot, two-enzymes approach is showed in (**Scheme 4.4**).

Scheme 4.4: One-pot, two-enzymes entry to arylalkyl glucosides.

X = OH, H, OCH₃
Y = H, OCH₃
n = 0, 1

Rutinosidase from *A. niger*

Rhamnosidase
from *A. terreus*

4.3 Reaction optimization: toward a one-pot synthesis

Transglycosylations are kinetically controlled reactions in which both the products and the reactants may become substrates for a subsequent hydrolysis catalyzed by the same enzyme, virtually lowering the overall yield (**Scheme 4.5**).
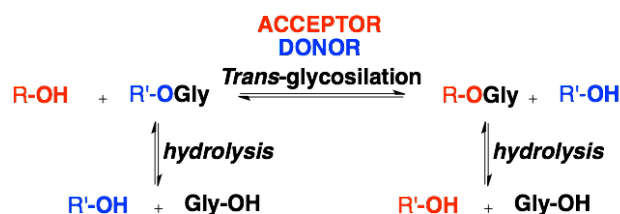
Scheme 4.5: Transglycosylation and hydrolysis.

Therefore, the first critical point of our investigation was the thorough optimization of the rutinosidase-catalyzed reaction, to promote a neat transgycosylation between rutin and the desired alcohol. As shown in **Scheme 4.6**, coniferyl alcohol (**4.7**), the aglycone of the natural hypotensive agent coniferin (**4.7a**), was chosen as a model glycosyl acceptor.
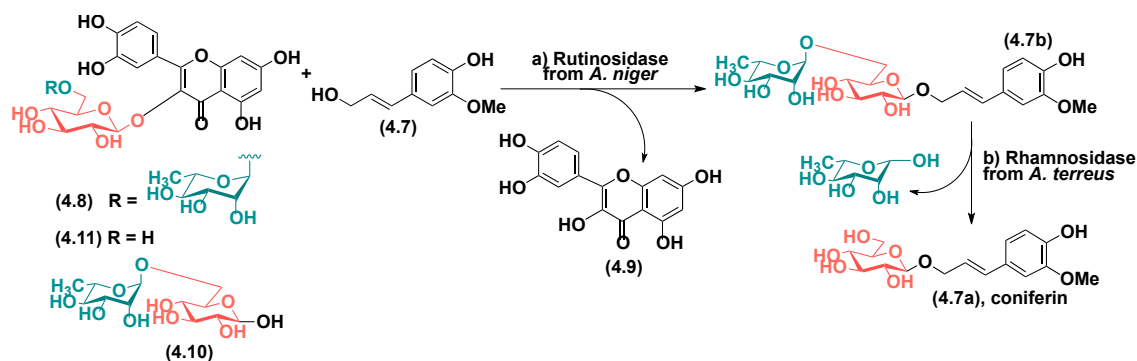
Scheme 4.6: Two-enzymes entry to **4.7a**.

According to the published transglycosylation protocol (50 mM 1:1 mixture of rutin and glycosyl acceptor dissolved in a 50 vol% DMSO solution in citrate/phosphate buffer at pH 5, incubated at 35 °C for 7 h with 0.026 U $mmol_{alcohol}^{-1}$), a set of biotransformations was carried out to investigate the influence of four selected key parameters: **a**) enzyme loading, **b**) relative stoichiometry of the reactants, **c**) concentration of glycosyl donor (rutin) and **d**) amount of cosolvent (DMSO).

a) **Enzyme loading**. Different loads of biocatalyst were used: 0.0065, 0.013, 0.026 or 0.052 U $mmol_{alcohol}^{-1}$ of rutinosidase. The obtained results showed that the highest was the amount of the enzyme, the fastest the hydrolysis of rutin to quercetin was. Moreover, when 0.0065 U $mmol_{alcohol}^{-1}$ of rutinosidase were used, almost no transglycosylation was observed and only a slow hydrolysis occurred under these conditions. For all this reason, loading of rutinosidase was set to 0.013 U $mmol_{alcohol}^{-1}$: the hydrolysis reaction was in this case slow enough to permit a modest accumulation of the target disaccharide **4.7b** in a reaction time of 7 hours.

b-c) **Stoichiometry/rutin concentration**. The stoichiometric ratio between rutin and coniferyl alcohol was deeply investigated. Four different biotransformations were run using a 0.5:1, a 1:1, a 2:1 and a 4:1 stoichiometric ratio of glycosyl donor/acceptor, respectively. When a 1:1 or a 2:1 mixture of rutin and alcohol was used, the conversion of coniferyl alcohol into the rutinoside was rather low (15 %, evaluated by HPLC) as quercetin was obtained as major product. Furthermore, when a 4:1 ratio was used, no reactions were catalyzed by the enzyme - neither the hydrolysis nor the transglycosylation. However, when a 0.5:1 mixture of rutin and alcohol was used, the conversion of the arylalkyl alcohol to the target disaccharide was higher (up to the 50 %, evaluated by HPLC). Thanks to these results, it was concluded that an excess of glycosyl acceptor was needed to promote the transglycosylation reaction over hydrolysis. Moreover, a strong inhibitory effect was observed for the enzyme at high concentrations of rutin.

c-d) Stoichiometry/cosolvent. The amount of DMSO (in terms of % v/v) was investigated, as the reaction mixture appearance was strongly dependent to it: both rutin and quercetin are in fact almost completely insoluble in water at acid pHs, unless more than the 40 % v/v of DMSO is used as cosolvent. Therefore, different concentrations of DMSO were used to run control biotransformations (40, 30, 20, 15 and 10 vol%), with a 1:1 stoichiometric ratio between rutin and coniferyl alcohol. The reaction run in the presence of 40 % v/v DMSO was a clear solution that gave just a 10 % (HPLC) conversion into the desired product. When 15 % v/v of DMSO was used, the system appeared as a solid-liquid biphasic system with rutin (and quercetin) just partially dissolved while the glycosyl acceptor

was in solution. Interesting enough, in this case conversion, evaluated by HPLC, was more than the 40 %.

On the base of these results, **4.7** was subjected to the action of rutinosidase (ca. 0.013 U mmol$_{alcohol}^{-1}$) using an initial excess of alcohol acceptor relative to the glycosyl donor (rutin/alcohol = 0.5:1 equiv.). To limit the significant substrate inhibition caused by rutin, a 15 % v/v of DMSO was used to decrease the active concentration of rutin in the reaction media as, in this system, the donor was just suspended and only partially dissolved. Moreover, to make this procedure fully scalable and green, a purification strategy avoiding the use of silica gel chromatography was developed. By fully exploiting the physicochemical differences between the starting alcohol **4.7**, the rutinoside product **4.7b**, the residual rutin **4.8** (if any), the produced quercetin **4.9** and the free disaccharide rutinose always formed as a byproduct **4.10**, it was possible to purify **4.7b** by means of **i)** centrifugation; **ii)** extraction with organic solvents and **iii)** solid-phase extraction on Amberlite® XAD4 non-ionic resin.[49] Accordingly, the produced **4.9** was removed by centrifugation, the unconsumed coniferyl alcohol **4.7** was extracted with AcOEt, and the hydrolyzed rutinose **4.10**, the buffer salts, and the residual DMSO cosolvent were easily removed in the eluate. Product **4.7b** was instead adsorbed on the XAD4 resin and then eluted using MeOH. The cosolvent DMSO did not compromise the green concept of this protocol: its toxicity is very low (DMSO is currently used in cosmetics and medications to increase skin permeability) and its residual presence could not be detected in the isolated products by NMR spectroscopy.

The preparative-scale transrutinosylation of **4.7** was conducted starting from a 1 g alcohol. Rutin (a total of 1.5 equiv.) was added portion-wise (0.5 equiv. each time) over 8 h (its disappearance was monitored by TLC). Following the described protocol, product **4.7b** was finally isolated in 70% yield and fully characterized by MS (m/z 511.3 [M+Na$^+$]) and NMR spectroscopy. In addition to the expected signals owing to the coniferyl moiety, the presence of a disaccharide unit was clearly demonstrated by the respective signals in the ^{1}H NMR spectrum. Specifically, the anomeric protons of the rhamnopyranose and glucopyranose units gave rise to doublets (J 1.6 and 7.8 Hz, respectively) centered at 4.80 and

4.37 ppm. The presence of the rhamnopyranose unit was further confirmed by the signal of its methyl group (δ_H =1.30, d, J 6.3 Hz). Moreover, the initial transglycosylation reaction was not only stereospecific (production of a β-glycoside from a β-glycosyl donor), but it was also highly regioselective, as no formation of phenolic glycoside was observed.

Once the first transglycosylation step had been optimized, the synthesis of the target natural glucoside **4.7** was straightforward. The enzymatic trimming of the rhamnose unit was easily obtained by incubating **4.7b** in a citrate phosphate solution (50 mM, pH 5) at 45 °C for 3 h with *ca.* 2 U $mmol_{alcohol}^{-1}$ of a rhamnosidase from *A. terreus*. After a solid phase extraction on XAD4 resin, the purified glucoside **4.7** was obtained in 90 % yield. Compound **7a** was characterized by MS (m/z 365.2 [$M+Na^+$]) and ^{1}H and ^{13}C NMR spectroscopy, which showed the presence of both the coniferyl aglycone and the glucopyranosyl moiety, in perfect agreement with literature data.[50]

Once **4.7** was successfully obtained *via* this novel two-enzymes catalyzed entry, the target one-pot approach was investigated by merging the two enzymatic reactions. A so-called telescoping synthesis was studied: the reactants were added sequentially to the reactor without any intermediate purification or work-up and the reactions were run in one pot. In this way, the rutinose grafting by glucosylation of coniferyl alcohol was achieved by sequentially combining the transglycosylation grafting and the rhamnose trimming by hydrolysis. The two enzymes, in fact, demonstrated to conveniently share the same optimal operational conditions, being both stable and active at the same pH and temperature. However, rutinosidase had to be thermally inactivated prior to adding the rhamnosidase (0.5 U $mmol_{alcohol}^{-1}$) and stirring the final reaction mixture overnight. The target glucoside **4.7a** was isolated in 75% yield after purification following the previously described procedure based on XAD4 resin.

The above described and optimized one-pot synthesis was then applied to the alcohols **4.1–4.8**. As shown in (**Table 4.1**), all compounds were accepted by the rutinosidase, except for sinapyl alcohol **4.8**. Compounds **4.4**-**4.6** behaved analogously to **4.7**, and with coumaryl alcohol **4.5** the transglycosylation reaction was also fully regioselective.

Compounds **4.1**-**4.3** were also glycosylated, but, apparently, they were less reactive as the yields of isolated products were lower. Kinetic studies of the enzymatic glycosylation of **4.1** and **4.2**, evaluating the formation of the rhamnosidase derivatives **4.1b** and **4.2b** (**Figure 4.7**), showed how the lower yield could be a consequence of an inevitable enzymatic hydrolysis of the target monosaccharide. Therefore, the reactions needed to be carefully monitored to maximize the yields.

	Product	Yield[a] %
1[b]	1a	12
2[b]	2b	24
3[b]	3a	44.5[c]
	3c	4.5[c]
4	4	70
5	5a	68
6	6a	58
7	7a	75
8	--	--

Table 4.1: One-pot, two-enzymes synthesis.
Reagents and conditions: **i)** rutinosidase (0.013 U $mmol_{alcohol}^{-1}$), arylalkyl alcohol (130 mM, 1 equiv), rutin (1.25 equiv.), citrate-phosphate buffer 50 mM pH 5/dimethyl sulphoxide = 85 % : 15 %, 35 °C and 750 rpm; **ii)** rhamnosidase (0.5 U $mmol_{alcohol}^{-1}$), 35 °C and 750 rpm , overnight. Centrifugation, extraction, XAD4 solid phase extraction. [a] Yields of isolated products. [b] Reactions with substrates 1, 2, and 3 were performed for 24 h instead of 8 h.
[c] Relative ratio estimated by ^{1}H NMR spectroscopy.

The structural rigidity of the fully conjugated system characterizing compounds **4.4-4.7** apparently made them suitable substrates for the transglycosylation reactions, as they proved to be good acceptors and bad donors. Therefore, the enzymatic hydrolysis of their corresponding rutinoside derivatives was almost completely avoided. Tyrosol (**4.3**) on the contrary, behaved similarly to compounds **4.1** and **4.2**, possessing neither a rigid π-system nor a 3-long carbon chain connecting the nucleophilic primary alcohol to the phenyl ring. The differences between the streoelectronic features of compounds **4.1**-**4.3** and **4.4**-**4.7** could have led to the different performances that the two family of nucleophiles showed in the one-pot synthesis. This was especially the case with compound **4.3**.
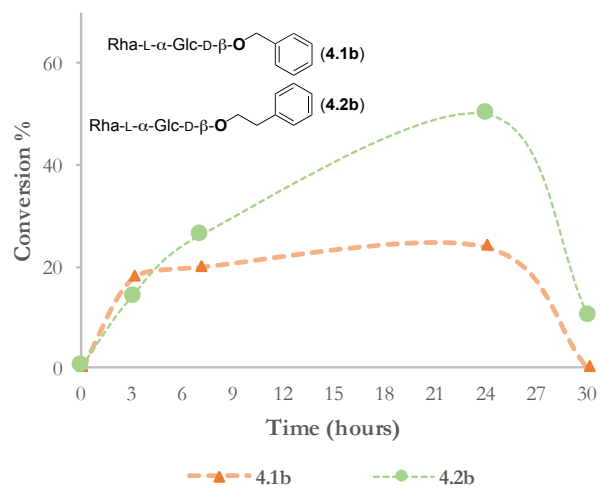
Figure 4.7: Kinetic profiles of the production of **4.1b** and **4.2b**.

4.4   The case of tyrosol

Tyrosol (**4.3**) behaved differently also in terms of regioselectivity. In fact, along with the lower isolated yield, the desired glucoside **4.3a** was obtained in a 10 : 1 mixture with the regioisomer **4.3c** (**Figure 4.8**).
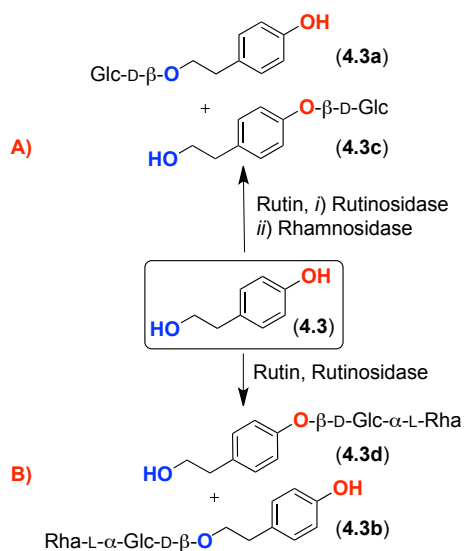

Figure 4.8: Glycosides of tyrosol (**4.3**). **A)** Two-enzyme synthesis of tyrosol glu- cosides **4.3a** and **4.3c**. **B)** Rutinosidase-catalyzed synthesis of tyrosol rutinosides **4.3b** and **4.3d**. © 2017 VILEY Wiley-VCH

The mass spectrum of the isolated product (m/z 232.2 [M+Na$^+$]) confirmed the introduction of a glucose moiety. However, the ^{1}H NMR spectrum clearly showed the presence of two products in 10 : 1 ratio. The signal resulting from the α-anomeric proton of the major product, a doublet with J 7.8 Hz resonating at 4.29 ppm, could be overlapped with the corresponding signal of the glucoside of phenylethanol (**4.2a**). As a consequence, it could be possible to assign the structure **4.3a** to this compound. The significant downfield shift of the aromatic protons of the minor product [the two coupled doublets (J 8.4 Hz) resulting from the AA'BB' aromatic system resonate at 7.18 and 7.03 ppm in the case **4.3b**, whereas they were recorded at 7.08 and 6.71 ppm in **4.3a**], indicated, instead, the glucosylation of the phenolic OH group (**4.3c**).

To further investigate the glycosylation of this compound, the intermediate tyrosol rutinosides **4.3b** and **4.3d** were isolated and a set of kinetic experiments conducted.

Following the previously described protocol, a mixture of the expected regioisomers **4.3b** and **4.3d** (MS and ^{1}H NMR spectrum in accordance with the proposed structures) was again obtained, this time in 3 : 1 ratio.

The different regioisomeric ratio observed between **4.3a**/**4.3c** (10:1) and **4.3b**/**4.3d** (3:1) could be kinetically rationalized by considering the different reaction time allowed for the transrutinosylation step in the two protocols, which was longer in the telescopic synthesis. In fact, kinetics studies performed by monitoring the reactions by reversed-phase HPLC clearly showed that the phenolic rutinoside **4.3d** could be hydrolyzed faster than alkyl rutinoside **4.3b** (**Figure 4.9**).
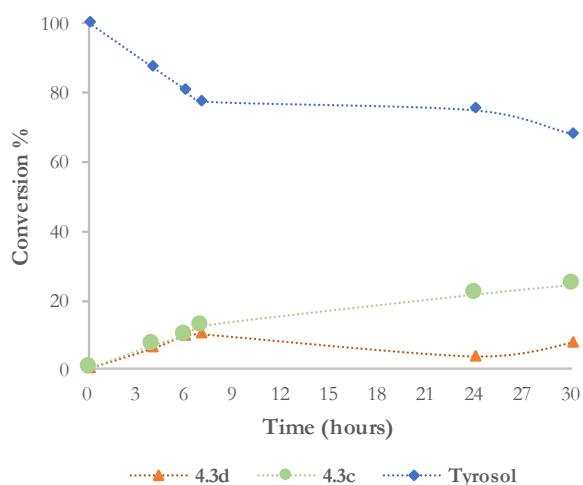

Figure 4.9: Kinetic profiles of the production of **4.3d** and **4.3c**.

The separation of the two regioisomeric glycosides (**4.3a** from **4.3c**, **4.3b** from **4.3d**) proved to be quite troublesome, and several techniques failed, including silica-gel flash chromatography and reverse phase preparative HPLC. On the contrary, the separation of the regioisomeric rutinosides **4.3b** and **4.3d** could be achieved by gel filtration with Biogel P2 (BioRad), and the major product **4.3b** could be obtained in a 94% purity, as determined by ^{1}H NMR spectroscopy.

4.5   Conclusions

A small library of naturally occurring bioactive glucosides was successfully synthetized by combining the action of a promiscuous diglycosidase rutinosidase from *Aspergillus niger* and of a rhamnosidase from *A. terreus* (both cloned and expressed in *Pichia pastoris*) in a biocatalytic process characterized by complete control over the stereochemical outcome. The target natural β-glucosides were obtained in isolated yield up to the 80% via a convenient telescoping synthesis that avoided the need of intermediate isolation and product purification by flash column chromatography.

In comparison, the chemical synthesis of, *i.e.*, **4.7a** required seven reactions (protection of carbohydrate hydroxyl groups, deprotection of the anomeric OH group, activation of the anomeric OH group, protection of the phenolic OH group, condensation between activated sugar and aglycone, deprotection of the phenolic moiety, deprotection of the sugar OH groups) and two silica-gel chromatography steps.

Therefore, the proposed enzymatic approach is superior to the chemical one in terms of better atom economy.[51] Both enzymes used in this work, that is, rutinosidase and rhamnosidase, do not need to be recycled. They are both produced heterologously by *P. pastoris* and their production costs are very low. In fact, the typical activity obtained is approximately 0.15 U mL^{-1} cultivation broths. This means that less than 1 mL of the medium is required for 1 g coniferyl alcohol. The previously described experiments were run in the presence of purified rutinosidase, but it was also verified that even the crude enzyme (that is just using the fermentation medium) could be equivalently used. By rough estimation, the substrate used for the optimization study (coniferyl alcohol) is significantly (ca. 100–1000 times) more expensive than the enzymes, thus making not economical the additional work required to regenerate the biocatalysts. Moreover, the use of immobilized enzymes was not compatible with the proposed protocol: ss the reactions were run with a suspension of substrates, soluble enzymes were needed.

On the contrary, polystyrene microporous resin Amberlite XAD4 could be well reused in tens of cycles and refreshed by simple washing with MeOH or acetone. Moreover,
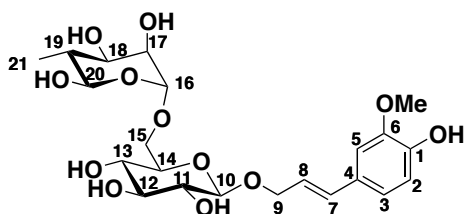
well-assessed regeneration protocols are available in the case resin starts to lose capacity. Therefore, the resin can be technically used for tens to hundreds of cycles.

Some of the synthetized glycosides, specifically compounds **4.5a** and **4.7a**, were also tested as substrates for a laccase-mediated oxidative-dimerization to synthesize, in a one-pot process, 2,3-dihydrobenzofuran-based analogues of these bioactive compounds. This topic will be discussed later in the paragraph *'Oxidative dimerization of glycosylated lignols'* of the chapter *'Laccases'*.

4.6 Experimental

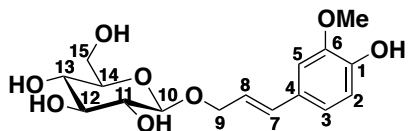### 4.5.1 Two-step two-enzymatic synthesis of *coniferin* (4.7a)

a) A suspension of rutin (1.70 g, 2.78 mmol) in a 15 % solution of DMSO in citrate-phosphate buffer (50 mM pH 5) containing coniferyl alcohol (1.00 g, 5.56 mmol) and rutinosidase from *A. niger* (0.073 U) were prepared and incubated at 35 °C and 750 rpm. The consumption of the glycosyl donor was checked by TLC analysis and 1.70 g of rutin was added again to the reacting mixture after 3 and 5 h. After 8 h the obtained yellow suspension was heated to 100 °C for 10 minutes and then cooled again to room temperature, diluted with ten 400 mL of citrate-phosphate buffer and centrifuged, recovering only the supernatant. The pH was changed from 5 to 7.5 – 7.7 and the water layer was extracted with AcOEt (2 × 200 mL) and then, after removing the residual AcOEt via concentration in *vacuo*, it was loaded to a column (5 × 30 cm) with Amberlite XAD4 resin (300 g) in water (elution with slow gradient H_2O to MeOH), affording the pure rutinoside **4.7b** (yellow solid, 755 mg, 70 %). The resin can be simply reused after washing with pure MeOH followed by extensive washing with water. **^{1}H-NMR (400 MHz; MeOD, 25 °C)**: δ 7.04 (d, *J* = 1.9 Hz, 1H: H-5), 6.89 (dd, *J* = 8.2, 1.9 Hz, 1H: H-3), 6.76 (d, *J* = 8.1 Hz, 1H: H-3), 6.60 (d, *J* = 15.9 Hz, 1H: H-7), 6.21 (ddd, *J* = 15.8, 6.8, 5.9 Hz, 1H: H-8), 4.80 (d, *J* = 1.6 Hz, 1H: H-16), 4.48 (ddd, *J* = 12.3, 5.8, 1.3 Hz, 1H: H-9$_A$), 4.37 (d, *J* = 7.8 Hz, 1H: H-10), 4.28 (ddd, *J* = 12.3, 7.0, 1.1 Hz, 1H: H-9$_B$), 4.01 (dd, *J* = 11.3, 1.7 Hz, 1H: H-15$_A$), 3.88 (s, 3H: OCH$_3$), 3.73-3.64 (m, 3H: H-15$_B$, H-18, H-20), 3.44-3.21 (m, 6H: H-11, H-12, H-13, H-14, H-17, H-19), 1.30 (d, *J* = 6.3 Hz, 3H: H-21). **^{13}C-NMR (101 MHz; MeOD, 25 °C)**: δ 147.7, 146.3, 133.1, 128.9, 122.1, 119.7, 114.8, 109.2, 101.6, 100.9, 76.7, 75.5, 73.7, 72.6, 70.97, 70.83, 70.3, 69.5, 68.4, 66.8, 54.9, 29.3, 16.7. **EI-MS, *m/z*** 511.3 [M+Na]$^+$.

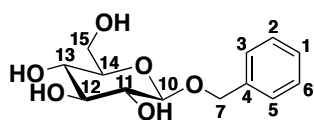**b)** Rhamnosidase from *A. terreus* (0.82 U) was dissolved in citrate-phosphate buffer (50 mM, pH 5) solution of **4.7a** (200 mg, 0.41 mmol, 2.5 mL). The resulting mixture was incubated at 35 °C and 750 rpm for 3 h. After checking the complete conversion of the starting rutinoside into the target glucoside by TLC analysis, heated to 100 °C for 10 minutes and then cooled again to room temperature to be subjected to an Amberlite XAD4 solid phase extraction (loaded and washed with H_2O; eluted with MeOH), affording pure coniferin, **4.7a** (yellow solid, 126 mg, 90%). **^{1}H-NMR (400 MHz; MeOD, 25 °C)**: δ 7.03 (d, *J* = 1.9 Hz, 1H: H-5), 6.87 (dd, *J* = 8.2, 1.9 Hz, 1H: H-3), 6.76 (d, *J* = 8.1 Hz, 1H: H-2), 6.59 (d, *J* = 15.9 Hz, 1H: H-7), 6.21 (ddd, *J* = 15.9, 6.7, 6.0 Hz, 1H: H-8), 4.51 (ddd, *J* = 12.4, 5.9, 1.4 Hz, 1H: H-9$_A$), 4.39 (d, *J* = 7.8 Hz, 1H: H-10), 4.32 (ddd, *J* = 12.4, 6.8, 1.2 Hz, 1H: H-9$_B$), 3.90 (dd, *J* = 11.9, 2.0 Hz, 1H: H-15$_A$), 3.88 (s, 3H: OCH$_3$), 3.70 (dd, *J* = 11.9, 5.4 Hz, 1H: H-15$_B$), 3.41-3.23 (m, 4H: H-11, H-12, H-13, H-14). **^{13}C-NMR (101 MHz; MeOD, 25 °C)**: δ 147.7, 146.3, 132.9, 129.0, 122.4, 119.8, 114.8, 109.3, 101.8, 76.74, 76.57, 73.7, 70.3, 69.6, 61.4, 55.0. **EI-MS, *m/z*** 365.2 [M+Na]$^{+}$.

4.5.2 Telescoping two-enzymatic glucosylation: general procedure. arylalkyl alcohol (1 eq, 128 mM) and rutinosidase from *A. niger* (0.013 U mmol^{-1}$_{substrate}$) were dissolved in a 15 % solution of DMSO in citrate-phosphate buffer (50 mM pH 5) and incubated at 35 °C and 750 rpm. The glycosylation reaction was started by adding 0.5 eq of rutin. Monitoring the consumption of the glycosyl donor by TLC analysis, two portions of rutin, 0.5 eq each, were added. The transglycosylations were conducted for 8 or 16 h, depending on the substrate used. When all the rutin was consumed, the suspension was heated to 100 °C for 10 minutes and then cooled again to 35 °C and rhamnosidase from *A. terreus* (0.5 U mmol^{-1}$_{substrate}$) was added to the mixture, which was incubated overnight at 35 °C and 750 rpm. The complete conversion of the intermediate disaccharide to the target β-glucopyranoside was checked by TLC analysis and then the resulting yellow suspension was cooled to room temperature,

diluted with ten volumes of citrate-phosphate buffer and centrifuged. The solid proved to be the expected quercetin (**10**) containing ca 20-25 % of unreacted rutin. The supernatant water layer, after shifting the pH from 5 to 7.5 – 7.7, was extracted twice with half the volume of AcOEt and then, after removing the residual AcOEt in vacuo, subjected to an Amberlite XAD4 solid phase extraction (mobile phase H_2O : MeOH, from 100 : 0 to 0 : 100), affording the pure arylalkylglucoside.

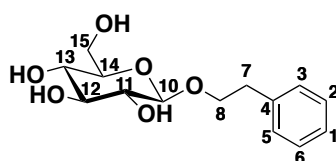**Compound 4.1a:** According to the General Procedure, compound **4.1a** (30 mg, 0.11 mmol, isolated yield: 12 %, yellow oil, 24 h) was obtained from 100 mg of benzyl alcohol and 846 mg of rutin. **^{1}H-NMR (500 MHz; MeOD, 25 °C)**: δ 7.44 (d, J = 7.3 Hz, 2H: H-2, H-6), 7.35 (t, J = 7.4 Hz, 2H: H-3, H-5), 7.29 (t, J = 7.3 Hz, 1H: H-1), 4.95 (d, J = 11.8 Hz, 1H: H-7$_A$), 4.69 (d, J = 11.8 Hz, 1H: H-7$_B$), 4.38 (d, J = 7.7 Hz, 1H: H-10), 3.92 (d, J = 10.2 Hz, 1H: H-15$_A$), 3.72 (dd, J = 11.8, 5.5 Hz, 1H: H-15$_B$), 3.39-3.26 (m, 6H: H-11, H-12, H-13, H-14). **^{13}C-NMR (101 MHz; MeOD, 25 °C)**: δ 132.4, 122.55, 122.48, 122.0, 96.6, 71.41, 71.36, 71.33, 71.32, 68.49, 68.44, 65.04, 65.03, 56.1, 33.7. **EI-MS, *m/z*** 293.1 [M+Na]$^+$.

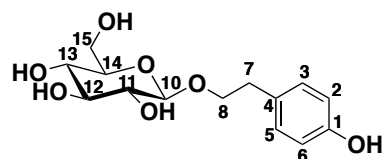**Compound 4.2a:** According to the General Procedure, compound **4.2a** (36 mg, 0.20 mmol, isolated yield: 24 %, yellow solid, 24 h) was obtained from 100 mg of 1-phenyl ethanol and 750mg of rutin. **^{1}H-NMR (500 MHz; MeOD, 25 °C)**: δ 7.27 (d, J = 4.5 Hz, 4H: H-2, H-3 H-5, H-6), 7.19 (q, J = 4.4 Hz, 1H: H-1), 4.32 (d, J = 7.8 Hz, 1H: H-10), 4.11 (dt, J = 9.5, 7.5 Hz, 1H: H-8$_A$), 3.88 (dd, J = 11.7, 1.5 Hz, 1H: H-15$_A$), 3.81-3.76 (m, 1H: H-8$_B$), 3.69 (dd, J = 11.8, 5.2 Hz, 1H: H-15$_B$), 3.39-3.19(m, 4H: H-11, H-12, H-13, H-14), 2.96 (td, J = 7.3, 1.6 Hz, 2H: H-7). **^{13}C-NMR (101 MHz; MeOD, 25 °C)**: δ 133.4, 123.3, 122.67, 122.64, 120.53, 120.50, 97.7, 71.43, 71.29, 68.4, 65.0, 56.1, 33.7, 30.6. **EI-MS, *m/z*** 307.0 [M+Na]$^+$.
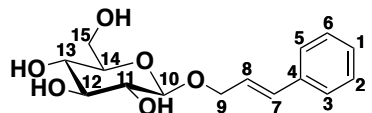
Compound 4.3a, *salidroside*: According to the General Procedure, compound **4.3a** (106 mg, 0.35 mmol, isolated yield: 49 %, yellow solid, 24 h) was obtained from 100 mg of tyrosol and 663 mg of rutin. **¹H-NMR (500 MHz; D₂O, 25 °C)**: δ 7.05 (d, *J* = 8.3 Hz, 2H: H-3, H-5), 6.69 (d, *J* = 8.3 Hz, 2H: H-2, H-6), 4.29 (d, *J* = 7.8 Hz, 1H: H-10), 4.04-3.99 (m, 1H: H-8$_A$), 3.85 (d, *J* = 10.7 Hz, 1H: H-15$_A$), 3.68 (td, *J* = 13.2, 5.8 Hz, 3H: H-7$_A$, H-8$_B$, H-15$_B$), 3.36 (t, *J* = 8.7 Hz, 1H: H-11), 3.31-3.24 (m, 3H: H-7$_A$, H-12, H-14), 3.18 (t, *J* = 8.4 Hz, 1H: H-13). **¹³C-NMR (101 MHz; D₂O, 25 °C)**: δ154.3, 128.45, 128.26, 113.7, 101.8, 75.59, 75.41, 72.6, 69.6, 69.1, 60.3, 38.0, 33.9. **EI-MS, *m/z*** 323.2 [M+Na]⁺.
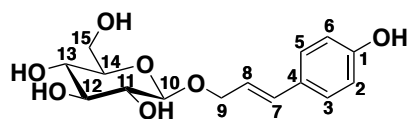
Compound 4.4a, *rosin*: According to the General Procedure, compound **4.4a** (140 mg, 0.47 mmol, isolated yield: 70 %, yellow solid, 8 h) was obtained from 100 mg of cinnamyl alcohol and 684 mg of rutin. **¹H-NMR (400 MHz; MeOD, 25 °C)**: δ 7.44-7.42 (m, 2H: H-2, H-6), 7.31 (dd, *J* = 8.2, 6.7 Hz, 2H: H-3, H-5), 7.23 (t, *J* = 7.3 Hz, 1H: 1), 6.70 (d, *J* = 16.0 Hz, 1H: H-7), 6.39 (ddd, *J* = 16.0, 6.4, 5.8 Hz, 1H: H-8), 4.55 (ddd, *J* = 12.8, 5.7, 1.5 Hz, 1H: H-9$_A$), 4.39 (d, *J* = 7.8 Hz, 1H: H-10), 4.35 (ddd, *J* = 12.8, 6.5, 1.4 Hz, 1H: H-9$_B$), 3.91 (dd, *J* = 11.9, 2.0 Hz, 1H: H-15$_A$), 3.71 (dd, *J* = 11.9, 5.3 Hz, 1H: H-15$_B$), 3.42-3.24 (m, 4H:H-11, H-12, H-13, H-14). **¹³C-NMR (101 MHz; MeOD, 25 °C)**: δ 136.8, 132.4, 128.2, 127.3, 126.1, 125.3, 102.0, 76.72, 76.59, 73.7, 70.3, 69.4, 61.4. **EI-MS, *m/z*** 319.2 [M+Na]⁺.

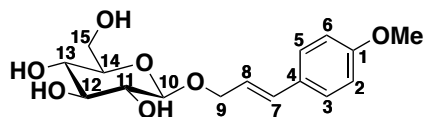**Compound 4.5a, *triandrin*:** According to the General Procedure, compound **4.5a** (141 mg, 0.45 mmol, isolated yield: 68 %, yellow solid, 8 h) was obtained from 100 mg of 4-hydroxycinnamyl alcohol (**5**) and 603 mg of rutin (**9**). **¹H-NMR (400 MHz; D₂O, 25 °C)**: δ 7.32 (d, *J* = 8.0 Hz, 2H: H-3, H-5), 6.83 (d, *J* = 7.8 Hz, 2H: H-2, H-6), 6.58 (d, *J* = 15.9 Hz, 1H: H-7), 6.16 (dt, *J* = 15.0, 7.1 Hz, 1H: H-7), 4.47-4.40 (m, 2H: H-9$_A$, H-10), 4.31-4.27 (m, 1H: H-9$_B$), 3.86 (d, *J* = 12.6 Hz, 1H: H-15$_A$), 3.69-3.66 (m, 1H: H-15$_B$), 3.44-3.24 (m, 4H: H-11, H-12, H-13, H-14). **¹³C-NMR (101 MHz; D₂O, 25 °C)**: δ 215.4, 155.6, 133.6,

128.9, 128.2, 122.3, 115.7, 101.1, 75.92, 75.90, 73.2, 70.5, 69.7, 60.8, 38.8, 30.3. **EI-MS, *m/z*** 335.1 [M+Na]$^+$.

Compound 4.6a, *vimalin*: According to the General Procedure, compound **4.6a** (115 mg, 0.35 mmol, isolated yield: 58 %, yellow solid, 8 h) was obtained from 100 mg of 4-methoxycinnamyl alcohol and 558 mg of rutin. **^{1}H-NMR (500 MHz; MeOD, 25 °C)**: δ 7.35 (d, *J* = 8.7 Hz, 2H: H-3, H-5), 6.87 (d, *J* = 8.8 Hz, 2H: H-2, H-6), 6.61 (d, *J* = 16.0 Hz, 1H: H-7), 6.22 (dt, *J* = 15.9, 6.3 Hz, 1H: : H-8), 4.51 (ddd, *J* = 12.5, 5.8, 1.3 Hz, 1H: H-9$_A$), 4.38 (d, *J* = 7.8 Hz, 1H: H-10), 4.30 (ddd, *J* = 12.4, 6.8, 1.1 Hz, 1H: H-9$_B$), 3.90 (dd, *J* = 11.9, 2.2 Hz, 1H: H-15$_A$), 3.78 (s, 3H: OCH$_3$), 3.71 (dd, *J* = 11.9, 5.5 Hz, 1H: H-15$_B$), 3.41-3.24 (m, 4H: H-11, H-12, H-13, H-14). **^{13}C-NMR (101 MHz; MeOD, 25 °C)**: δ 154.1, 127.0, 124.1, 122.0, 117.5, 108.3, 96.5, 71.36, 71.20, 68.4, 64.9, 64.3, 56.1, 49.0, 33.7. **EI-MS, *m/z*** 349.2 [M+Na]$^+$.

Compound 4.7a, *coniferin*: According to the General Procedure, compound **4.7a** (508 mg, isolated yield: 75 %, yellow solid, 8 h) was obtained from 250 mg of coniferyl alcohol and 1.30 g of rutin. The NMR and mass spectra were in accordance with those described above.

4.5.3 HPLC analysis: methods

Biotransformations were run following protocol **4.5.1a**. Substrates were incubated for 30 hours at 35 °C and 750 rpm. Rutin was added at 3h, 7h until a total amount of 1.5 equiv. were reached. When all the rutin added was consumed, the mixtures were left reacting to investigate the hydrolysis of the obtained disaccharide in the absence of the glycosyl donor.

Sample preparation. 50 μL of the reaction mixtures were diluted with three volumes of distilled water, incubated at 100 °C and then centrifuged, recovering only the supernatant. The obtained clear solutions were used for the HPLC analysis.

Analysis conditions.

- *Column* = Kinetex C18 HPLC 5μm EVO C18 100Å, 150x4.6 mm

- Flow = 0.8 mL/min; *- Loop* = 20 μL; *- Detection Lambda* =: 270 nm; *- Injection* = 10 μL of the sample prepared flowing the listed procedure.

- Gradient A = CH_3CN = A; H_2O (0.1 ppm TFA, pH 3) = B

  0 min: 20 % of A; 1-10 min: 30 % of A; 11-14 min: 90 % of A; 15-17 min: 20 % of A;

- Gradient B = CH_3CN = A; H_2O (0.1 ppm TFA, pH 3) = B

  0 min: 10 % of A; 1-10 min: 20 % of A; 11-14 min: 90 % of A; 15-17 min: 10 % of A

5. Amine transferases: from hot spring metagenomes to chiral amines

The discovery of novel, convenient and efficient methods for the selective preparation of stereogenic carbon-nitrogen bonds is a prosperous research topic in the field of synthetic organic chemistry. Specifically, organocatalytic, organometallic and biocatalytic entries to enantiomerically enriched chiral amines, valuable building blocks for the preparation of pharmaceutical agents that span a range of therapeutic areas (including antihypertensive, antibiotics, antidepressants, antihistamines, and antidiabetics), have been and are being proposed nowadays.

In the last two decades, biocatalysis has emerged as an interesting alternative to conventional chemical methods in generating also chiral amine compounds. Specifically, amine transferases (ATAs) represent an attractive option for chiral amine synthesis and have been demonstrated to be suitable tools for application on industrial scale.

However, the number of useful enzymes that are commercially and industrially available is still pretty limited. This is especially true for thermostable ATAs which are needed for industrial processes run under harsh (*i.e.* conditions such as high temperature and/or in the presence of organic solvents).

In the work described in **Paper VI**, in the quest of a selective and robust biocatalyst to perform the asymmetric synthesis of chiral amines, a metagenomics-based approach was exploited to find novel thermostable ATAs. The identified new ATAs were then fully characterized in terms of stability (*i.e.* high temperatures and organic co-solvents) and screened for their ability to selectively produce chiral amines.

5.1   Biocatalysis and chiral amines: amine transferases

Transaminases (TAs, EC 2.6.1.x) are ubiquitous enzymes in Nature where they play a key role in nitrogen metabolism.[52,53] These pyridoxal-5'-phosphate (PLP)-dependent biocatalysts are capable of transferring an amino group between an amino donor and a carbonyl acceptor, creating a novel stereogenic center in the transamination reaction, when the carbonyl is prochiral group (**Figure 5.1**).
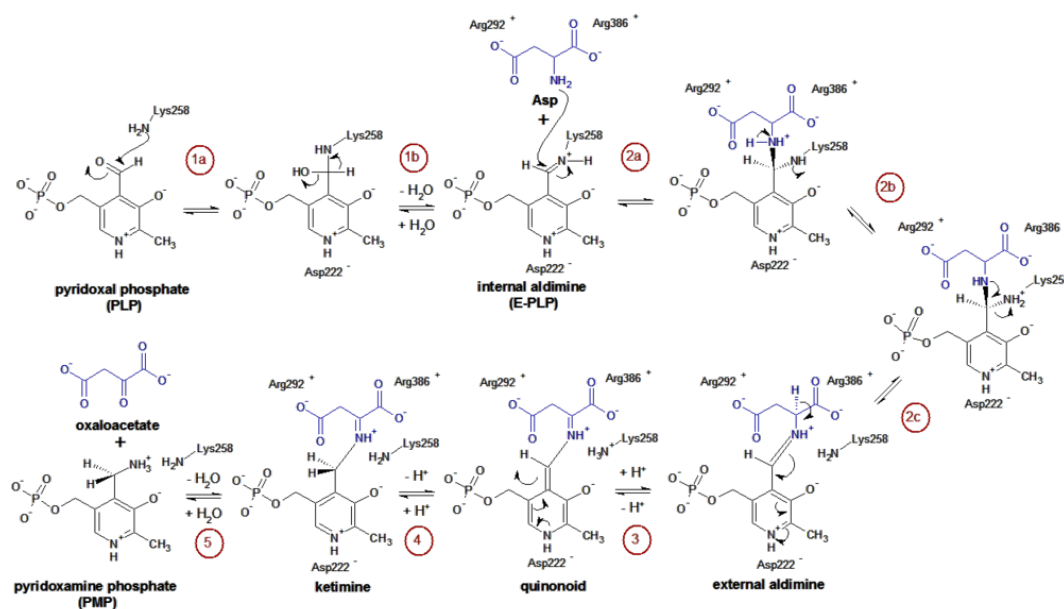

Figure 5.1: Example of a aminotransferase PLP-dependent mechanism.
In this case, an aspartate transaminase converting aspartate to oxaloacetate.

Generally, TAs are classified into α-TAs, which represent the majority of TAs and are able to interconvert only α-amino and α-keto acids, and ω-TAs, which can have amino acids with a distal carboxylic acid group as substrates/products.[53, 54]

Among ω-TAs, the class of amine transaminases (ATAs) is of particular interest for synthetic applications, as they also convert amines lacking a carboxylic acid group in addition to α-amino acids and ω-amino acids. The action of a proper ATA can in fact promote the selective (both regio- and enantio-) preparation of chiral amines as synthons or late-structural modification of drugs and chemical intermediates. Moreover, these promising selectivity

47

features do not depend on the use of metal catalysts (*i.e.* Ru, Pd and/or Ni) at high pressure, as often reported in chiral amine chemical syntheses.[55]

Both (*S*)- and (*R*)-selective ATAs could be found in Nature and exploited both for the kinetic resolution of racemic amines and the synthesis of chiral amines starting from the corresponding ketones,[52, 56, 57] thus allowing a fully-biocatalytic entry to both the enantiomers of a selected chiral amine (**Figure 5.2**) and confirming the synthetic potential of amine transferases.
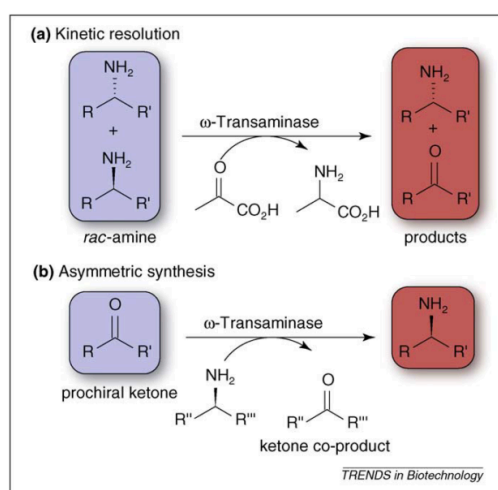

Figure 5.2: Complementary approaches for the preparation of enantio-enriched primary amines.
(**a**) Kinetic resolution starting with racemic (rac) amines is (limited by 50% maximum yield);
(**b**) Asymmetric synthesis of prochiral ketones.

For example, both enantiomers of mexiletine (**Figure 5.3a**) [1-(2,6-dimethylphenoxy)-2-propanamine], a chiral antiarrhythmic agent, were prepared by deracemization of commercially available racemic amine using two different enantioselective ATAs.[58]

In another interesting application of ATA-chemistry the stereoselective synthesis of (*R*)-4-phenylbutan-2-amine, a precursor of the antihypertensive dilevalol (**Figure 5.3c**), and of (*R*)-1-(4-methoxyphenyl)ethylamine, an important building block for the biologically active compound formoterol (**Figure 5.3d**), was successfully achieved.[59, 60]

However, many challenges inherent to transaminase stability under industrial process conditions still remain to be tackled before developing large-scale processes, the most important regarding the stability of ATAs in the presence of organic solvents.
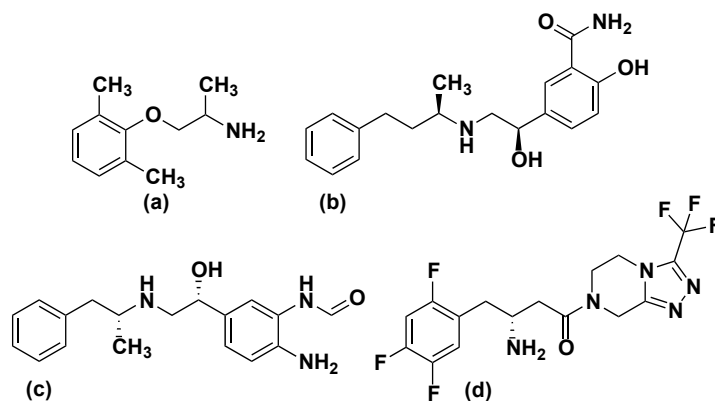

Figure 5.3: Amine containing bioactive compounds.
(**a**) mexiletine; (**b**) dilevalol; (**c**) formoterol; (**d**) sitagliptin.

In fact, even if the promising ATAs' performances in the stereoselective formation of C-N bonds is attested by the wide number of examples found in literature[52,61] (among them it surely deserves to be cited the outstanding case of sitagliptin reported by companies Merck® and Codexis® **Figure 5.3d**), transamination processes on preparative scale are often impaired by the need of organic co-solvents, that might be 'toxic' to the biocatalysts.[62] Moreover, increased reactions temperatures are often required (for example for the stripping of volatile co-products, i.e., acetone, to shift the equilibrium of the transamination reaction toward product formation).[63]

In an attempt to tackle this drawback, hot spring metagenomics was exploited to develop novel thermostable ATAs able to catalyze the stereoselective production of chiral amines and possessing an enhanced structural tolerance and stability toward the presence of organic co-solvents and working at higher temperature.

5.2   From hot spring metagenomics to novel biocatalysts

In general, biocatalysts produced by thermophiles, organisms that thrives at relatively high temperatures between 41 and 122 °C, show attractive inherent properties such as high stability in the presence of organic solvent, under operational conditions and during long-term storage.[64, 65] So that, the use of thermophiles genomes as source for the search and development of novel thermostable transaminases has lately revealed to be a promising tool.[66, 67] Recently, a (*S*)-selective ATA with a broad substrate scope showing a remarkable thermostability has been identified from *Thermomicrobium roseum* and was successfully exploited in asymmetric syntheses and kinetic resolutions at high temperatures to produce enantiomerically enriched amines.[68]

As an alternative to selected genomes mining, metagenomics, *i.e.*, the study of the genetic material (*metagenome*) recovered directly from environmental samples[69, 70] was selected to find new thermostable ATAs. The potential of this innovative approach for the identification of novel active and stable biocatalysts has been recently demonstrated with enzymes of different classes.[71, 72, 73]

To this purpose, samples were collected from three different hot springs in Iceland, China and Italy at very high temperature (76-90 °C), ideal environments for (hyper)thermophilic microorganisms. Their metagenome was extracted and sequenced to generate a database of DNA sequences potentially coding for different biocatalysts, as described by Menzel *et al.*[74] This database was then subjected to bioinformatic search to find *in silico* sequences coding for the target biocatalysts ATAs: the query sequences were aligned with database sequences using the program LAST (http://last.cbrc.jp/) with default settings.[75]

Three sequences (B3-TA, Is3-TA, and It6-TA) showing similarity with known (*S*)-selective ATAs were found in metagenomes collected in Iceland (B3-TA, hot spring at 85 °C, pH 7.0; Is3, TA-hot spring at 90 °C, pH 3.5) and in Italy (It6-TA, hot spring at 76 °C, pH 3.5), respectively, while only partial sequences were found in a sample collected in China (hot spring at 55 °C, pH 7.0). These proteins can be classified as class III aminotransferases (IPR005814), which is the class that comprises most of the known (*S*)-selective ATAs; no

sequences similar to (R)-selective ATAs were found in the investigated metagenomes. The three identified ATAs sequences were then cloned for recombinant expression in *E. coli,* (up to 180 mg of pure protein from 1 L of culture).[76] The three novel thermostable potential biocatalysts were then to be tested for their ability of producing chiral amines from prochiral ketones and hypothesized enhanced stability. The whole discovery and expression process is summarized in (**Figure 5.4**).
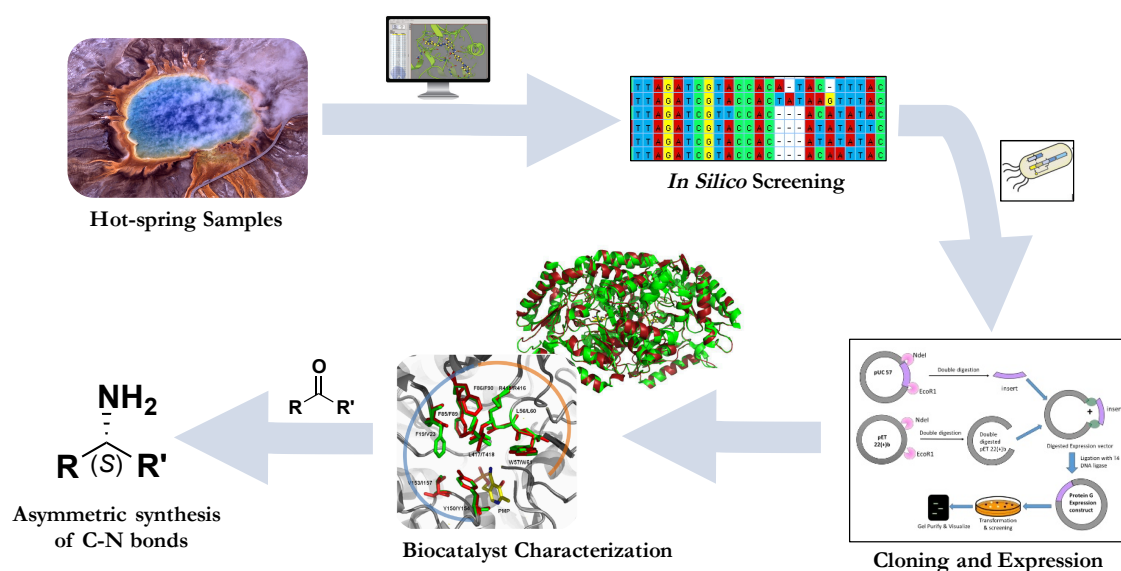

Figure 5.4 From hot-spring metagenome to chiral amines.

5.3   Functional properties of the novel ATAs

Scheme 5.1: Model reaction.

At first, the functional characterization of the ATA homologs was started by evaluating the effect of different reaction conditions in the transamination reaction between the benchmark and common substrates (*S*)-MBA (methylbenzyl amine) and pyruvate (**Scheme 5.1**).
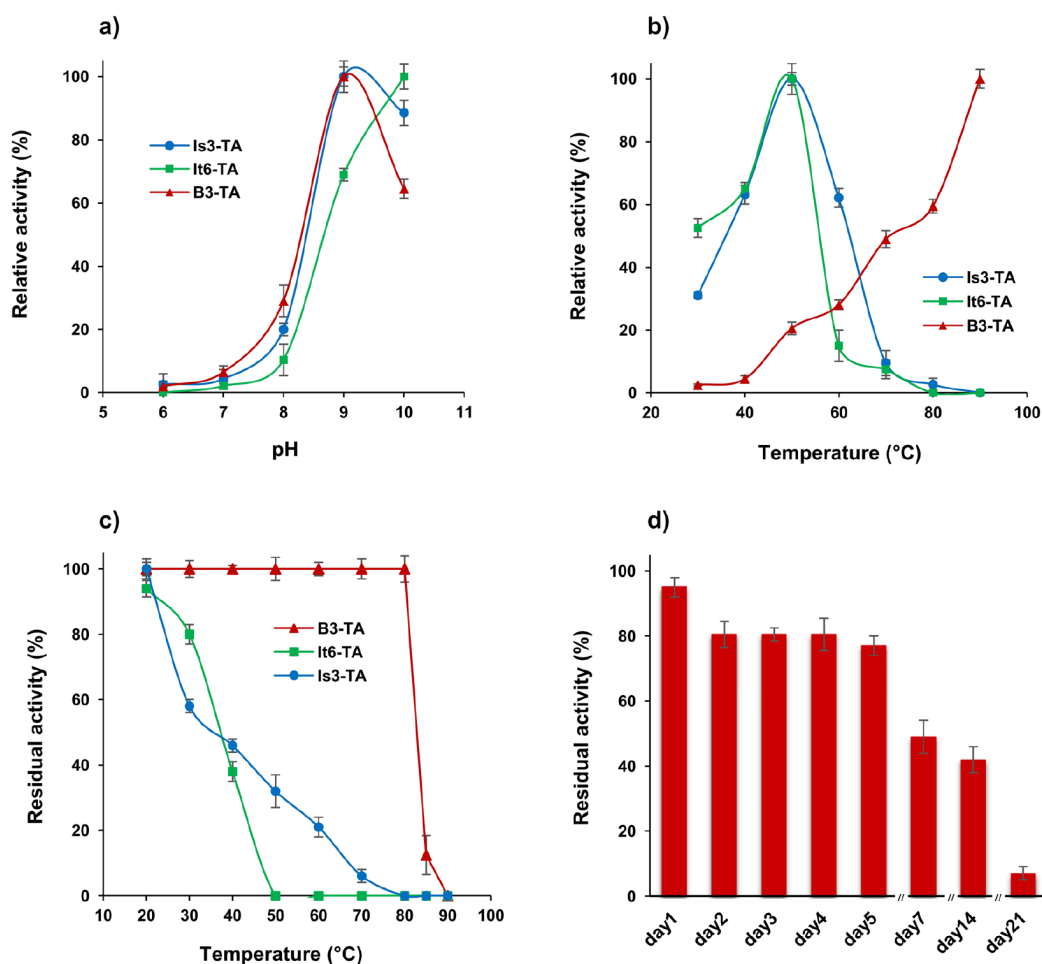

Figure 5.5: Influence of pH (**a**) and temperature (**b**) on ATA activity, influence of temperature (**c**) on ATA stability, and long-term stability of B3-TA at 80 °C (**d**).

Specifically, their stability toward temperature and co-solvents was determined, as all the three enzymes displayed high levels of activity under alkalophilic conditions, this result being in agreement with the average pH optimum of 9.0 the typical of ATAs (**Figure 5.5a**).[77]

The hypothesized thermophilic character of three new biocatalysts was confirmed as the three ATAs showed optimal activity at high temperatures: in particular, both It6-TA and Is3-TA presented optimal activity at temperatures around 50 °C and retained >10% relative activity at 60 and 70 °C, respectively (**Figure 5.5b**). Even more interesting, the activity of B3-TA increased constantly with temperature up to 90 °C, showing a typical hyperthermophilic behavior. Moreover, thermal stability studies performed by incubating the three enzymes at different temperatures between 20 and 90 °C for 3 h and estimating their residual activity by spectrophotometric analysis, demonstrated that Is3-TA and It6-TA maintained about 40% of the starting activity at 40 °C, while B3-TA remarkably retained 100% activity after 3 h thermal treatments between 20 and 80 °C (**Figure 5.5c**). Furthermore, the long-term thermal stability of B3-TA resulted outstanding, as after five days of incubation at 80 °C the biocatalyst retained the 85 % of its initial activity. After two weeks at 80 °C, the enzyme was still alive showing 40 % residual (**Figure 5.5d**).
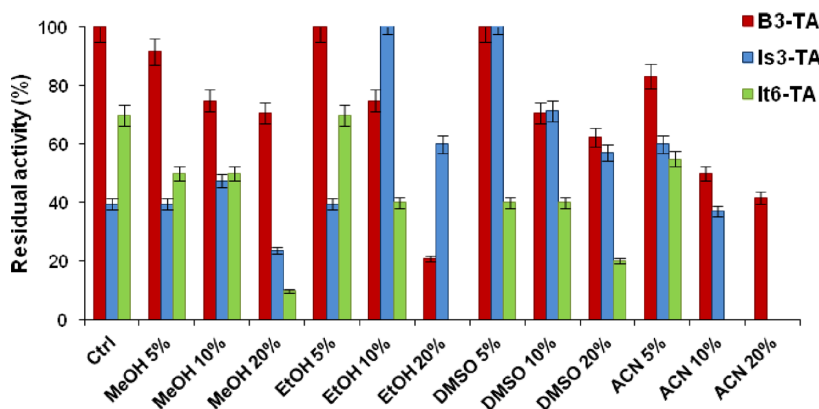

Figure 5.6: Influence of organic co-solvents on ATA stability.
Residual activity was estimated after 5 h of incubation at room temperature.

The stability of the three enzymes was tested in the presence of 5–20% (v/v) organic co-solvents, *i.e.*, MeOH, EtOH, DMSO, and CH_3CN, by measuring their residual activities

at 25 °C after a 5 h incubation (**Figure 5.6**). The residual activity of B3-TA under any condition tested (with the exception of 20% (v/v) EtOH) was always above 40%, thus indicating this enzyme, the most thermophilic, as the most tolerant to organic co-solvents among the three new ATAs.

Considering the superior performances shown by B3-TA, its stability in buffer/organic solvent biphasic systems was investigated as well. The enzymatic aqueous solution was incubated in the presence of either tert-butyl methyl ether, ethyl acetate, toluene, or petroleum ether (1:1 v/v) under vigorous shaking, and the residual activity was evaluated after 5 and 24 h. As shown in **Figure 5.7**, B3-TA was quite tolerant to toluene and petroleum ether, retaining more than 50% of its activity in the presence of these two organic solvents after 24 h of incubation. It proved to be sensitive to tert-butyl methyl ether and ethyl acetate, retaining only 25% activity in the presence of these two organic solvents after 5 h of incubation.
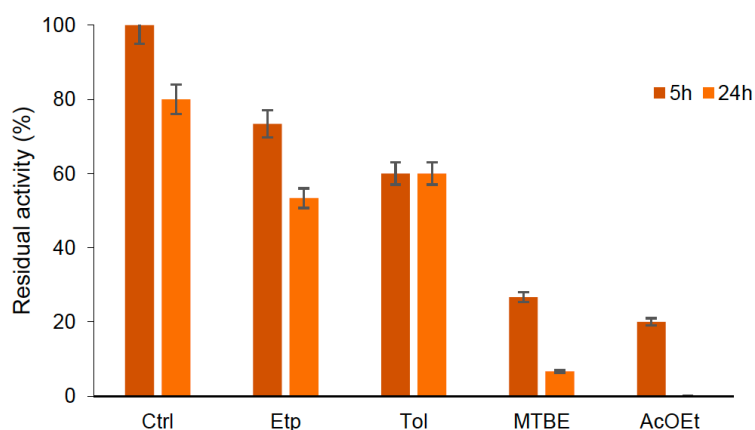

Figure 5.7: Influence of organic co-solvents on B3-TA stability. Residual activity was estimated after 5 h of incubation at room temperature. Ctrl = control; Etp = petroleum ether; Tol = toluene; MTBE = methyl *tert*-butyl ether; AcOEt = ethyl acetate.

5.4 Asymmetric synthesis of chiral amines: ATAs' substrate scope

Once the stability of the three novel biocatalysts had been investigated, the B3-TA being the most promising one, their synthetic exploitation to produce enantiomerically enriched (S)-chiral amines was explored by studying their substrate scope. As the transamination reaction catalyzed by ATAs requires a 'sacrificial' amine donor and a suitable acceptor, the investigation was focused on both the partner. Moreover, obtained results were compared to those achieved using the well-known ATA from *Vibrio fluvialis* (Vf-TA)[78, 52] obtained by recombinant expression in *E. coli* from its synthetic gene, to better evaluate the practical synthetic utility of the novel ATAs.

To this purpose, several keto acids, ketones, and aldehydes were considered as potential acceptors (amino donor: (*S*)-methyl benzyl amine, MBA), as well as a series of aliphatic and aromatic amines and amino acids were investigated as potential donors (amino acceptor: pyruvate). Reaction conversions were estimated after 24 h and analyzed by HPLC or GC/MS and performed in triplicate. Standard deviation was below 5%, and no significant degradation of substrates/products or formation of by-products was observed.
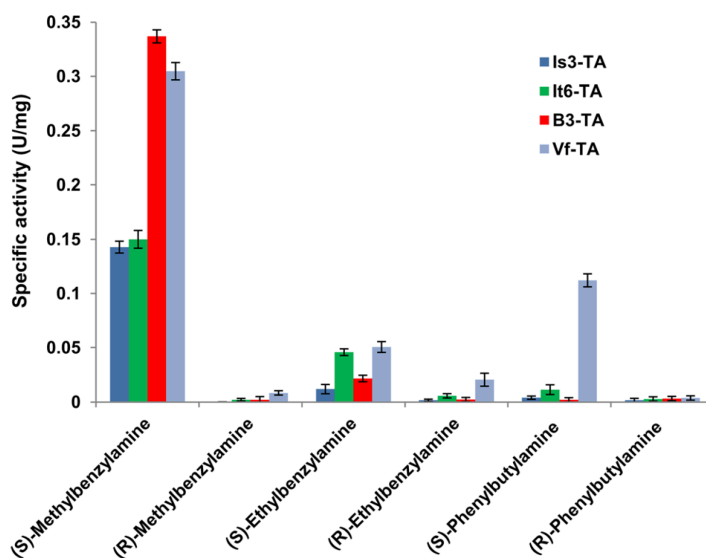

Figure 5.8: Enantioselectivity of the novel ATAs. Specific activities (U/mg) of ATAs and Vf-TA toward different (*S*) and (*R*) aromatic amines were determined spectrophotometrically as described by Nobili *et al.*[79]
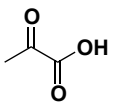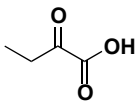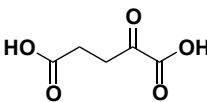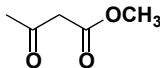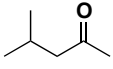
As shown in **Figure 5.8** , the (*S*)-selectivity of the novel ATAs inferred by sequence analysis was confirmed by determining spectrophotometrically their specific activity using as substrates either (*R*) or (*S*) aromatic amines, bearing a methyl, ethyl, or propyl side chain adjacent to the amine function. As previously stated, Vf-TA was included in this study for comparison. The obtained data indicate a very strict (*S*)-selectivity for all the novel ATAs that showed very low or negligible activity toward the tested (*R*)-amines.

As reported in **Table 5.1**, the novel ATAs and Vf-TA displayed a quite similar behavior in the transamination reactions using different keto acids and aliphatic ketones as amino acceptors. Specifically, concerning the use of keto acids as acceptors, it was possible to appreciate that an increase in the acceptor side chain length from pyruvate to 2-oxobutyrate resulted in higher conversions, while the presence of a second carboxylic group in the acceptor, such as α-ketoglutarate, significantly decreased the substrate conversions. Furthermore, conversions were significantly lower also in case of methyl acetoacetate (the carboxylic group of the keto acid is protected as methyl ester) or aliphatic ketones as amine acceptors. On the other hand, in some cases, the use of aldehydes in place of ketones resulted in a significant increase of conversions. In particular, quantitative conversions were obtained with Is3-TA, B3-TA, and Vf-TA using glyoxylate, while acetaldehyde demonstrated to be a very good amino acceptor for B3-TA, as well as propionaldehyde for Is3-TA.

As far as the amino donor specificity is concerned (**Table 5.2**), the three novel ATAs showed a good activity toward phenyl-substituted secondary amines bearing either a methyl or an ethyl group, while significant decreases in conversions were observed when (*S*)-α-phenylbutylamine was the substrate. When testing the primary amine 2-phenylethylamine, the best performances were observed with B3-TA, while 1-aminoindan was well accepted by all the tested enzymes. Among nonaromatic amines, isopropylamine was the best donor for all the novel enzymes, lower conversions being observed when using aliphatic primary mono- and diamines as donors. Interestingly, all the novel ATAs converted β-alanine, which, in agreement with literature data,[57] was instead not accepted by Vf-TA. However, no

detectable activities were measured in the presence of more sterically hindered β-amino acids, such as (DL)-β-phenylalanine and (DL)-β-homoleucine.

Table 5.1: Amino acceptors screening.

Conversion (%)				
	Is3-TA	**It6-TA**	**B3-TA**	**Vf-TA**
Amino Acceptor				
Pyruvate	48	45	51	50
2-Oxobutyrate	>99	>99	>99	>99
α-Ketoglutarate	8	1	4	8
Methyl acetoacetate	16	6	5	15
Acetone	7	2	8	5
2-Butanone	3	2	5	11
Methyl isobutyl ketone	1	1	5	10
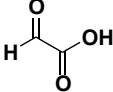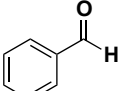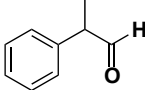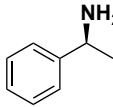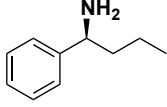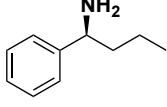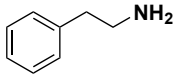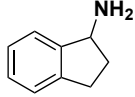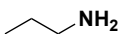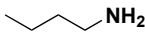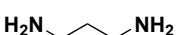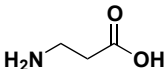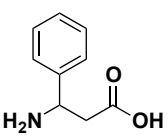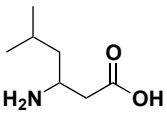
2-Oxoacetic acid	>99	62	>99	>99
Acetaldehyde	6	6	68	18
Propionaldehyde	74	10	33	34
Benzaldehyde	3	10	10	15
2-Phenylpropionaldehyde	16	3	16	19

Table 5.2: Amino donors screening.
a) n.d. below detection limit

Conversion (%)				
	Is3-TA	**It6-TA**	**B3-TA**	**Vf-TA**
Amino Donor				
(*S*)-α-Methylphenylamine	50	41	43	>99
(*S*)-α-Ethylphenylamine	63	46	23	>99
(*S*)-α-Phenylbutylamine	2	3	1	>99
2-Phenylethylamine	8	18	30	15
(±)-1-Aminoindan	97	89	43	99
Isopropylamine	12	27	13	28

Propylamine	6.5	3.7	n.d.[a]	28
Butylamine	1.4	3.5	1	1.2
1,3-Diaminopropane	0.7	3	2	n.d.
β-Alanine	67	57	29	n.d.
(±)-β-Phenylalanine	n.d.	n.d.	n.d.	n.d.
(±)-β-Homoleucine	n.d.	n.d.	n.d.	n.d.

5.5   Conclusions

This work further demonstrated the potential of metagenomics in the search of relatively rare enzymatic activities, such as thermostable ATAs from extreme environments. The three novel ATAs, identified as a subfamily of mostly uncharacterized B3-TA-like transaminases and all from thermophilic microorganisms, showed the desired thermophilic character and, in the case of B3-TA, an outstanding stability toward organic co-solvents, both in mono and biphasic systems. Moreover, structural stability data obtained by CD analysis (comparison of the data collected at 20 and 80 °C to get some information about any conformational changes) reveled an apparent melting temperatures of 57.32 ± 0.55 and 79.23 ± 0.31 °C for It6-TA and Is3-TA, respectively and remarkably, of 88.15 ± 1.17 °C for B3-TA.

The catalytic performances of these new ATAs were investigated in the asymmetric synthesis of commonly reported chiral amines, exploring the scope of amino donors/acceptors and demonstrating their strictly (*S*)-selectivity. At the same time, given their origin and stability features, it can be foreseen that members of this subfamily could possess useful applicative features, such as high stability under harsh reaction conditions and different substrate specificities.

Moreover, this biochemical study on the discovery of new thermostable enzymes to assess stability issues in the biocatalytic preparation of enantiomerically enriched amines, can be regarded as a way for the rational modification of an existing (bio)catalyst aimed at achieving enhanced catalytic performances. As for organo- and/or metallorganics a lead catalyst can be structurally modified to fulfill desired new features, the genetic information collected from the hot-spring metagenomes were filtered and refined on the base of well-known families of ATAs sequences found literature. In fact, at variance to what can be and is usually done with chemical catalysis, biocatalysis gathers strength from the exploitation of what Nature offers in the struggle for life: forms of stereoselective organic synthesis against unselective processes.

5.6 Experimental

Acceptor spectrum of ATA homologs was determined at 30 °C in 0.5 mL reaction mixture containing 20 mM KP buffer, pH 9.0, 10 mM acceptor, 10 mM (*S*)-MBA, 1 mM PLP, and 0.5 mg of purified enzyme. Conversion of (S)-MBA (after acetylation) into acetophenone was determined after 24 h by GC-MS analysis.

Donor spectrum of ATA homologs was determined at 30 ° C in 0.5 mL reaction mixture containing 20 mM KP buffer, pH 9.0, 10 mM donor, 10 mM pyruvate, 1 mM PLP, and 0.5 mg of purified enzyme. Conversions were determined after 24 h by GC-MS analysis or, alternatively, by estimating the formation of L-alanine (after OPA derivatization) through HPLC analysis.

GC/MS analysis Samples of amine derivatives were acetylated before injection as follows: transamination reactions (0.5 mL) catalyzed by TAs were recovered after 24 h, then reaction pH was adjusted to 11.0 by adding 6 M NaOH (50 μL) and products were extracted with ethyl acetate (350 μL). To 100 μL of organic phase dried over anhydrous Na_2SO_4, pyridine and acetic anhydride (15 μL each) were subsequently added and the mixture was kept overnight at room temperature before analysis. The following temperature program was employed: 60 °C (1 min)/6 °C min−1/150 °C (1 min)/12 °C min^{-1}/210 °C (5 min).

HPLC analyses were conducted using a Kinetex 5-μm EVO C18 100-Å 150 Å~ 4.6-mm column (Phenomenex, Torrance, CA). L-Alanine derivatization was achieved by diluting the reaction samples (50 μL) in 1 mM HCl and then adding 50 μL of phthaldialdehyde (OPA) reagent (Sigma-Aldrich). The mobile phase consisted of MeOH/THF/50 mM phosphoric acid (20:20:960), pH adjusted to 7.5 with NaOH (eluent A) and MeOH/H2O (65:35) (eluent B). L-alanine-OPA derivative was eluted at a flow rate of 0.5 mL min^{-1} with the following gradient: t = 0 min, 80% A; t = 17min, 70%A; t = 32min, 20%A; t = 37min, 20%A; t = 47 min, 80% A. Peaks were detected at 340 nm and calibration curves were prepared using standard solutions of L-alanine-OPA derivative.

6.   Unspecific peroxigenases: the asymmetric sulfoxidation of arylalkyl sulfides

Unspecific peroxygenases (UPOs, EC 1.11.2.1) represent an emerging class of biocatalysts with a wide range of potential applications in different oxyfunctionalization reactions.[80, 81, 82, 83] They are extracellular heme-thiolate enzymes (**Figure 6.1**), a class of hemoproteins in which a thiolate group, typically from a cysteine residue, is the axial ligand of heme iron.
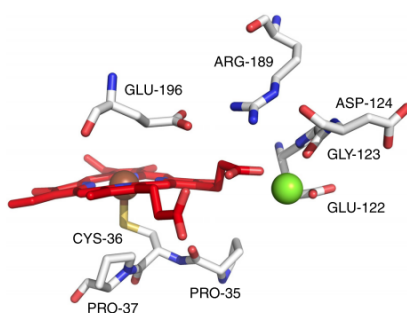
Figure 6.1: Heme-thiolate structure with its typical cysteine axial ligand. © Elsevier.

UPOs are usually produced by several fungi (**Figure 6.2**), and they show no significant sequence homology to cytochrome P450s and are only distantly related to CPO (Chloride peroxidase,~ 30% sequence similarity).
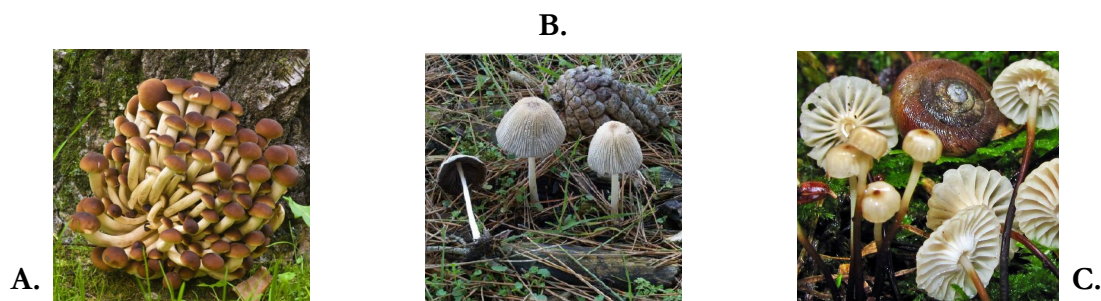
Figure 6.2: UPOs have been isolated form: **A.** *Agrocybe aegerita* (edible, pioppino), *Aae*UPO; **B.** *Coprinellus radians*, *Cra*UPO and **C.** from *Marasmius rotula*, *Mro*UPO.

UPOs systematic classification appears to be tricky: they use hydrogen peroxide as electron-acceptor during their redox processes, like *peroxi*dase do, but they work *via* a catalytic cycle resembling the 'peroxide shunt' (yellow section, **Figure 6.3**) pathway of P450s-mediated reactions. Thanks to their 'peroxide shunt' mechanism, UPOs show a peroxide-dependent monooxygenase activity resulting *e.g.*, in the hydroxylation of different alkanes and aromatic compounds, in alkene epoxidation and *O-* and *N-*dealkylation reactions.
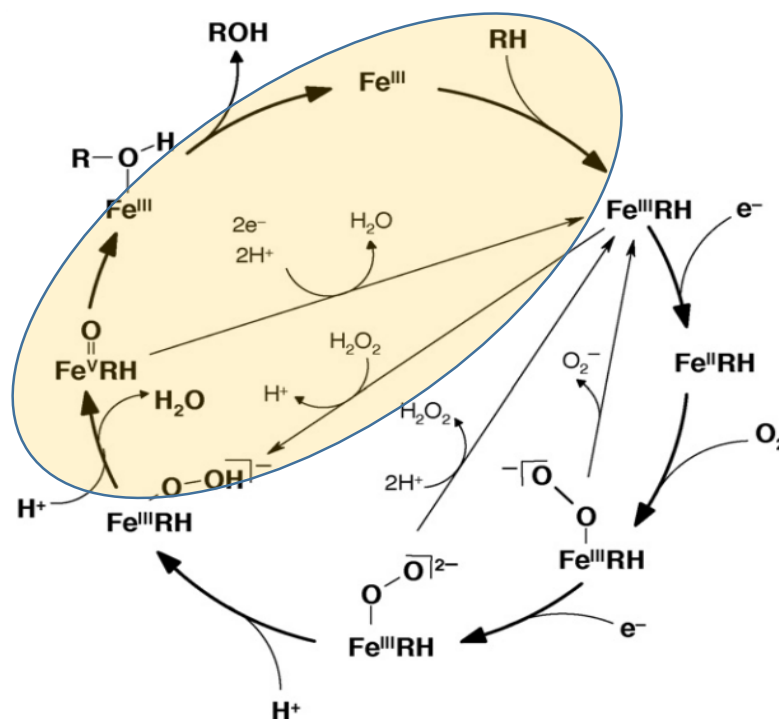
Figure 6.3: P450-peroxyde shunt mechanism. © Elsevier

The best characterized UPO (*Aae*UPO, **Figure 6.4**) has been identified in 2004 from the edible mushroom *Agrocybe aegerita*.[84] Its structural and functional features have been largely investigated in the last years.[85, 86, 87, 88, 89] Moreover, the practical application of *Aae*UPO in useful synthetic biotransformations has been recently implemented by developing improved systems for enzyme production/optimization[90, 91] and for the efficient set-up of preparative-scale reactions.[92, 93, 94]
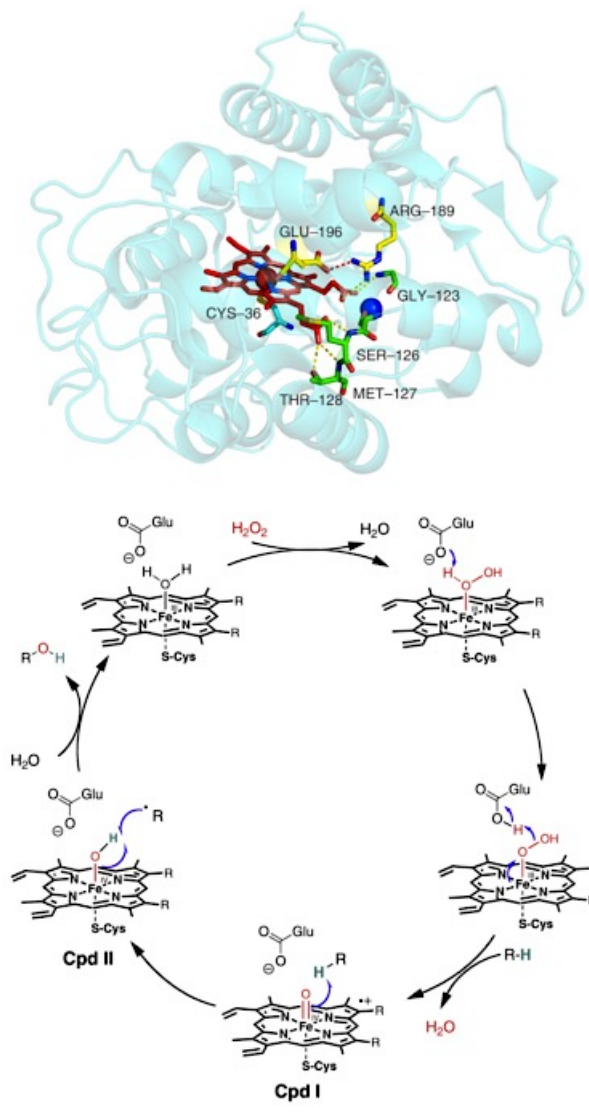
Figure 6.4: *Aae*UPO structure and proposed catalytic cycle. © Elsevier

6.1   Chiral sulfoxides

Chiral sulfoxides are valuable compounds that find several applications as synthons in the preparation of biologically active molecules as well as chiral auxiliaries in asymmetric synthesis (**Figure 6.5**).[95, 96]
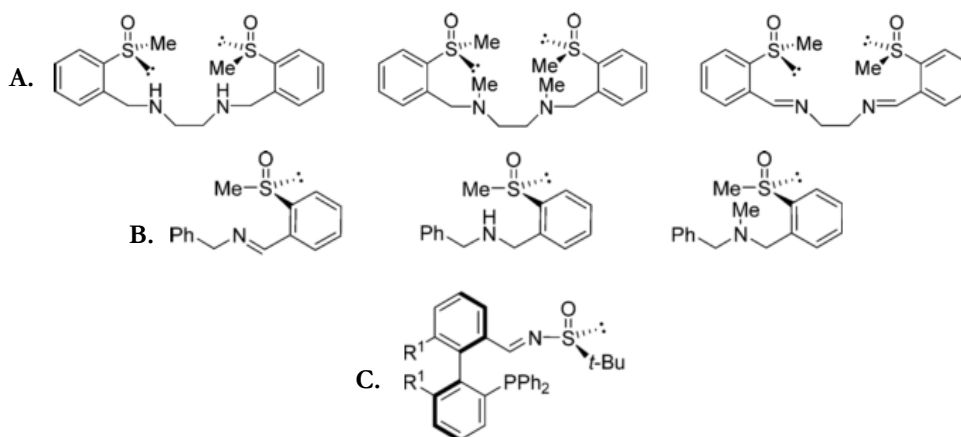
Figure 6.5: Sulfur-containing chiral ligands/catalyst for asymmetric synthesis **A.** Tetradental bis-sulfoxides ligands; **B.** chiral imino- and aminosulfoxides and **C.** biphenyl sulfinimines containing diphenylphospphine moieties.

Among the different methods aimed at the efficiently prepare optically enriched sulfoxides, enzyme-catalyzed enantioselective oxidation of prochiral sulfides has been widely investigated in the last decades.[97] In particular, the best results, in terms of both enantioselectivity and conversions, have been obtained with the chloroperoxidase (CPO) from *Caldariomyces fumago*,[98, 99, 100] and different Baeyer-Villiger monooxygenases (BVMOs), in the presence of either H_2O_2 or O_2 as oxidant, respectively. [101,102, 103, 104, 105]

In recent reviews about the current state-of-the-art on the applications of peroxygenases, sulfoxidations are commonly listed among the wide number of possible reactions catalyzed by UPOs.[80, 81, 82, 83] However, to the best of our knowledge, only a few preliminary data were available so far about the exploitation of UPOs, including *Aae*UPO, in the (enantioselective) oxyfunctionalization of sulfides to sulfoxides.
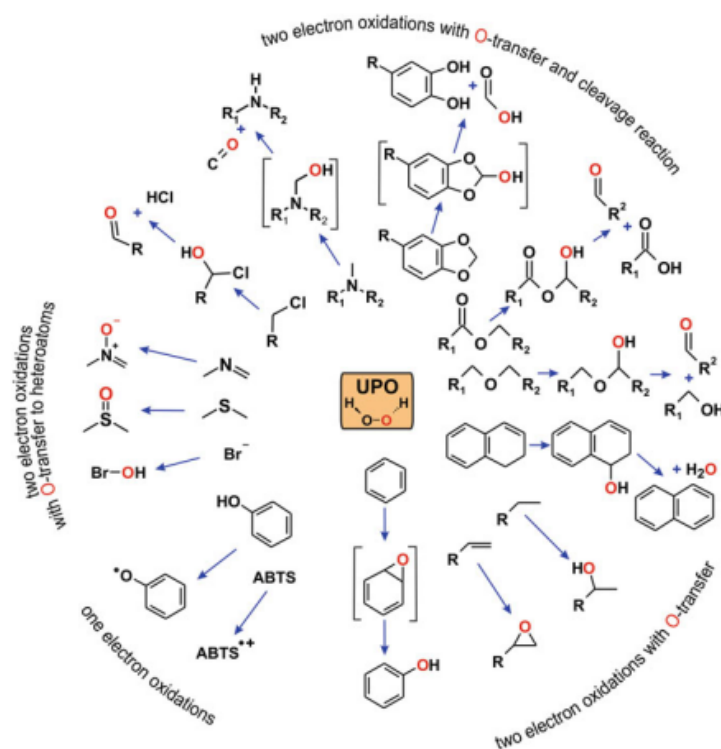
Figure 6.6: Synthetic potential of *Aae*UPO. © Elsevier

Specifically, the enantioselective oxidation of thioanisole **6.1** to the corresponding (*R*)-sulfoxide **6.1a** was previously reported in a poster presentation presented by A. Horn, R. Ullrich, M. Hofrichter, K. Scheibner, U. Kragl at the 8th International Conference on Biocatalysis & Biotranformations (BIOTRANS), Oviedo (Spain); while the *S*-oxidation of the heterocyclic compound dibenzothiophene has been investigated to a deeper extent by using both whole cells of basidiomycetes and purified UPOs.[106] In particular, the authors obtained a mixture of oxidized products, involving both the oxidation of the *S*-atom to the correspondent sulfone and the un-selective hydroxylation of the two aromatic rings.

The aim of the presented work (**Paper V**) was to assess the performances of *Aae*UPO in the asymmetric synthesis of different chiral sulfoxides (compounds **6.1a**-**6.10a**, **Scheme 6.1**) starting from differently substituted arylalkyl sulfides (compounds **6.1**-**6.10**, **Scheme 6.1**), thus filling this gap in the knowledge of the biocatalytic potential of this unspecific peroxygenases.

6.2   Biocatalyzed asymmetric sulfoxidation

(6.1) R' = CH$_3$; R = H
(6.2) R' = CH$_3$; R = o-Cl
(6.3) R' = CH$_3$; R = m-Cl
(6.4) R' = CH$_3$; R = p-Cl
(6.5) R' = CH$_3$; R = p-CH$_3$
(6.6) R' = CH$_3$; R = p-CN
(6.7) R' = CH$_3$; R = m-OCH$_3$
(6.8) R' = CH$_2$=CH$_2$; R = H
(6.9) R' = c-propyl; R = H
(6.10) R' = CH$_2$OCH$_3$; R = H

(6.1a) R' = CH$_3$; R = H
(6.2a) R' = CH$_3$; R = o-Cl
(6.3a) R' = CH$_3$; R = m-Cl
(6.4a) R' = CH$_3$; R = p-Cl
(6.5a) R' = CH$_3$; R = p-CH$_3$
(6.6a) R' = CH$_3$; R = p-CN
(6.7a) R' = CH$_3$; R = m-OCH$_3$
(6.8a) R' = CH$_2$=CH$_2$; R = H
(6.9a) R' = c-propyl; R = H
(6.10a) R' = CH$_2$OCH$_3$; R = H
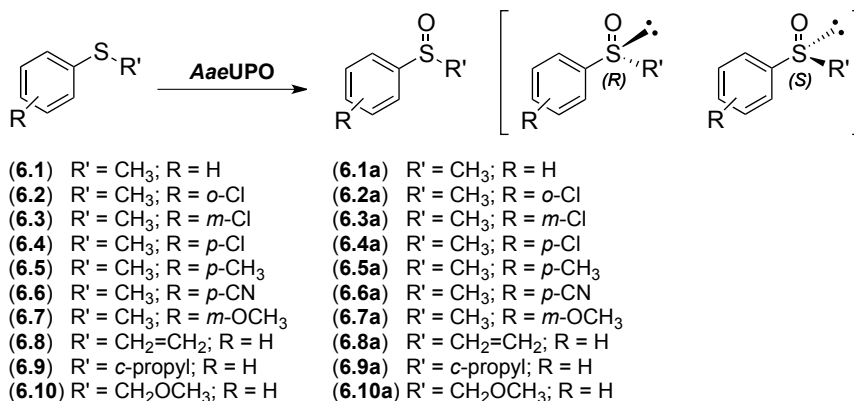
Scheme 6.1: Biocatalyzed sulfoxidation.

To investigate the ability of *Aae*UPO to catalyze the sulfoxidation of the model substrate thioanisole (**6.1**), a peroxygenase preparation was easily obtained from the wild-type *Agrocybe aegerita* TM-A1 (DSM 22459) strain as described in the literature (**Figure 6.7**).[80]
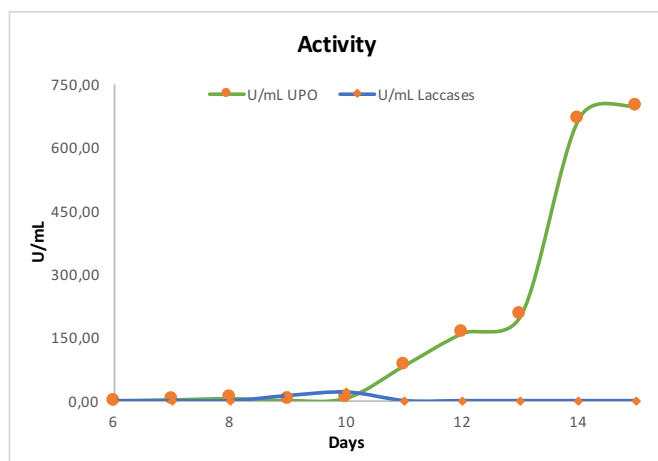
Figure 6.7: *Agrocybe aegerita* strain TM-A1 (DSM 22459) was grown in 2 L-shaken flasks containing 0.5 L of 30 g L^{-1} soybean peptone. The culture was maintained at 25°C and monitored daily for laccase and UPO activity. After 14-15 days, the mycelium was filtrated and the crude *Aae*UPO was recovered from the culture medium by ammonium sulphate precipitation.

In a first set of experiments, the starting concentration of both the substrate **6.1** and the oxidant H$_2$O$_2$ were kept at 1 mM to avoid the well-described peroxide-dependent inactivation of the enzyme.[82, 92, 107] Reactions with *Aae*UPO were carried out at 20 °C in citrate phosphate buffer (10 mM, pH 7.0) in the presence of 20 % CH$_3$CN as cosolvent and stopped

at scheduled times by extraction with ethyl acetate to analyze the obtained crude mixtures by means of direct-phase HPLC on a chiral column. Control reactions were performed in the absence of the enzyme or the oxidant. Under these reaction conditions, the (*R*)-sulfoxide **6.1a** could be obtained after 20 min in quantitative conversions and 80% enantiomeric excess (*ee*) (**Table 6.1**).
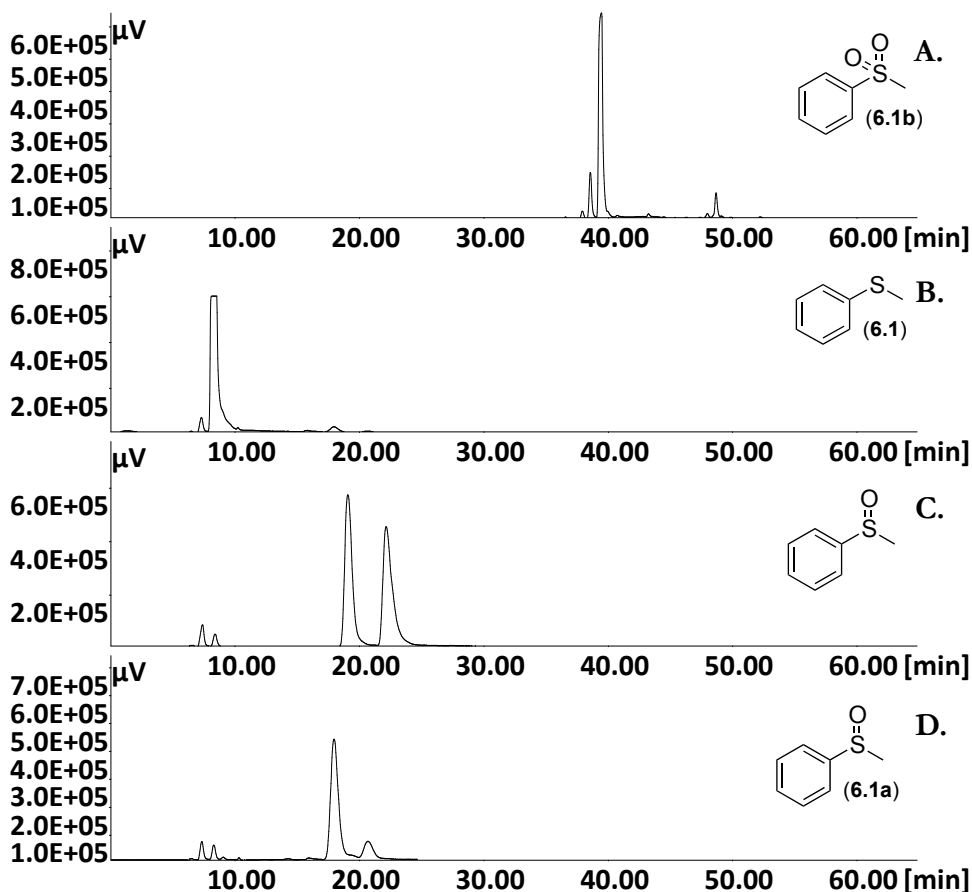
Figure 6.8: HPLC chromatograms of **A.** standard sulfone **6.1b**; **B.** thioanisole **6.1**; **C.** standard racemic **6.1a** and **D.** reaction of **6.1** with *Aae*UPO: quantitative conversion, 80 % *ee* (*R*)-enantiomer.

*Aae*UPO showed a good operative stability, retaining >90% of the starting activity for at least 2 h, as assayed by spectrophotometric measurement of the activity with 2,2'-azino-bis(3-ethylbenzthiazoline-6-sulphonic acid) (ABTS) as substrate. Moreover, no formation of by-products, and of the corresponding over-oxidation sulfone products was observed (**Figure 6.8**) even when in a control reaction the racemic mixture of sulfoxides **6.1a** was used as

substrate. The same result was previously reported also for a number of CPO-catalyzed sulfoxidations on different aryl and alkyl substrates.[99, 100, 80]

To study the possibility of overcoming the well-known peroxide-dependent inactivation of the *Aae*UPO, the same reaction conditions were used in the presence *tert*-butyl hydroperoxide (*t*-BuOOH) as oxidant. Differently from the performances of CPO in the same conditions, *Aae*UPO showed negligible activity (<1% conversion). However, this finding was not surprising since the use of *t*-BuOOH as an alternative to H_2O_2 showed to be more challenging also in other oxyfunctionalization reactions catalyzed by *Aae*UPO.[93]

To assess the practical utility of this biotransformation, the concentration of **6.1** was increased to 10 mM (35 μmol in 3.5 mL final volume) and 20% (v/v) CH_3CN was used to keep it in solution. The presence of cosolvent in the reaction medium had no significant effect on enzyme stability and was strictly needed to ensure the substrate solubility. Instead, as mentioned before, the *in situ* H_2O_2 concentration was the critical point in the stability/efficiency of this peroxygenase.

Among the several options described in the literature to face this issue,[80,92] it was decided to use a simple step-wise addition of a 100 mM H_2O_2 solution (35 μmol added in 10 aliquots at 30 min intervals in the first 4.5 h, then the reaction was maintained for additional 2.5 h without further oxidant addition). The residual *Aae*UPO activity in the reaction solution, conversion of substrate **6.1** and *ee* value of the formed product were monitored at scheduled times.

As shown in **Figure 6.9**, the controlled supplementation of H_2O_2 allowed to obtain a quantitative conversion of **6.1** without observing dramatic drops of enzyme activity during oxidant addition (~60% residual activity after the first 5 h).

In agreement with previous studies, the application of an optimized substrate/H_2O_2/enzyme ratio allowed a minimization of the catalase side-activity, which has been suggested as the main responsible of UPOs inactivation. In fact, only one equivalent of oxidant was required to obtain almost a complete conversion of the target substrate, thus suggesting the lack of

significant H_2O_2 consumption by dismutation to O_2 and H_2O. A possible protective effect of the substrate toward peroxide-induced inactivation, previously investigated by Alexander and coauthors for UPO-catalyzed hydroxylation reactions,[107] was suggested also in this case by the superior operative stability shown by *Aae*UPO at low (<50%) conversion degrees. The *ee* value of the formed (*R*)-sulfoxide **6.1a** was unaltered (80%) during the whole reaction time.
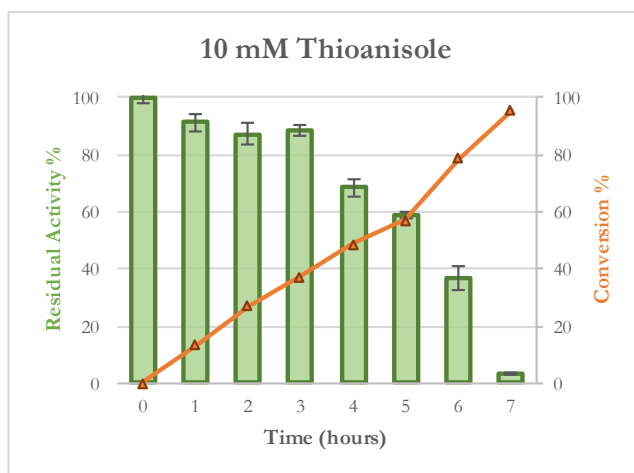
Figure 6.9: step-wise addiction of H_2O_2 to a 10 mM thioanisole reacting solution: profiles of conversion into sulfoxide **6.1b** and enzyme stability in terms of residual activity.

In addition to thioanisole **6.1**, the versatility of *Aae*UPO in promoting enantioselective sulfoxidations was further studied by testing a panel of differently substituted aryl alkyl sulfides (compounds **6.2**-**6.10**, **Table 6.1**).

The obtained conversions and *ee* values of the sulfoxide products were compared with those available in the literature for CPO and three different BVMOs (CHMO, PAMO and HAPMO) for the biooxidation of the same compounds.

In general, *Aae*UPO converted the tested arylalkyl sulfides into the corresponding sulfoxides with good conversions, except for the *o*-substituted substrate **6.2** (35%) and the *p*-cyanophenyl methyl sulfide **6.6** (<5%). The formation of the *R* enantiomer of the sulfoxide products was always observed (the *S* product was obtained only in the case of **6.10a** due to a change in the CIP priority rules) with good to excellent enantioselectivity (70-99% *ee*). The

stereochemical outcomes of the biotransformations was assessed by confrontation with the literature data reported for compounds **6.1a**-**6.10a** by means of chiral HPLC. Respective references are reported in paragraph 6.3, '**Experimental**'.

Both electron donating and 'neutral' groups in the para position of the aromatic ring seemed to be well tolerated (entry 4, 5 and 7), as well as substitution on the meta carbon atom (entry 3), while the presence of an electron withdrawing substituent in para dramatically affected the biocatalytic oxidation (entry 6). The best results in terms of enantiomeric excess were obtained when a substituent was introduced on the R'-group: the vinyl thioanisole **6.8**, as well as the cyclopropyl derivative **9**, were converted into the corresponding (*R*)-sulfoxides with >99% *ee*. However, a decrease of both conversion and *ee* value was observed with compound **6.10** whose flexible CH_2-OMe R' substituent and higher of conformational freedom could have allowed more than one energetically equivalent conformations during the binding with the active site. Moreover, the presence a coordinating oxygen atom on the R' substituent could have impaired the enantioselectivy of the *S*-oxidation as well.

Interestingly, during the biocatalytic sulfoxidation of **6.8** only the *R* enantiomer of sulfoxide **6.8a** was recovered, suggesting a faster kinetic for the sulfoxidation in comparison with olefin epoxidation, another example of UPO-catalyzed reactions largely reported in the literature.[80,81,82,83]

Regarding the comparison with other biocatalyzed sulfoxidations, it is not surprising to observe pretty similar results in terms of conversions and enantioselectivity with CPO, as it is, as mentioned before, an enzyme structurally related to UPOs. Except for **6.5**, *Aae*UPO usually achieved better conversions, but slight lower *ee* values than CPO, the stereoselectivity being in both cases toward the formation of the (*R*)-enantiomer.

As far as BMVOs concern, only few data are available with the panel of substrates used with the enzymes from *Acinetobacter calcoaceticus* (CHMO)[102] and *Thermobifida fusca* (PAMO)[104], in most cases showing less impressive performances than UPO (and CPO) both in terms of conversion and enantiomeric excesses. Instead, a full set of data was reported on the asymmetric sulfoxidation of **6.1**-**6.10** catalyzed by the HAPMO enzyme from *Pseudomonas*

fluorescens.[105] Interestingly, satisfactory results were obtained with HAPMO. In most cases, the formation of the (*S*)-enantiomers of sulfoxides **6.1a**-**6.10a** was achieved with good conversion (except for substrates **6.3** and **6.4**) and very good enantiomeric excesses, with the only exception of compound **6.4**.

The strict (*S*)-selectivity previously shown by HAPMO is herein well complemented by the preference toward the formation of the (*R*)-sulfoxides demonstrated by *Aae*UPO, thus enabling a fully biocatalytic entry to both the enantiomers of sulfoxides **6.1a-6.10a**

Substrate	R	R'	UPO[a]		CPO[b]		CHMO[c]		PAMO[d]		HAPMO[e]	
			c [%][f]	ee [%][f]	c [%]	ee [%]	c [%]	ee [%]	c [%]	ee [%]	c [%]	ee [%]
6.1	CH$_3$	H	>99	80 (R)	>99	98 (R)	88	99 (R)	94	44 (R)	96	99 (S)
6.2	CH$_3$	o-Cl	35	74 (R)	33	85 (R)	35	32 (R)	n.a.[g]	n.a.	76	96 (S)
6.3	CH$_3$	m-Cl	>99	90 (R)	n.a.	n.a.	n.a.	n.a.	n.a.	n.a.	42	93 (S)
6.4	CH$_3$	p-Cl	>99	93 (R)	77	90 (R)	78	51 (S)	n.a.	n.a.	37	44 (S)
6.5	CH$_3$	p-CH$_3$	83	90 (R)	98	91 (R)	94	37 (S)	68	10 (R)	77	99 (S)
6.6	CH$_3$	p-CN	<5	n.d.[h]	n.a.	n.a.	n.a.	n.a.	n.a.	n.a.	64	96 (S)
6.7	CH$_3$	p-OCH$_3$	87	70 (R)	72	90 (R)	81	51 (S)	47	25 (R)	78	99 (S)
6.8	CH=CH$_2$	H	85	>99 (R)	n.a.	n.a.	n.a.	n.a.	n.a.	n.a.	78	98 (S)
6.9	c-propyl	H	95	>99 (R)	n.a.	n.a.	n.a.	n.a.	67	48 (R)	74	97 (S)
6.10	CH$_2$OCH$_3$	H	50	81 (S)[i]	n.a.	n.a.	n.a.	n.a.	n.a.	n.a.	63	98 (R)[i]

Table 6.1: Comparison of UPO-catalyzed sulfoxidations with literature data for CPO and the Baeyer-Villiger monooxygenases CHMO, PAMO, and HAPMO. [a] substrate, 1 mM; H$_2$O$_2$, 1 mM, UPO, 40 U mL^{-1}; 10 mM citrate phosphate buffer, pH 7.0, 2% (v/v) CH$_3$CN; 20°C; 20 min. [b] substrate, 9 mM; H$_2$O$_2$, 2 eq. (added portionwise in 13 aliquots), CPO, 0.144 µM; 50 mM citrate buffer, pH 5.0; 25°C; 1 h.[100] [c] substrate, 40 mM; NADP$^+$, 0.15 mM; glucose-6-phosphate (G6P), 0.1 M; CHMO, 0.3 U mL^{-1}; glucose-6-phosphate dehydrogenase (G6PDH), 2.5 U mL^{-1}; 50 mM Tris/HCl buffer, pH 8.6; 25°C; 24 h.[102] [d] substrate, 20 mM; NADP$^+$, 0.02 mM; G6P, 2 eq.; PAMO, 1 U mL^{-1}; G6PDH, 10 U mL^{-1}; 50 mM Tris/HCl buffer, pH 9.0; 25°C; 24 h.[104] [e] substrate, 20 mM; NADP$^+$, 0.02 mM; G6P, 1.5 eq.; HAPMO, 1 U mL^{-1}; G6PDH, 10 U mL^{-1}; 50 mM Tris/HCl buffer, pH 9.0; 25°C; 24 h.[105] [f] Conversions and enantiomeric excesses calculated on the basis of chiral HPLC analysis (see Supporting Information for details). [g] n.a.: not available from literature data. [h] n.d.: not determined. [i] Absolute configuration is reversed due to a change in the substituent priority according to the sequence rules.

6.3   Conclusions

The performances of the *Aae*UPO in the asymmetric synthesis of chiral sulfoxides were investigated. To the best our knowledge, this is the first example of a systematic investigation of the *Aae*UPO synthetic potential in the asymmetric oxidation of hetero atoms, *i.e.* the pro-stereogenic sulfur of sulfides.

A small library of differently substituted arylalkyl sulfoxides **6.1a**-**6.5a**, **6.7a**-**6.10a** was successfully synthetized by incubating the arylalkyl sulfides in the presence of the *Aae*UPO and H_2O_2. All the sulfoxides were obtained as (*R*)-enantiomers, regardless the substitution pattern both on the aromatic ring and the alkyl chain.

To furnish a complete overview on the biocatalytic entries to chiral sulfoxides, the performances of the *Aae*UPO were confronted with the literature data available for the sulfur oxidation mediated by CPO and different species of BVMOs. While, with no surprise, the *Aae*UPO performances were in very good agreement with the ones obtained using the structurally-related CPO, the stereo-complementary showed by the HAPMO from *P. fluorescens* allowed a general biocatalytic entry to both the enantiomers of compounds **6.1a**-**6.5a**, **6.7a**-**6.10a**. Moreover, as it was shown by Gonzalo de Gonzalo *et al.*, monooxygenase PAMO form *Thermobifida fusca* could also be used to produce chiral sulfoxides by kinetic resolutions of racemic mixtures of (*R*) and (*S*). This was not the case with *Aae*UPO, as this peroxygenase successfully catalyzed asymmetric *S*-oxidation of sulfides but did not accept sulfoxides as substrates.[104]

Furthermore, the performances of the *Aae*UPO in the presence of arylalkyl sulfides as substrates were remarkably better in terms of chemo- and regio-selectivity when compared with the results obtained by Aranda *et al.* in the biooxidation of dibenzothiophene.[106] Specifically, as previously mentioned, the *Aae*UPO-mediated oxidation of dibenzothiophene led to a complex mixture of products in which an un-tunable *S*-oxidation gave the correspondent sulfone and a plethora of hydroxylated products on both the aromatic rings. On the contrary, enantiomerically enriched chiral sulfoxides were obtained regio-, chemo-

and stereo-selectively. No aromatic hydroxylation products were in fact obtained, as clearly demonstrated by the HPLC chromatograms shown in **Figure 6.8**.

Despite the tricky scaling up of *Aae*UPO-catalyzed reactions, a preliminary investigation on the possibility of conducing preparative scale biotransformations to access chiral synthons containing a stereogenic sulfur atom was undertaken. As follow-up, the immobilization of the *Aae*UPO on a suitable solid phase in under investigation to evaluate the possibility of conducing preparative-scale *S*-oxidations *in flow*. The use of a flow system could in fact avoid the mentioned peroxide-dependent inactivation of the enzyme, increasing the stability of the biocatalyst in the reaction media thanks to the possibility of working in continuous with low substrates and H_2O_2 concentrations, thus allowing the accumulation of considerable amounts of products.

6.4   Experimental

6.3.1 Enzyme production

Unspecific peroxygenase (UPO) from *Agrocybe aegerita* strain TM-A1 (DSM 22459) was produced with slight modifications of the method reported in the literature.[84] Specifically, fungal stock cultures were maintained on malt extract agar slants at 4°C and precultured on MEA ([g L^{-1}]: glucose, 20; malt extract, 20; peptone, 2; agar, 20) plates at 25°C for two weeks. Mycelial suspensions prepared by homogenization were used to inoculate 0.5 L of 30 g L^{-1} soybean peptone (Sigma-Aldrich) in 2-L baffled flasks. The cultures were maintained at 25°C and monitored daily for the release of laccase and UPO activity in the culture medium using 2,2'-azino-bis(3-ethylbenzthiazoline-6-sulphonic acid) (ABTS) as substrate, either in the absence and in the presence of H_2O_2, respectively. Enzyme assays were performed in 0.1 M citrate phosphate buffer, pH 4.5, 0.33 mM ABTS, and 3 mM H_2O_2, and monitored spectrophotometrically at 436 nm (ε_{436} = 29300 M^{-1}cm^{-1}). Laccase activity was negligible throughout the all cultivation period, while production of UPO started typically after 7-9 days from the inoculum and reached a plateau after 14-16 days. The mycelium was thus removed by filtration and proteins secreted into the culture medium were recovered by ammonium sulfate precipitation (85% saturation). After centrifugation (5000 rpm, 20 min, 4°C), the protein precipitate was resuspended in saturated ammonium sulfate solution (10 mL) and stored at 4°C. Purified UPO samples were prepared by hydrophobic interaction chromatography as previously described, and used for control reactions.[91]

6.3.2 Asymmetric biocatalyzed sulfoxidation of substrates 1-10

H_2O_2 (1 eq, 1 mM) and UPO (40 U mL^{-1}, 25 μL mL^{-1} of reacting solution) are added to a solution of arylalkyl sulfide (1 eq, 1 mM) in citrate phosphate buffer (10 mM, pH 7.0, 1 mL final volume). The resulting mixture is incubated at 20 °C and 500 rpm for 20 min. Extraction with AcOEt allowed the recovery of the desired oxidized product to be analyzed by HPLC on chiral column. The absolute configurations of the obtained products were determined by

comparing the t_R reported in literature for the *R* and *S* enantiomers of compounds **1a**-**5a** and **7a**-**10a** in the same analytic conditions (see below).

6.3.3 Preparative-scale chemical synthesis of racemic 1a-10a

To obtain suitable racemic mixtures of sulfoxides to be used as NMR and HPLC standards, preparative scale chemical sulfoxidation reactions were carried out at 0 °C by adding dropwise *m*CPBA (1.2 eq, 0.5 M in CHCl$_3$) to a CHCl$_3$ solution of the desired arylalkyl sulfide (substrates **1-10**, 1 eq, 50 mM, 2 mL final volume). After stirring the mixture for 30 – 60 min (TLC analysis: MeOH:CHCl$_3$ = 0.25:9.75, UV) racemic sulfoxides **1a-10a** were obtained by extraction with AcOEt, drying over sodium sulfate and *in vacuum* concentration. Product were obtained in good isolated yields (70-90%) and characterized by ^{1}H NMR and HPLC analysis on chiral column.

Phenyl Methyl Sulfoxide, 6.1a
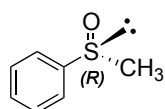
 ^{1}H NMR (400 MHz, CDCl$_3$, rt), δ: 7.62-7.64 (m, 2 H), 7.46-7.54 (m, 3 H), 2.72 (s, 3 H) ppm. **HPLC**: t_R (R) = 19.0 min, t_R (S) = 22.1 min (Chiralcel OD column, petroleum ether/iPrOH = :1, flow rate = 0.5 mL min^{-1}, wavelength = 254 nm). [108]

o-Chlorophenyl Methyl Sulfoxide, 6.2a
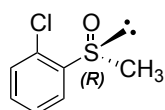
 ^{1}H NMR (400 MHz, CDCl$_3$, rt), δ: 7.90 (d, *J* 7.8 Hz, 1H), 7.52 (m, 1H), 7.43 (m, 1H), 7.34 (d, *J* 7.8 Hz, 1H), 2.81 (s, 3H) ppm. **HPLC**: t_R (R) = 25.1 min, t_R (S) = 29.2 min (Chiralcel IA column, petroleum ether/iPrOH = 9:1, flow rate = 0.4 mL min^{-1}, wavelength = 254 nm). [109]

m-Chlorophenyl Methyl Sulfoxide, 6.3a
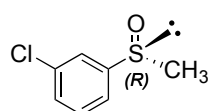
 ^{1}H NMR (400 MHz, CDCl$_3$, rt), δ: 7.95 (t, *J* 1.8 Hz, 1H), 7.85 (ddd, *J* 7.8, 1.7, 1.1 *Hz*, 1H), 7.56-7.48 (m, 2H), 3.08 (s, 3H) ppm. **HPLC**: t_R (R) =

34.3 min, t_R (S) = 35.3 min (Chiralcel IA column, petroleum ether/iPrOH = 9:1, flow rate = 0.4 L min^{-1}, wavelength = 254 nm).[109]

p-Chlorophenyl Methyl Sulfoxide, **6.4a**
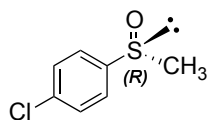
^{1}H NMR (400 MHz, CDCl$_3$, rt), δ: 7.56-7.59 (m, 2 H), 7.48-7.52 (m, 2 H), 2.71 (s, 3 H) ppm. **HPLC**: t_R (R) = 58.8 min, t_R (S) = 68.8 min (Chiralcel OD column, petroleum ether/iPrOH = 9:1, flow rate = 0.25 mL min^{-1}, wavelength = 254.[110]

p-Tolyl Methyl Sulfoxide, **6.5a**

^{1}H NMR (400 MHz, CDCl$_3$, rt), δ: 7.84 (d, J 8.3 Hz, 2H), 7.38 (d, J 8.3 Hz, 2H), 3.04 (s, 3H), 2.46 (s, 3H). ppm. **HPLC**: t_R (R) = 55.0 min, t_R (S) = 62.0 min (Chiralcel OD column, petroleum ether/iPrOH = 95:5, flow rate = 0.25 L min^{-1}, wavelength = 254 nm).[104]

p-Methoxyphenyl Methyl Sulfoxide, **6.7a**
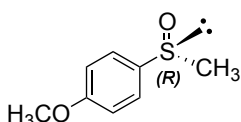
^{1}H NMR (400 MHz, CDCl$_3$, rt), δ: 7.91 (d, J 8.7 Hz, 2H), 7.57 (d, J 8.7 Hz, 2H), 3.07 (s, 3H), 2.44 (s, 3 H) ppm. **HPLC**: t_R (R) = 37.4 min, t_R (S) = 40.6 min (Chiralcel OD column, petroleum ether/iPrOH = 95:5, flow rate = 0.5 mL min^{-1}, wavelength = 254 nm).[111]

Phenyl Vinyl Sulfoxide, **6.8a**
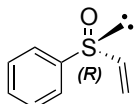
^{1}H NMR (400 MHz, CDCl$_3$, rt), δ: 7.64-7.59 (m, 2 H), 7.55-7.47 (m, 3 H), 6.59 (dd, J 16.5, 9.6 Hz, 1 H), 6.20 (dd, J = 16.5, 0.5 Hz, 1 H), 5.89 (dd, J = 9.6, 0.5 Hz, 1 H) ppm. **HPLC**: t_R (R) = 37.5 min, t_R (S) = 46.3 min (Chiralcel OD column, petroleum ether/iPrOH = 9:1, flow rate = 0.25 mL min^{-1}, wavelength = 254 nm).[111]

Phenyl Cyclopropyl Sulfoxide, **6.9a**

¹H NMR (400 MHz, CDCl₃, rt), δ: 7.71-7.68 (m, 2H), 7.57-7.52 (m, 3H), 2.22 (ddd, J 7.4, 4.4, 3.0 Hz, 1H), 1.11-1.07 (m, 2H), 0.74-0.70 (m, 2H) ppm. **HPLC**: t_R (R) = 28.6 min, t_R (S) = 39.6 min (Chiralcel OD column, petroleum ether/iPrOH = 8:2, flow rate = 0.3 mL min⁻¹, wavelength = 254 nm).[105]
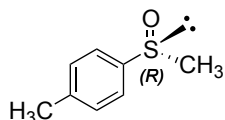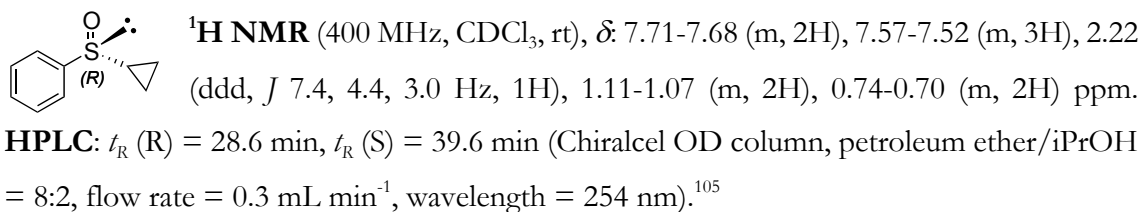
Phenyl Methoxymethyl Sulfoxide, **6.10a**

¹H NMR (400 MHz, CDCl₃, rt), δ: 7.65-7.56 (m, 2 H), 7.58-7.43 (m, 3 H), 4.39 (d, J 10.1 Hz, 1 H), 4.35 (d, J 10.1 Hz, 1 H), 3.69 (s, 3 H) ppm. **HPLC**: t_R (S) = 52.3 min, t_R (R) = 68.1 min (Chiralcel OD column, petroleum ether/iPrOH = 95:5, flow rate = 0.25 mL min⁻¹, wavelength = 254 nm).[110]
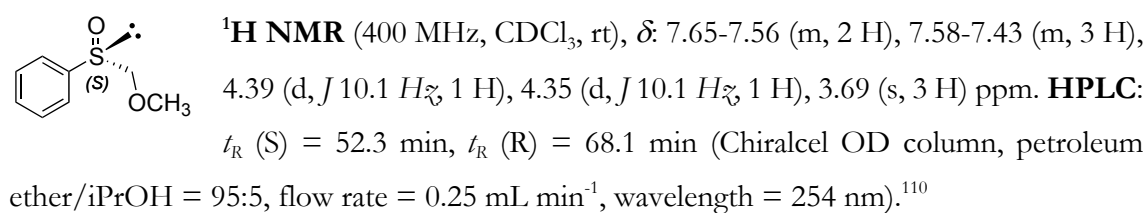
7.   Laccases: selective Csp^2-H bonds activators

7.1   2,3-dihydro benzofurans-based scaffolds

Laccases (benzenediol:oxygen oxidoreductases, EC 1.10.3.2) are redox metalloproteins widely known as 'blue oxidases' thanks to the presence of a tetraatomic copper cluster in their active site (**Figure 7.1**).

In Nature, they are generally produced by the fungi *basidiomycetes* and *ascomycetes* as biocatalysts involved in the degradation of lignin, a cross-linked phenolic polymer, *via* complex oxidative mechanisms that involve the production of free radicals.[112]
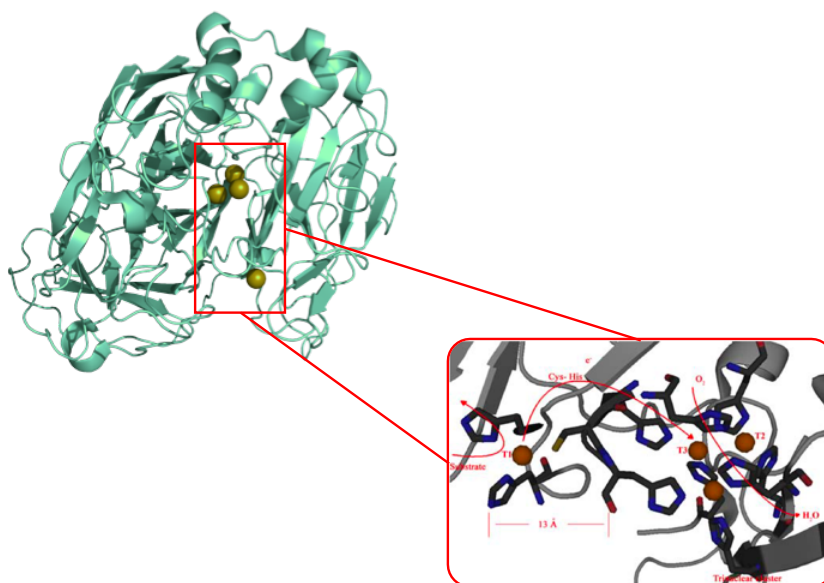
Figure 7.1: Ribbon representation of the X-Ray determined crystal structure of a laccase from *Trametes versicolor* (**left**); detail of the copper-cluster (**right**).

The tetraatomic copper cluster represents the pivotal-core of laccases catalytic activity as the key redox processes occurs on its copper centers. Specifically, four organic compounds are oxidized in the presence of molecular oxygen producing four highly reactive radicals and water as the only (theoretical) by-product.
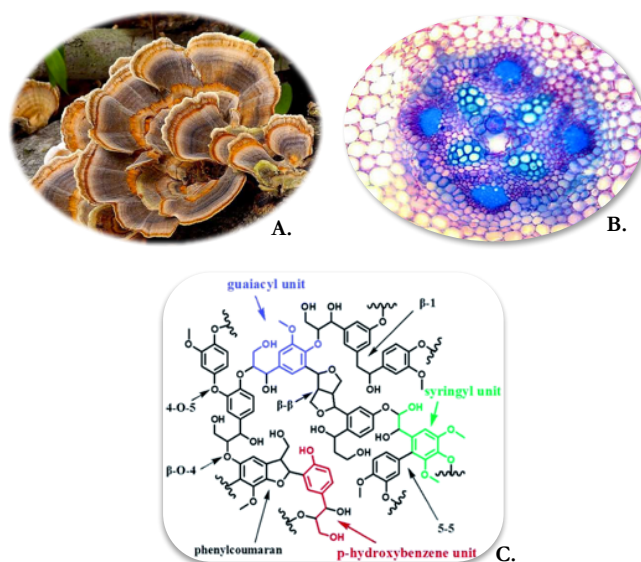
Figure 7.2: **A.** *Trametes versicolor*; **B.** A microscope detail of a plant tissue. The blue coloration indicates lignified cell-walls; **C.** Detail of lignin structure.

Among the four copper atoms (**Figure 7.3**), the so-called 'T1' copper site acts as the primary electron acceptor site. It is the place where the single-electron oxidations of four molecules of a reducing substrate, the rate determining step of laccase-mediated processes, occurs. The other tree metal centers, arranged in a triangular-shaped semi-cluster, 'T2/T3' copper site, catalyze the reduction of molecular oxygen to water.[113, 114, 115]

Figure 7.3: Detailed description of the tetratomic cupper cluster of laccases. The charge transfer transition S*cys*→Cu(II) provides the enzyme its deep blue coloration.

Interestingly, the laccase-catalyzed formation of radicals, with the concomitant reduction of oxygen and water production, can be exploited in biocatalyzed organic synthesis as a green entry to activated organic compounds. In fact, the laccase oxidation of differently substituted aromatic amines and phenols offers the possibility of a conve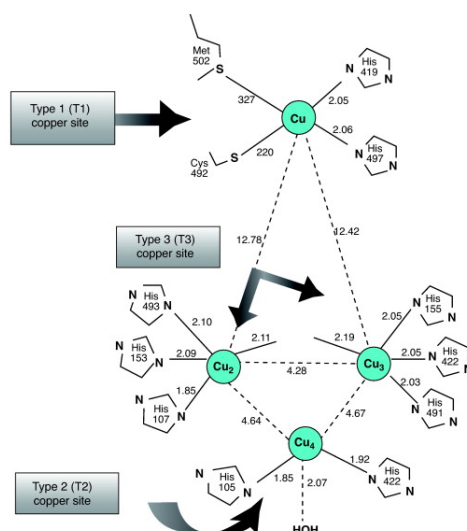nient biocatalytic activation of normally inert Csp^2-H bonds. Thanks to mesomeric resonance(s), the radical species formed by the biooxidation, which at first occurs on the more electronegative heteroatom (*N* or *O*), can be delocalized along all the carbonaceous skeleton of the π-system, allowing the formation of new C-C or C-Het bonds (radicals **ii, v, vi** and quinon or quininon-like specie **iv, Scheme 7.1**).
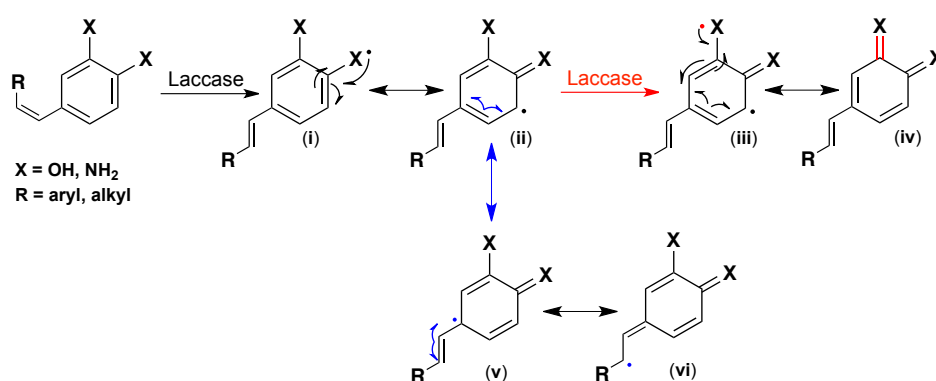
Scheme 7.1: Laccase-catalyzed activation of Csp^2-H bonds *via* mesomeric resonance.

These highly reactive radical species usually undergo different reaction pathways, *ndr* quenching processes, to be transformed into more stable species, as shown in **Figure 7.4**.

Figure 7.4: Quenching processes allowed for laccase-produced radicals.

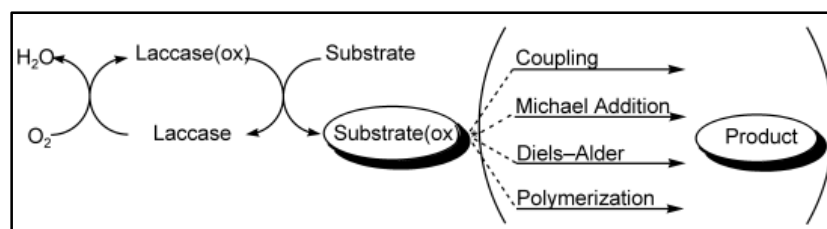By conducing these transformations in the proper reacting media, the quenching processes can be controlled, or at least guided, to promote the formation of fine chemical as products, with modest to very good chemoselectivity in the formation of the target new C-C and C-Het bonds.

A wide number of example have been reported on the synthetic application of laccases as Csp^2-H bonds activators and two main classes of processes can be identified:

a) aromatic nucleophilic substitution (1,4-conjugate addictions to quinones, mechanism shown in **Scheme 7.2**) to form novel C-Het bonds[116, 117, 118, 119, 120, 121, 122]

b) radical C-C couplings to form biaryl compounds[123, 124, 125, 126]
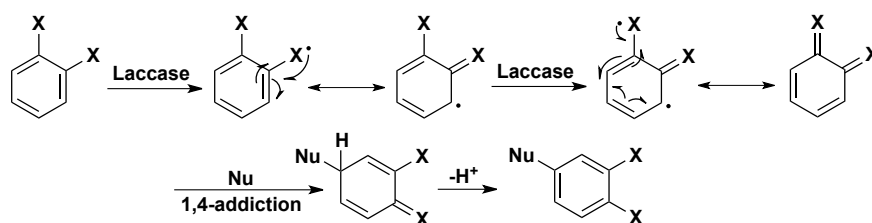
Scheme 7.2: Laccase-promoted 1,4-conjugate addictions to quinones.

Moreover, one of the most interesting synthetic application of laccase Csp^2-H bonds activation, are the biocatalyzed ring closure reactions. In fact, by the rational design of a proper substrate and an accurate optimization of the reaction conditions, the listed mechanisms can be merged to obtain domino and cascade processes for the one-pot synthesis of substituted (hetero)cyclic compounds. An outstanding example of this strategy is the work done by professor Beifuss *et al.* regarding the use of aromatic 1,3-dicarbonyls as carbon nucleophiles. When reacted with and 1,2-dihydroquinones in the presence of laccases, 1,3-dicarbonyls are successfully and selectively transformed into oxygenated heterocycles *via* a domino process that involves two nucleophilic 1,4-conjugate addictions to *in situ* generated quinon intermediates, as shown in **Scheme 7.3**.[127, 128, 129, 130, 131] Moreover, their investigation was expanded to *S*- and *N*-containing equivalents of 1,3-dicarbonyls, as in their elegant biocatalytic entry to pirimidobenzothiazoles bases on the use of 2-thioxo

pirimidine as nucleophiles (**Scheme 7.4**).[132] It's noteworthy that no expensive, toxic and/or hazardous metal-based chemical catalysts, that usually require inert atmosphere and specific experimental conditions, are needed to perform this biocatalytic Csp^2-H bond activation.
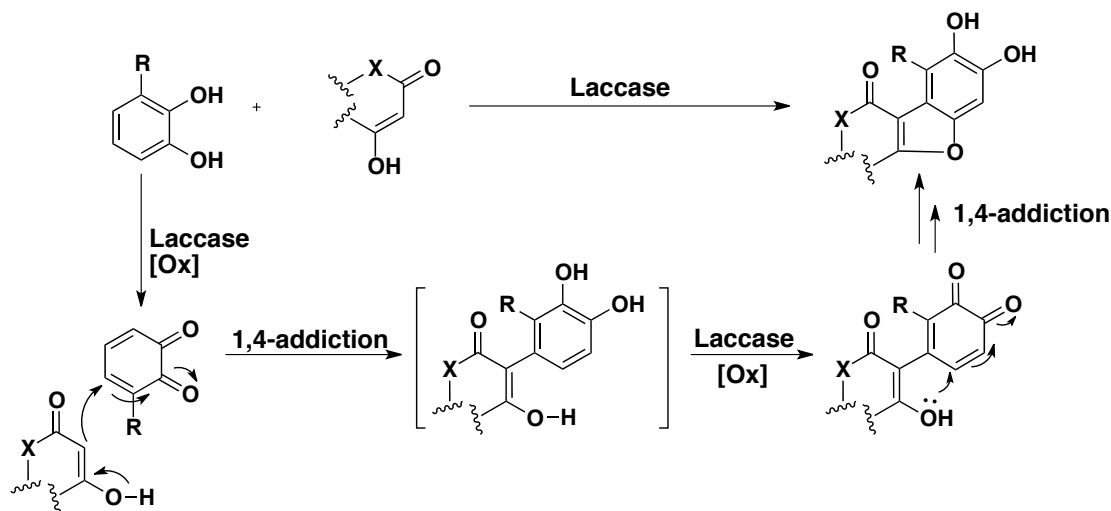
Scheme 7.3: 1,3-dicarbonyls-based laccase chemistry investigated by Beifuss.
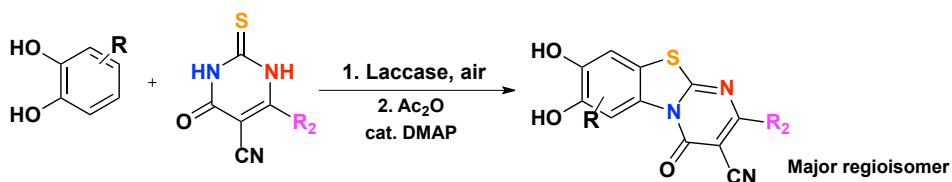
Scheme 7.4: Biocatalytic entry to pirimidobenzothiazoles.

A domino process to afford oxygen-containing heterocyclic compounds can also be built by exploiting the oxidative (homo)coupling of phenolic substrates. In the past years, our research group has extensively investigated the laccase-mediated coupling of substituted vinyl phenols and stilbenes.[133, 134, 135, 136] In **Scheme 7.5**, the different class of chemical structures that were obtained by the oxidative coupling of substituted phenolic substrates is presented.

When the R' group is second phenolic group and R is both an alkyl or an aryl substituent, a dioxane hetocyclic (**ii**) ring is usually obtained as major product, while in the presence of a 'spectator group' in the R' position and an allylic alcohol as the R substituent, the formation

of racemic pinoresinol (**iii**) is preferred. The obtainment of the 2,3-dihydrobenfofuran structures (β-5 type dimers, **i**) is instead preferred when the R' group is, again, a 'spectator group' (*i.e.* hydrogen, alkyl chains, protected phenols) and the R substituent is both an alkyl or an aryl group.
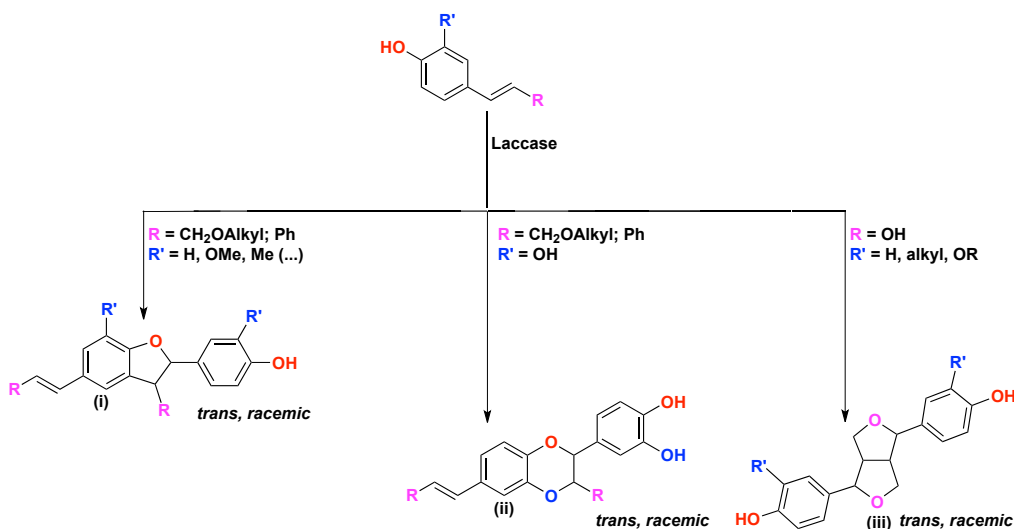
Scheme 7.5: Overview about the possible heterocyclic products obtained *via* laccase-mediated couplings.

Thanks to these results, it was discovered that, working under optimum conditions and with the proper substrate, the selective formation of 2,3-dihydrobenzofurans could be achieved by laccase-mediated oxidations. From a mechanistic point of view, the target dihydrobenzofuran skeletons are obtained by a formal oxidative homocoupling reaction *via* a process involving the C-C coupling of two activated radicals formed by the biooxidation of two substrate molecules followed by an intramolecular 1,4-conjugate addiction, as shown in **Scheme 7.6**. During these oxidative couplings, two new stereocenters are formed. In general, due to steric hindrance and thermodynamics, dimeric products are formed as *trans*-stereoisomers, whose absolute configuration is unfortunately randomized. The lack of enantioselectivity is a serious synthetic drawback of these biocatalyzed oxidative couplings. Nature has solved this problem developing the so-called 'dirigent proteins', a group of proteins that act as chiral templates and direct the stereochemical outcome of these

processes. A significant example of these 'dirigent proteins' was isolated from the plant *Forsythia intermedia* and used by Davin et al. for the *in vitro* stereoselective biocatalyzed synthesis of (+)-pinoresinol (**iii**, R' = H) by the laccase-catalyzed oxidation of coniferyl alcohol.[137] Later on, in 2010, Pickel et al. isolated and cloned an enantiocomplementary dirigent protein, able to guide the bio-oxidative coupling toward the formation of (-)-pinoresinol.[138] However, this elegant biomimetic approach is of scarce synthetic appeal as, for any substrate and desired enantiomer of a dimeric product, a specific dirigent protein should be isolated, providing that it does exist in Nature.

To overcome this limitation, in previous works our research group has exploited the 'classical' lipase-catalyzed kinetic resolution protocols. The racemic mixtures of *β*-5-type dimers derived from the laccase-mediated oxidation of different vinyl phenols were separated obtaining both the possible enantiomers as enriched species. The target products could be isolated with *e.e.* up to 98 %.[139, 140]
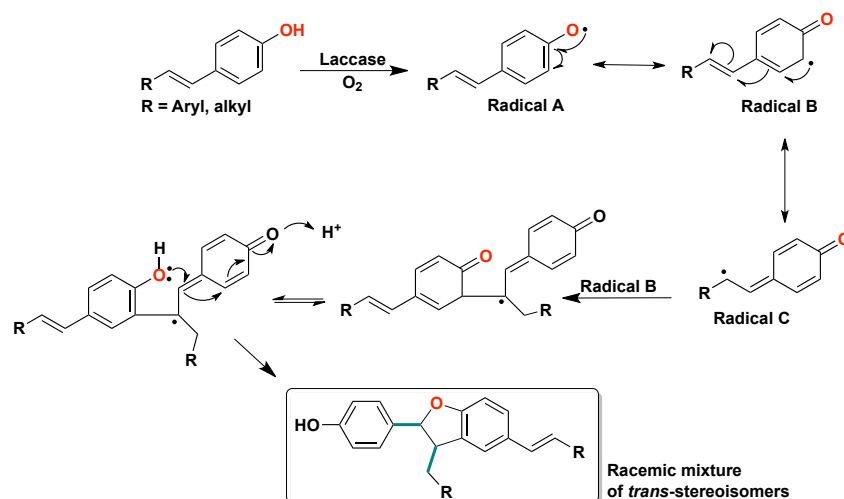
Scheme 7.6: Domino process to dihydrobenzofurans *via* oxidative homocoupling.

More recently, both the enantiomers of the *β*-5-type dimers of resveratrol could be isolated on a preparative scale starting from the laccase-mediated oxidation of piceid, a natural D-glucoside of resveratrol (**Figure 7.5**).[141] A mixture of *trans*-2R,3R and *trans*-2S,3S glucosylated dihydrobenzofurans–based dimers was easily isolated in good yield, and the two

diastereomers were separated by preparative HPLC on a chiral column. The target enantiomers of resveratrol dimers were eventually obtained with *e.e.* values up to 97 % by glycosidases-catalyzed hydrolysis of the glucose units.
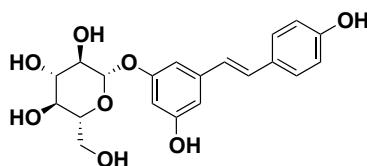
Figure 7.5: Piceid.

Paper VI described the possibility of extending this approach to other compounds, specifically to phenylpropanoid glucosides (PPGs, also known as glucosylated lignols) a family of bioactive arylalkyl glucosides whose biocatalytic synthesis has been extensively discussed in chapter 4. Looking for a possible sugar-induced stereochemical enrichment, the laccase-catalyzed oxidative coupling of a small family of glycosylated phenylpropanoids (using different carbohydrate moieties), has been investigated. Novel structurally modified analogues of these bioactive natural compounds have been isolated and characterized. These results will be discussed in 7.2.

To further investigate the laccase-mediated coupling of vinyl phenols and stilbenes to produce benzofuran-containing moieties, the possibility of conducting an intramolecular oxidative dimerization was investigated, using a substrate a small library of linked compounds (**Figure 7.11**), obtained by exploiting the lipase-mediated transacylation reaction discussed in chapter 3. Paragraph 7.3 will be focused on the presentation of these laccase-catalyzed biotransformations.

Moreover, this convenient, chemo- and regio-selective biocatalytic entry to 2,3-dihydrobenzofurans has been exploited to perform a chemo-enzymatic synthesis of potential allosteric modulators of the 90 kDa heatschok protein (Hsp90) (**Submitted Manuscript I**), as it will be discussed in paragraph 7.4.

7.2   Oxidative dimerization of glycosylated lignols

In **Paper VI**, the laccase-catalyzed oxidative coupling of a small family of water-soluble phenylpropenoid glucosides (PPGs), synthesized from coniferyl and *p*-coumaryl alcohol, has been investigated to produce 2,3-dihydrobenzofurans-based analogues of bioactive natural compounds. Moreover, to investigate the possibility of promoting a sugar-induced stereochemical enrichment of the obtained diasteromeric mixtures of dimers, different carbohydrate moieties (D-glucose, L-glucose and the disaccharide rutinose) were considered (**Figure 7.6**). In fact, in these compounds, the glycon moieties are linked very closely to the carbons (C-α and C-β, **Figure 7.6**) that were going to become novel stereocenters. The working hypothesis was that a bulky multi stereogenic chiral moiety near the reaction sites would have induced a discrimination among the possible diasteromeric products.
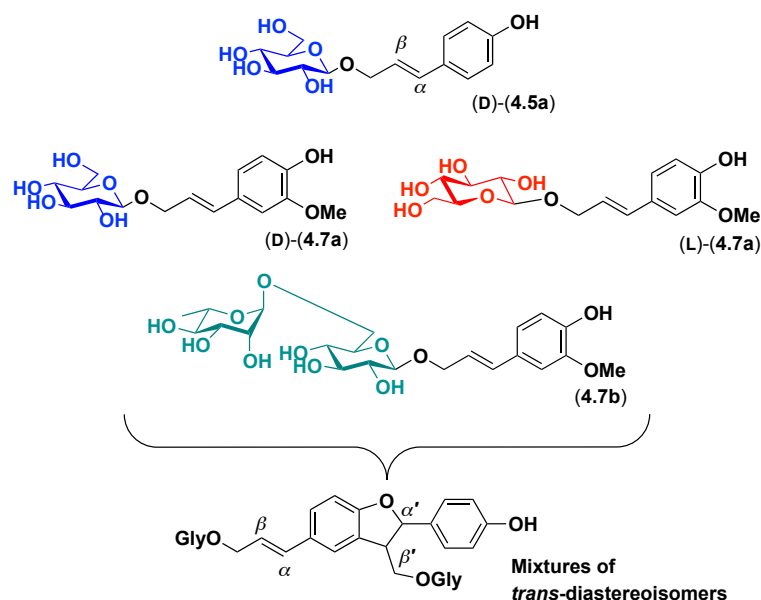
Figure 7.6: Glycosylated substrates.

At first, it was decided to study the laccase-mediated coupling of phenylpropanoid glucosides, synthetized as describes in chapter 4, compounds that had never been submitted before to the oxidative action of laccases. Furthermore, the presence of the sugar moiety linked to the primary alcohol of the propenol side chain, preventing the formation of

pinoresinol-like structures (**iv, Scheme 7.5**), would have allowed to limit the number of dimeric products obtained by the radical coupling.
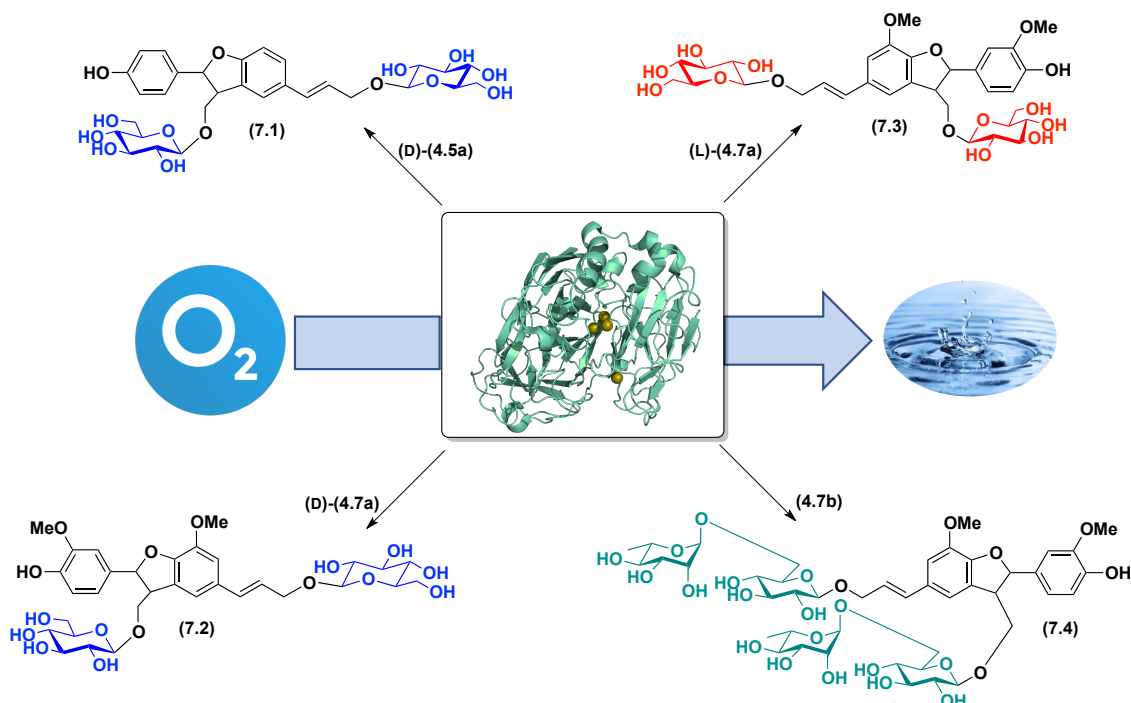
Scheme 7.7: Synthesis of compounds **7.1–7.4**.
Reagents and conditions: Phenylpropanoid glycoside (0.05 M), acetate buffer (20 mM pH 5), laccase (0.005 U $mmol_{substrate}^{-1}$), at 30 °C and 300 rpm, 6 - 8 hours. Isolated yields: **7.1**= 35 %; **7.2**= 34 %; **7.3** = 37 %; **7.4**= 33 %. All products were obtained as mixtures of *trans*-diasteroisomers..

At first, the naturally occurring PPGs (**D**)-**4.5a** and (**D**)-**4.7a** were submitted to the action of the laccase from *Trametes versicolor* and the corresponding main products, **7.1** and **7.2**, were isolated in 35 and 34 % yield, respectively (**Scheme 7.7**). Their mass spectra showed the expected values for dimeric products, the quasi molecular peaks ($[M + Na^+]$) being registered at 645.3 at 705.3 Da respectively.

The *trans β*-5-type dimeric structure of **7.1** was confirmed by the corresponding ^{1}H-NMR spectrum. In addition to the signals due to the expected seven aromatic and two olefinic protons, the ^{1}H-NMR spectrum showed the diagnostic signal due to H-α'.

Provided that **7.1** is a mixture of diasteroisomers, the signals were split in two base line separated doublets (relative ratio almost 1:1, **Figure 7.7**) centered at 5.574 and 5.234 ppm (*J* 6.4 Hz). Similarly, the signals due to the two anomeric protons (doublets) were split in two doublets each (resonating between 4.403 and 4.347 ppm). All the other signals appeared as multiplets, due to the duplication of the expected peaks.

Similarly, the ^{1}H-NMR spectrum of **7.2** showed the presence of the five aromatic and two olefinic protons. The signal due to H-*α'* was again split in two base line separated doublets centered at 5.547 and 5.503 ppm (*J* 6.4 Hz), **Figure 7.7**. However, the relative ratio of these two doublets, evaluated by signals integration, was approximately 1.5:1. Among the two anomeric protons, the first one resonated as a doublet at 4.217 ppm (*J* 8.0 Hz). The second one was split in two doublets, again in a 1.5:1 ratio, the most abundant being centered at 4.263 and the second one at 4.256 ppm (*J* 7.6 Hz). Both the two singlets due the two methoxy substituents were also split, resonating respectively at 3.807 and 3.800 ppm and at 3.751 and 3.742 ppm.

Intrigued by the observed difference in the relative ratio of the two diasteroisomers of **7.2**, it was decided to subject to the action of laccases the phenylpropanoid glucoside (**L**)-**4.7a**, carrying the enantiomeric sugar moiety, (L)-glucose. The synthesis of compounds (**L**)-**4.7a** was conducted following standard chemical glycosylation protocols, as it was shown in **Scheme 4.1** of chapter 4. The key step, again, was the coupling of the trichloroacetimidate of L-tetraacetylglucopyranoside to a TBDMS-protected (at the phenolic moiety) alcohol, that gave the target glucoside in isolated yield of 20 %. After subjecting (**L**)-**4.7a** to the laccase-catalyzed oxidation, the main product **7.3** was isolated in a yield similar to the previously described products (37 %) and the structure was confirmed by mass spectrometry and ^{1}H-NMR. As expected, its spectrum was mostly equivalent to the one previously obtained with **7.2**. Specifically, the presence of two diastereomeric substituted benzodihydrofuran moieties was confirmed by the two doublets resonating at 5.554 and 5.504 ppm (*J* 6.8 Hz). However, at variance to **7.2**, the relative ratio of the area of the two doublets of **7.3** was lower (1.1: 1) and, moreover, the most abundant dimer was the one whose doublet resonated at higher

fields (5.504 ppm, **Figure 7.7**), whereas with **7.2** it was the one resonating at lower fields (5.547 ppm); a result, that was coherent with the presence of two enantiomeric sugars in the starting substrates (**D**)-**4.7a** and (**L**)-**4.7a**. As a comparison, **Figure 7.7**, shows the relative abundance of the signals due to H-α' in compounds **7.1**-**7.4**.
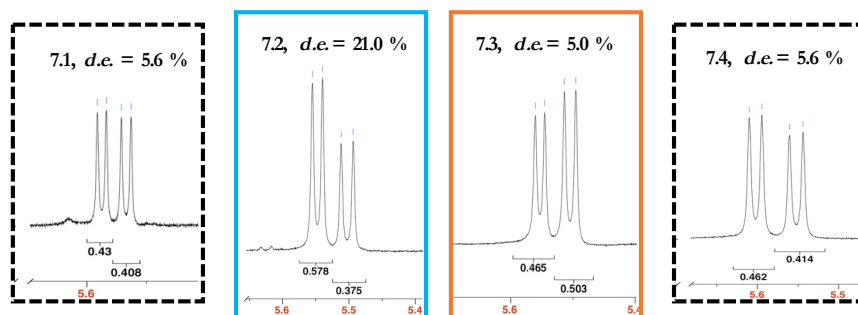
Figure 7.7: Diasteromeric excesses evaluation: ^{1}H-NMR.

The difference reaction outcomes, in terms of diastereomeric ratio of the dimeric products **7.1** and **7.2**, was also confirmed by HPLC analysis. Several chiral and achiral columns were tested and the best results were obtained with a Kinetex 5μm Biphenyl 100Å Column. **Figure 7.8** shows the baseline separated HPLC peaks of the diasteromeric mixtures **9** and **10**. The low *d.e.* (18 % and 6.0 %, respectively) and the stereo complementarity of the two reactions outcomes were confirmed.
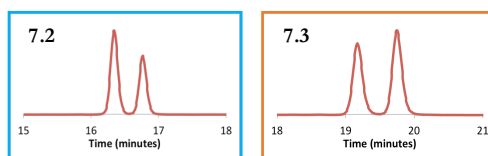
Figure 7.8: Diasteromeric excesses evaluation: HPLC.

Derivative **4.7b**, that was obtained by exploiting the biocatalytic entry described in chapter 4, containing a bulkier sugar moiety linked to coniferyl alcohol, was used as the last substrate for, again, a laccase-mediated oxidation. Its dimerization was performed following the usual protocol, and the main product **7.4** was isolated in 33 % yield. The mass spectrum was in accordance with the structure of a dimeric product ([M + Na$^+$] m/z = 997.3 Da) and the ^{1}H-NMR corroborated the structure. The spectrum was quite complex, due to the

presence of two disaccharide moieties and two diastereoisomers. The anomeric protons of the two glucopyranose units were doublets centered at 4.489 and 4.373 ppm. The presence of the rhamnopyranose units was confirmed, *i.a.*, by the signals due to the C-18 methyl groups resonating at 1.174 and 1.238 ppm. The diagnostic signals due to H-α' were two baseline separated doublets at 5.602 and 5.552 ppm (*J* 6.4 Hz, **Figure 7.7**) with a relative ratio of 1.16 : 1.

Thanks to this work, it has been shown that coumaryl and coniferyl glucosides are suitable substrates for a laccase-mediated Csp^2-H bond activation allowing an easy and convenient biocatalytic entry to 2,3-dihydrobenzfuran-based analogies of bioactive natural products. The presence of a carbohydrate moiety increased the water solubility of these compounds and reduced the number of dimeric products, as pinoresinol-like structures could not be formed. However, the sugar substituents had a minor effect on the stereochemical outcome of the radical coupling reactions, the best results being the 21 % *d.e.* observed in *β*-5-like dimer **7.2** obtained by the laccase-catalyzed dimerization of (**D**)-**4.7a**. Anyway, these low *d.e.* were surprisingly accounting for a stereocomplementarity in the reactions outcomes depending the configuration of the sugar moiety attached to the phenylpropanoid structure.

As future development, since a sugar-induced asymmetric synthesis of 2,3-dhydrobenzufyrans *via* a laccase-mediated oxidative coupling of glycosylated lignols appears unfeasible, the will be focus on the preparative scale isolation of enantiomerically enriched dimers of coumaryl and coniferyl alcohols following the protocol previously exploited with resveratrol glucoside.[141]

7.3   Studies on intramolecular oxidative couplings

It's commonly accepted that intramolecular reactions can often proceed with better degrees of stereo-, regio- and chemo-selection, when compared to their intermolecular versions. Accordingly, the intramolecular laccase-mediated oxidative couplings of suitable phenolic substrates were undertaken.
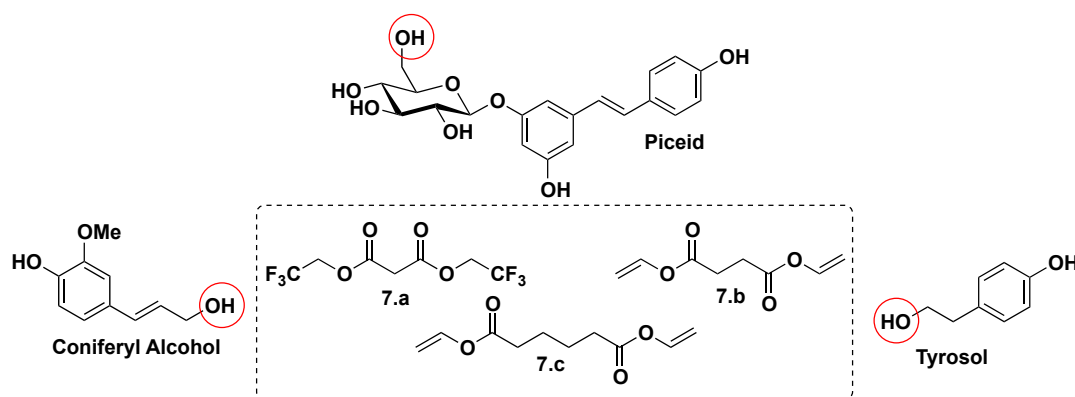
Figure 7.9: Representative phenolic substrates and linker.
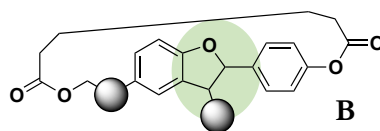
Figure 7.10: Target scaffolds (**B**).

In this study, different phenols, even chiral glucosylated substrates, were linked, *via* spacers of diverse chain lengths, to build omoderivatives (**Figure 7.9**) to be used as substrates for the laccase-catalyzed oxidation. The aim was to investigate whatever a macrocycle structure containing a (±)-2,3-*trans*-dihydrobenzofuran moiety could have been obtained this way (**Figure 7.10**). These families of scaffolds, could be used to build interesting analogues.

Using the activated diesters compounds (**7.a** – **7.c**) as acyl-donors in some Novozym435-catalyzed (*Candida antarctica* lipase B) transacylation reactions, a small library of linked omoderivatives (**7.d**-**7.m**) of coniferyl alcohol, tyrosol and piceid was built.
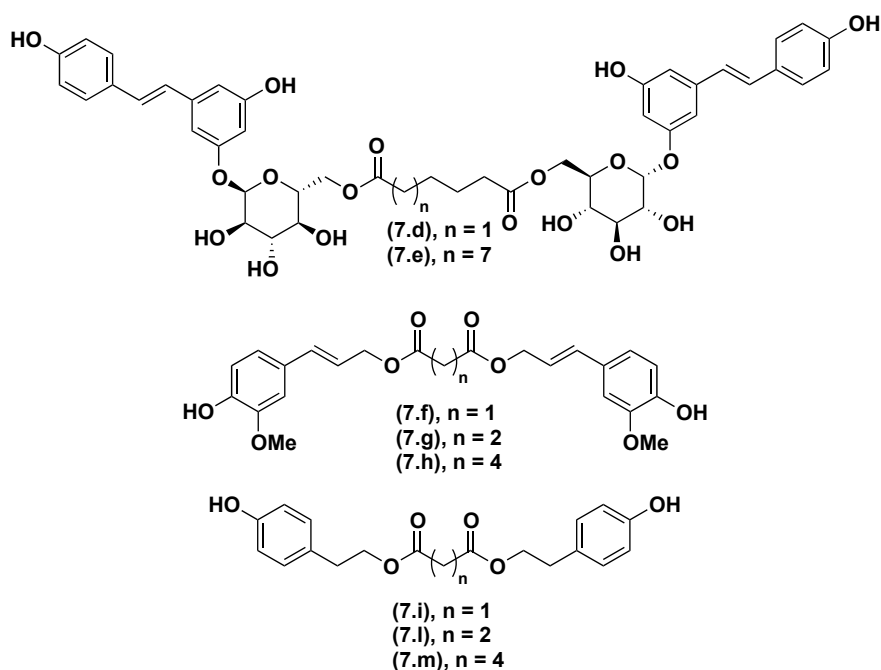
Figure 7.11: The bio-catalyzed synthesis of **7.d**-**7.m** were conducted using Novozym435 (0.25 mg/mg) at 45 °C, 200 rpm in dry acetone as solvent.
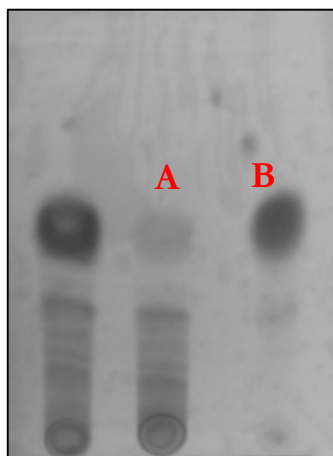
Figure 7.12: TLC plate of the reaction of **7.g** with *T. vesicolor* laccase: (**A**) reaction outcome; (**B**) starting substrate **7.g**. **Laccase-mediated oxidations, reagents and conditions:** 7.d-7.e =acetate buffer pH 5 20mM/acetone = 1:1, [2.5 mg/mL], 0.05 U/mg; **7.f-7.h** = acetate buffer pH 5 20mM/acetone = 1:1, [2.5 mg/mL], 0.018 U/mg; **7.i-7.m** = acetate buffer pH 5 20mM/MeOH = 1:1, [5 mg/mL, 0.5 U/mg.

Compounds **7.d**-**7.m** (whose sctructres were confirmed by ^{1}H-NMR) were than subjected to the action of laccases. Unfortunately, only complex mixtures of oxidized products were

always obtained, regardless the conditions used or the type of substrates. As an example, **Figure 7.12**, shows the reaction outcome of the laccase-mediated oxidation of compound **7.g**.

This investigation is now focused on the finding of more suitable linkage-modalities and/or reactions conditions to promote the formation of the target cyclic products and avoid the disruption of the starting material due to undesired radical decompositions.

7.4 Chemo-enzymatic synthesis of potential allosteric modulators of the 90 kDa heatschok protein (Hsp90)

Heat shock proteins as pharmacological target: Hsp90 and Hsc82

Heat shock proteins (Hsp) are molecular chaperones that facilitate the maturation of a wide range of proteins, known as 'clients' which usually are enriched in signal transducers, including kinases and transcription factors. The human heat shock protein 90 (Hsp90), and its homologue found in yeast Hsc82, are the most characterized member of this class of polypeptides.[142] In Nature, chaperones are required for essential housekeeping functions, such as *de novo* protein folding during nascent polypeptide-chain synthesis, translocation of proteins across membranes, quality control in the endoplasmic reticulum, and normal protein turnover. Chaperones also participate in many higher-order functions, such as the post-translational regulation of signalling molecules, the assembly/disassembly of transcriptional complexes and the processing of immunogenic peptides by the immune system (**Figure 7.13**). As such, they have been proposed as interesting target for the treatment of vascular disease,[143] neurodegeneration[144] and cancer.[145]

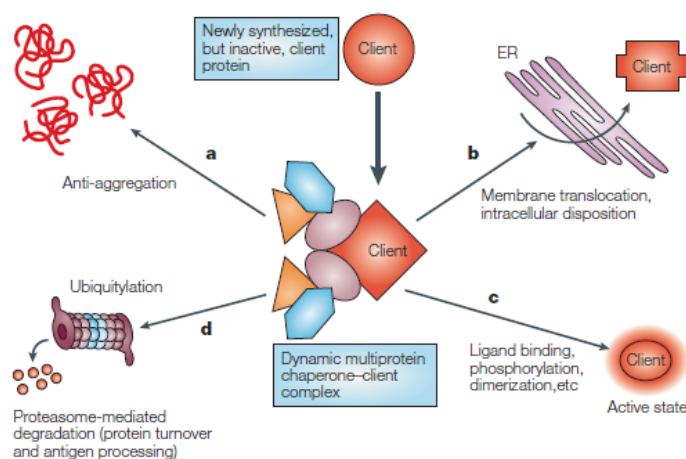**Figure 7.13**: Biological roles of chaperones.

In general, the intracellular expression of Hsp increase in response to protein-denaturing stressors, such as temperature change, as an evolutionarily conserved response to restore the normal protein-folding environment and to enhance cell survival. However, most chaperones are ubiquitously expressed under normal conditions: Hsp90, specifically,

comprises as much as 1–2 % of total cellular protein content, even under non-stressed conditions. Hsp90 important role in cellular functionality, *i.e.* its ability of prevent protein-denaturation, led researchers to develop a general approach to perturb this essential chaperone by impairing its pivotal functional dynamics through the modulation of its ATPase processes.[142]
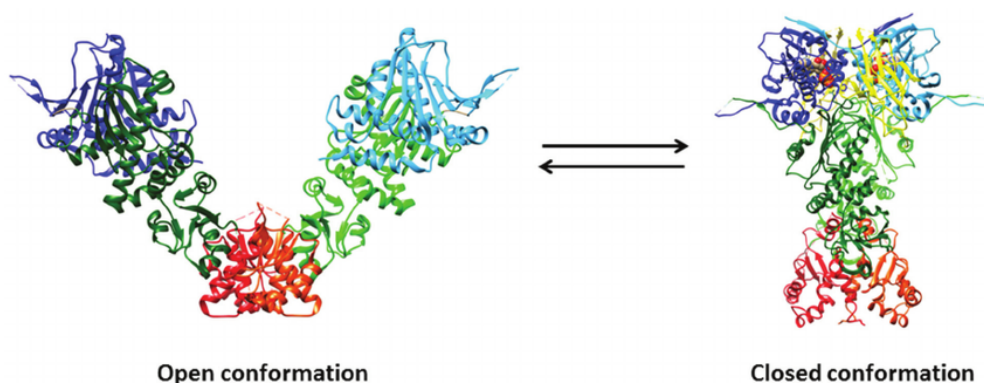
Figure 7.14: Crystal structures of open (ligand-free) full-length Hsp90 from *E. coli* and closed (ATP- and co-chaperone-bound) yeast Hsp90. The N -domain is depicted in blue and cyan, the middle domain in dark green and light green, and the C -domain in red and orange. The p23 co-chaperone is in yellow, whereas ATP is depicted through a space-filling representation.

Specifically, Hsp90 dynamics depend on ATP binding and hydrolysis, which underlies the onset of conformational transitions between substrates with different functional properties. Hsp90 works as a homodimer with a common modular organization in terms of *N*-terminal (NTD), middle (M) and *C*-terminal (CTD) domain. The CTD domain is the dimerization domain, while the NTD contains an ATP-binding site.[146] ATPase activity is essential for Hsp90 to work and requires transient dimerization of the NTD in a closed state of the dimer (**Figure 7.14**). The exact mechanism of coupling between ATP binding/hydrolysis and client folding remains elusive. A possible model, supported by biochemical data, involve a nucleotide binding at the NTD which propagates a conformational signal to the CTD. The chaperone undergoes conformational rearrangements that bring the two NTDs into close association in the ATP-state and into an open one in the ADP-state. The formation of the closed state can be therefore induced by ATP. After ATP hydrolysis, the protein cycles back to the open ADP-bound state.

In **Figure 7.15** interactions of Hsp90 with clients and co-chaperone and its consequent conformational changes are shown. As an example, the co-chaperone Aha1 is an Hsp90 ATPase activity activator, while Sba1 acts as inhibitor by binding selectively to the closed conformation, thus blocking the chaperone dynamics.

Figure 7.15: Hsp90 structure and its conformational equilibrium. AS= allosteric site; Aha1= co-chaperone; Sba1= co-chaperone; Δ131Δ= client protein.

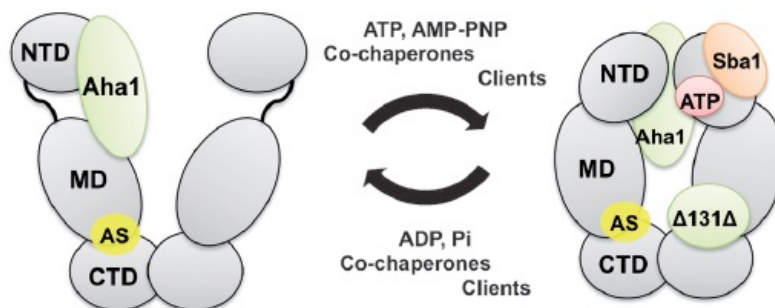Learning from Nature, the design of potential small-molecules modulators able to perturb Hsp90 ATPase activity, thus impairing its essential conformational dynamics, has emerged as a promising approach in the field of drug discovery.

Hsp90 synthetic allosteric modulators

The modulation of Hsp90 conformational dynamics using small-molecules modulators can potentially occur by the action of both inhibitors or activators of its ATPase activity.

Most of the known Hsp90 modulators acts as ATPase activity inhibitors by interacting with the chaperone at the NTD. Some of these compounds has also been tested as antitumor drugs. Interestingly, most of tested compounds, have shown some limitations due to their ability of completely inhibit the ATPase activity of Hsp90 inducing the so-called 'heat shock response' (**Figure 7.16**). As a prosurvival cell mechanism that cause a different aggregation of filament-forming proteins, the heat shock response can limit the action of a potential drug, especially in eukaryotes, where it leads to the disruption of the cytoskeleton, the loss of the correct localization of organelles and a breakdown of intracellular transport processes.[147]
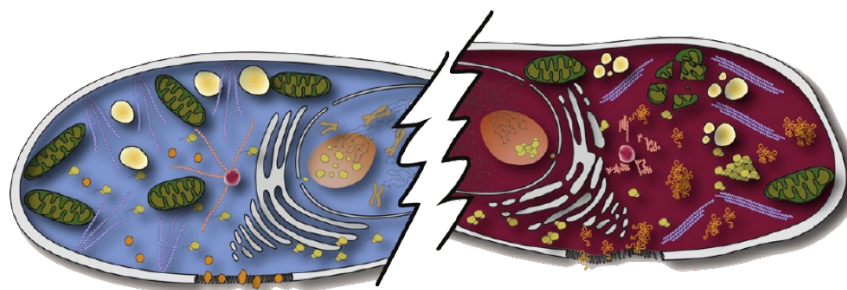
Figure 7.16: Effects of heat shock on the organization of the eukaryotic cell

In this context, Bernardi, Colombo *et al.* have investigated the rational design of chemical compounds to select and activate Hsp90 key substrates, avoiding the mentioned heat shock response and targeting an allosteric pocket 'AS' of protomer B (**Figure 7.15**). Moreover, the authors sought a connection between protein activities, cellular outcomes and small molecular scaffolds.[148,149,150] Thanks to their studies it was demonstrated that the three families of 2-(4-hydroxyphenyl)-3-methylbenzofuran-based Hsp allosteric ligands showed in **Figure 7.17** possess a structure-dependent ability to stimulate ATPase process and to alter conformational dynamics, favoring synergistic effects with the activating co-chaperone Aha-1, to modulate Hsp90 direct interactions with the co-chaperone Sba-1 (inhibitor of ATP-hydrolysis) and to compete with the client protein Δ131Δ (**Figure 7.15**).
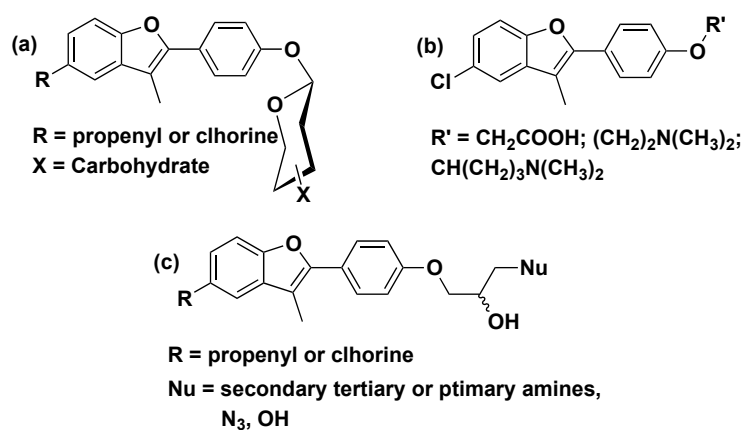
Figure 7.17: Novel Hsp90 allosteric ligands: first (**a**), second (**b**) and third (**c**) generation ligands. Their rational design was based on a set of computational experiments focused on targeting an allosteric site located at the MD/CTD interface, alternative to the ATP binding site. The best candidates were then synthetized and tested as allosteric modulators by measuring their effects on the ATPase activity of the Hsp90 yeast homologue (Hsc82). Following *in silico* experiments were run to optimize the structures afforded the second and third generations ligands by introducing substituents able to induce H-bonding.

2,3-Dihydrobenzofuran-based potential modulators

As described by Bernardi, Colombo *et al.*, allosteric ligands with 2-(4-hydroxyphenyl)-3-methylbenzofuran structure can act as activators of Hsp90's ATPase cycle. Moreover, their optimization may lead to new effective anticancer drugs with novel mechanisms of action, based on the perturbation of the Hsp90 machinery. Specifically, the acceleration of conformational dynamics could be translated into impaired chaperone functions and consequent cell death.

Intrigued by their elegant results, in **Submitted Manuscript I**, both the synthesis and the *in vitro* evaluation of a family of substituted (±)-*trans*-2,3-dihydrobezofurans (**i**) as potential allosteric modulators of the Hsp90's ATPase were investigated. At variance to the compounds proposed by Bernardi, Colombo *et al.*, it was decided to introduce a remarkable affinity for π-aryl interactions and more conformational freedom. Accordingly, our structure activity relation studies (SAR) were focused on the introduction of two aryl groups at the R and C_3-positions of the parental benzofuran moieties (**p**) (**Figure 7.18**), as the pivotal substitution at the R' group had been extensively investigated in the previous works reported by the authors. Moreover, as a convenient and easy entry to a broad family of analogues was cherished, it was decided to exploit the oxidative coupling of *E*-stilbenes which is reported to produce dihydrobenzofurans as racemic mixtures of *trans*-2,3-diastereosimoers. Thus, the C_2 and C_3-position of the benzofuran moieties (**i**) were fully saturated.
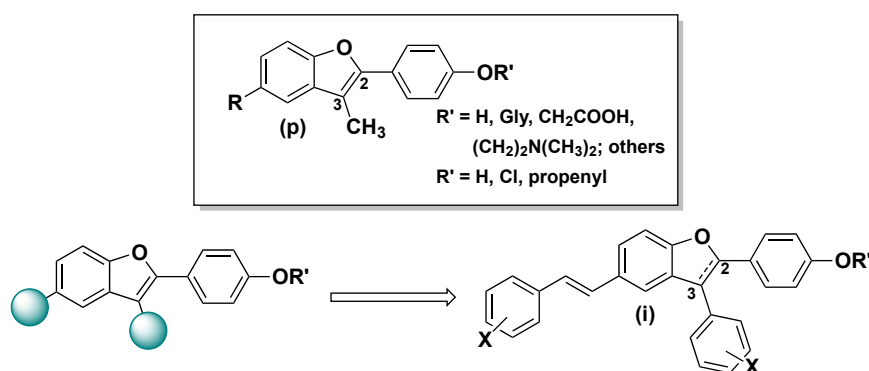
Figure 7.18: 2,3-dihydrobenxofurans-based potential modulators (**i**).

As previously introduced, a convenient, scalable and selective entry was needed to easily access a library of R, C_3-modiefied compounds to be tested for their potential Hsp90's dynamics modulating effects. After a careful evaluation of other commonly chemical oxidants available to access the target compounds staring from differently substituted (*E*)-4-styrylphenols (**ii**), the previously described laccase-mediated synthesis of oxygenated heterocycles was selected as the key synthetic step. The retrosynthetic approach is proposed in **Figure 7.19**.
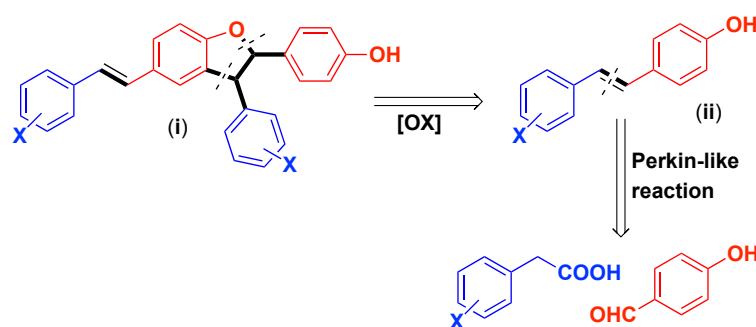
Figure 7.19: Retrosynthetic analysis.

Most of the modern synthetic entries to 4'-hydroxy-*E*-stilbenes (**ii**) relay on the use of Pd-catalyzed Heck reactions[151,152] or *trans*-selective reduction of alkynes,[153, 154] but a metal and catalyst-free, cheap and versatile methodology to easily synthetize a broad family of styrylphenols is still cherished. As such, the microwave-based strategy proposed by Sinha and co-workers[155] has been deeply investigated. The authors, starting from substituted benzaldehydes and phenylacetic acids could successfully produce various *E*-stilbenes under microwave irradiation in the presence of piperidine, imidazole and PEG.

To further simply this convenient strategy, a study proposed by De Filippis *et al.* was used as starting point.[156] The one-pot synthesis of (*E*)-4-styrylphenols has been achieved by heating to 130 °C a concentrated DCM-solution of 4-hydroxy benzaldehyde, a substituted phenylacetic acid and piperidine, distilling the solvent and reacting the obtained neat mixture for 12-24 h. Surprisingly, using these pretty harsh conditions, the authors reported that the target *E*-stilbenes could be obtained in modest to very good yield, depending on the

substitution pattern of the phenylacetic acid used. Specifically, electron-donating groups on the aromatic ring affected negatively the overall yield of the process by impairing the decarboxyative-formation of the C-C (*E*)-double bond, a key-step in mechanism of the transformation; the best results were instead obtained with electron-poor phenylacetic acids.
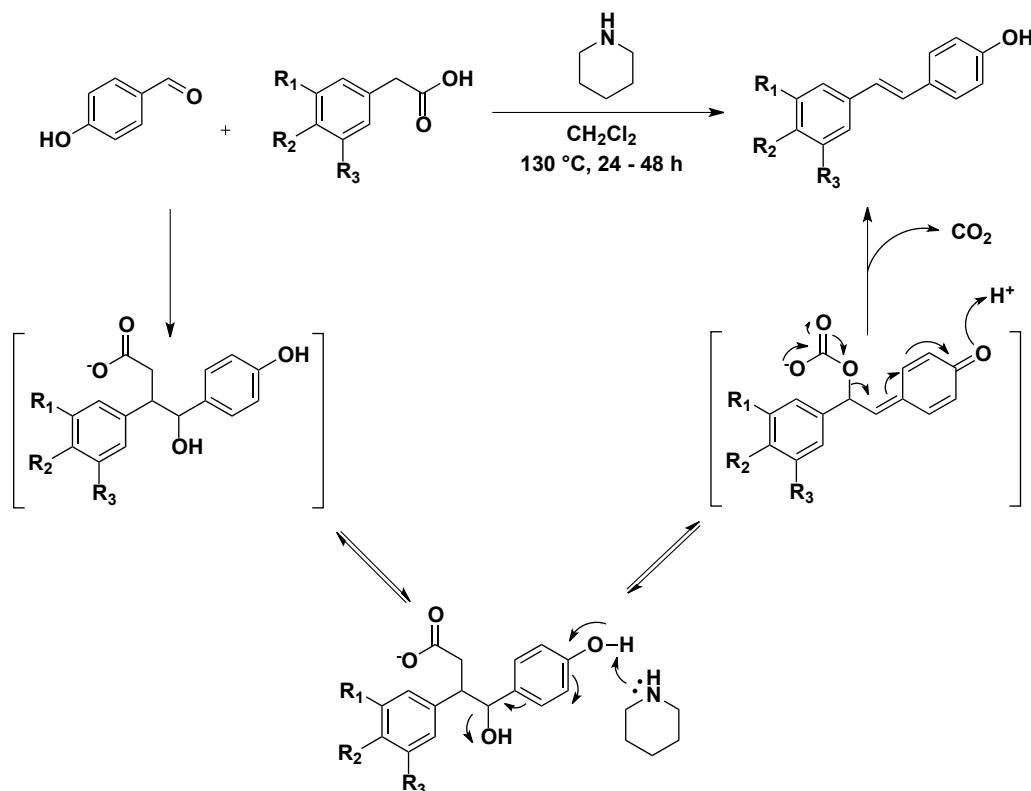
Scheme 7.8: Proposed mechanism for the catalyst-free synthesis of (*E*)-4-styrylphenols.

A proposed mechanism for this interesting transformation is shown in **Scheme 7.8**. At first, benzaldehyde and phenylacetic acid undergoes an aldol condensation to form an *α*-hydroxy carboxylate species that interacts with piperidine to give a quinone-like intermediate. A subsequent decarboxylation gives the final product hydroxy-*E*-stilbene. Along with a rational explanation of the lower yield obtained by the authors with electron-rich phenylacetic acids, this mechanistic proposal also underlines the key role of 4-hydroxy benzaldehyde, as its C-4 hydroxyl group appears essential for the good functioning of the reaction. Moreover, this

was further confirmed conducting a control-reaction between *p*-hydroxy-phenylacetic acid and benzaldehyde: no products were formed.

On the base of these results, the reaction conditions proposed in De Filippis's work were further investigated and optimized, focusing on reaction stoichiometry. After a small set of experiments, the best results in terms of isolated yield of the desired *E*-stilbenes were obtained using 2.4 equivalents of phenylacetic acid and 2.5 equivalent of piperidine. In this way, a library of p_{10}- and $m_{9(11)}$- substituted and m_9, m_{11} di-substituted (*E*)-4-styrylphenols was synthetized starting from commercially available phenylacetic acids, as summarized in **Table 7.1**.
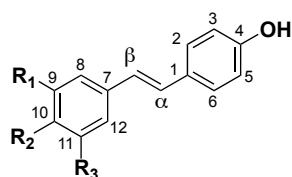
Entry	Compound	R₁	R₂	R₃	Yield %	Reaction Time (h)
1	7.5	H	H	H	52	24
2	7.6	H	CH₃	H	44	48
3	7.7	H	CN	H	64	24
4	7.8	H	NO₂	H	62	18
5	7.9	H	OCH₃	H	38	28
6	7.10	CH₃	H	H	28	24
7	7.11	CN	H	H	60	24
8	7.12	SCH₃	H	H	57	48
9	7.13	OCH₃	H	OCH₃	28	48
10	7.14	CH₃	H	CH₃	39	72

Table 7.1: Synthetized substituted (*E*)-4-styrylphenols.
Reagents and conditions: 4-hydroxybenzaldehyde, phenylacetic acid, piperidine, DCM, 130 °C, 24 h.

Evidence of the formation of the desired *E*-stilbenes came from ^{1}H-NMR analysis. Indeed, the spectra showed all the expected aromatic and (if any) aliphatic signals as well as the presence of a (*E*)-olefin bond (two doublets resonating between 7.20-7.50 ppm with

coupling constants of ca. 16.0-16.5 Hz, a typical value for a *E*-configured C-C double bonds). All the synthetized stilbenes were characterized by ^{1}H-NMR and, when possible, compared with previous literature reports. As expected, the presence of electron donating groups on phenylacetic acid *para* and *meta* position caused a decreasing in reaction rates and yields (entries **2, 5, 6** of **Table 7.1**). Again, the presence of two electron-donating groups on the phenylacetic acid moiety, *i.e.* two methoxy groups and two methyl groups (**9** and **10** of **Table 7.1**), produced a substantial decrease of reactivity.

Once compounds **7.5**-**7.14** have been synthetized, their oxidative coupling to give the target 2,3-dihydrobenzofuran-based scaffolds (**i**) was studied.

As previously stated, different chemical oxidants (MnO_2, $FeCl_3$ and $CuCl_2$) were investigated, using compound **7.5** as a model. Oxidations with iron(III) trichloride and copper(II) chloride, conduced in a solvent made by a monophasic mixture of ethanol and water as solvent, gave a complex mixture of oxidized products (TLC plate shown in **Figure 7.20**) and thus these compounds were discarded.

The oxidation with manganese(IV) oxide, run under the same experimental conditions, gave better results. The reaction run smoothly and, as shown **Figure 7.21A**, a single spot could be detected by TLC. Unfortunately, the ^{1}H-NMR spectrum of the isolated product showed the presence of an inseparable mixture of oxidized compounds, as further confirmed by reverse-phase HPLC analysis, containing as major product the desired di-hydrobenzofuran structure, (**Figure 7.21B**).

Given these selectivity issues, as more than one regioisomeric oxidized products were always obtained by chemical means, the mentioned laccase-mediated system for the activation of Csp^2-H bonds. Due to the design of the stilbenic substrates carrying only one oxidizable phenolic moiety, the synthesis of the target heterocyclic compound could be in principle selectively promoted by the redox action of laccases' tetratomic copper cluster.

As it was previously reported by our research group for the oxidation of resveratrol,[157] the oxidation of the model substrate **7.5** was conducted using the commercially available laccase

from *Trametes versicolor* and a 1:1 mixture of acetate buffer (pH 4.5, 50 mM) and acetone as solvent. The reaction proceeded smoothly, and the only detectable product (TLC analysis) was isolated by silica gel chromatography and analyzed by Mass spectroscopy, ^{1}H- and ^{13}C-NMR. The ^{1}H-NMR spectra underlined the formation of the dihydrodimers. Specifically, besides the signals of the aromatic protons, the presence of the target 2,3-*trans*-dihydrobenzofuran was verified by the presence of two doublets resonating at 5.53 and 4.60 ppm characterized by the typical value of trans-coupling constants in oxygenated 5-memberd rings (J ca. 8.58 Hz). Moreover, two doubles resonating at 7.06 and 6.92 and showing the typical value of *E*-configured C-C double bonds (J ca. 16.5 Hz) were detected, attesting the presence of *E*-double bond between C_α and C_β.
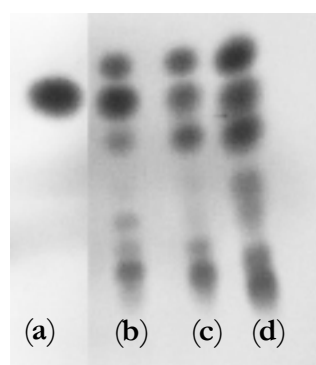
Figure 7.20: TLC plate of the reaction outcome of the CuCl$_2$-mediated oxidation of **7.5**:
(**a**) standard of **7.5**; (**b**) 3 h reaction; (**c**) overnight reaction; (**d**) 24 h reaction.
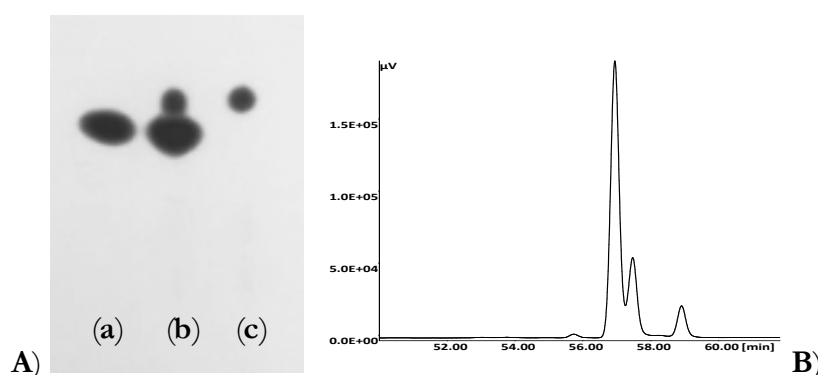
Figure 7.21: **A**) TLC plate of the reaction outcome of the MnO$_2$-mediated oxidation of **7.5**:
(**a**) standard of **7.5**; (**b**) co-chromatography of **a** and **c**; (**c**) 24 h reaction.
B) HPLC chromatogram of **c**.

Thanks to the action of laccases, the target oxygenated heterocycle **7.15** (with the proper stereochemistry) was obtained in a remarkable 76 % isolated yield from stilbene **7.5**. As a comparison, in **Figure 7.22** the HPLC chromatograms of **7.15** (**A**) and the mixture of inseparable products obtained by the oxidation mediated by MnO_2 (**B**).

These results pointed out how the use of the selected biocatalyst could allow a convenient and selective entry to **7.15**, working with a cheap, non-toxic and environmental-sustainable (oxygen is consumed and water produced) 'masked' metal catalysts under mild reaction conditions.
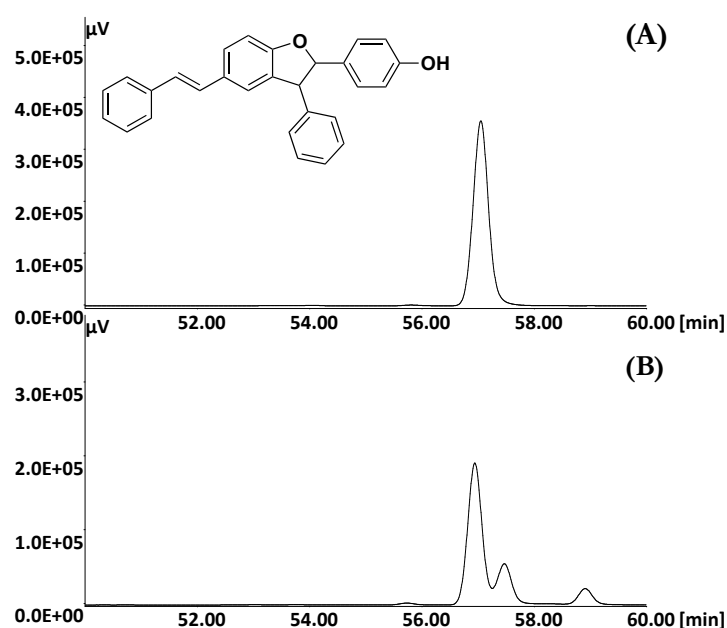
Figure 7.22: HPLC chromatograms of **7.15**, obtained by laccase-mediated oxidation (**A**), and the mixture of oxidized products obtained *via* the oxidation with MnO₂, enriched in **7.15** (**B**).

Once verified that the laccase catalyzed oxidation was the best method for the selective preparation of the target (±)-*trans*-dihydrobenzofuran **7.15** from stilbene **7.1**, the same protocol was applied to the other synthetized 4-(*E*)-styrylphenols. The commercially available resveratrol (**iii**), whose biooxidation usually gives different oxidized products, was also subjected to the action of laccases from *T. versicolor*, aiming at isolating its natural dimer ε-viniferin (compound **7.16**, **Figure 7.23**). This natural compound, in fact, possesses the

same (±)-*trans*-dihydrobenzofuran structure and four different OH groups, potential promoters of H-bonding bridges during the binding event with Hsp90.
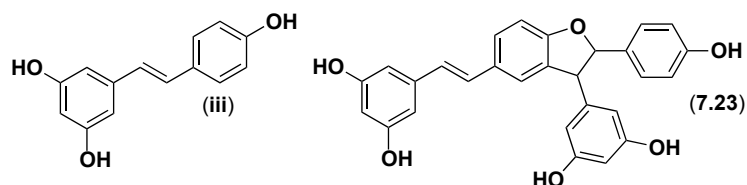
Figure 7.23: Structures of resveratrol (**iii**) and e-viniferin (**7.16**).

The obtained results are summarized in **Table 7.2**. In all cases the oxidations proceeded smoothly and the expected (±)-*trans*-dehydrodimers were isolated in 55-74 % isolated yield after 24 h of reaction.
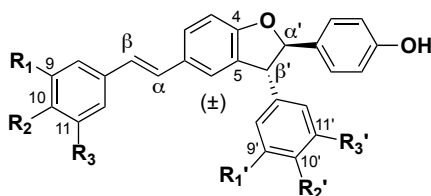
Entry	Substrate	Product	R_1	R_2	R_3	Yield %
1	7.5	7.15	H	H	H	52
2	7.6	7.16	H	CH_3	H	60
3	7.7	7.17	H	CN	H	74
4	7.8	7.18	H	NO_2	H	68
5	7.9	7.19	H	OCH_3	H	55
6	7.10	7.20	CH_3	H	H	46
7	7.11	7.21	CN	H	H	49
8	7.12	7.22	SCH_3	H	H	57
9	(**iii**)	7.23	OH	H	OH	33
10	7.13	7.24	OCH_3	H	OCH_3	58
11	7.14	7.25	CH_3	H	CH_3	69

Table 7.2: Synthetized racemic-*trans*-2,3-dihydrobenzofurans.
Reagents and conditions: laccases from *T. versicolor* (42 U $mmol_{substrate}^{-1}$) acetate buffer (pH 4.5, 50 mM), acetone, 27 °C, 160 rpm, 18 h.

The lower yield obtained with resveratrol could be due to presence of more than one oxidizable phenolic OH: by-products and over-oxidations are very likely to occur with such a reactive substrate. All products were fully characterized by means of mass spectroscopy and ^{1}H- and ^{13}C-NMR.

Moreover, in order to increase the number of compounds available for subsequent *in vitro* testing, it was decided to reduce the nitro groups of compound **7.18** to afford the di-amine derivative **7.26**. In this way, a potential H-bonding group could be inserted in the *para-* positions of scaffold (**i**). This task was accomplished exploiting the metal-free method developed by Benaglia and co-workers for the reduction of aromatic nitro compounds, which consisted in the use of trichlorosilane in combination with DIPEA.[158]

Form the reduction of **7.18**, the diamine **7.26** was obtained 21 % isolated yield, its sctructres being confirmed by both NMR and mass analysis. Moreover, during the purification process, the two mono-amines derivatives **7.27** and **7.28** were also isolated in 3 % and 8 % yield respectively (**Figure 7.24**).
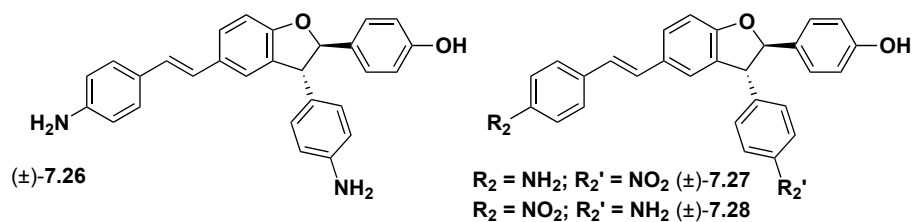
Figure 7.24: Reduced compounds from **7.18**.

The structural attribution of compounds **7.27** and **7.28** was far from being easy, as the two regioisomers shares the same molecular weight and shows very similar NMR spectra. Our hypothesis for the attribution was based on their TLC spots. The two compounds, in fact, showed different Uv-Vis-responses. One, as its parental compounds **7.8** and **7.18**, appeared yellow in the Vis-spectrum and responds with a bright spot when irradiated with Uv-light at 254 nm. At variance, the other was only Uv-responsive. Since the starting material showed a similar behavior, the structure of the mono-amine **7.27**, in which a fully conjugated nitro group is still present, was attributed to the yellow compounds.

In vitro screening

Having a battery of compounds available thanks to the described selective chemo-enzymatic synthesis, the potential activity of compounds **7.15**-**7.27** as allosteric modulators of the Hsp90's ATPase cycle was tested. As previously stated, the interaction of these chemicals with the allosteric binding site of Hsp90 can impair the natural chaperon functions of the protein by perturbing its essential conformational dynamics during ATP-hydrolysis, acting both as inhibitors or activators.

The homologue chaperone Hsc82 from yeast was used for the *in vitro* screening, thanks to its higher availability. The selected test, as reported by Sattin *et al.*, consisted in a colorimetric assay in which the hydrolysis of ATP, promoted by the previously discussed Hsp90's dynamics, was coupled with the final oxidation of NADH to NAD$^+$ (nicotinamide adenine dinucleotide, **Figure 7.25**) in a set of cascade reactions catalyzed by the enzymes pyruvate kinase and lactate dehydrogenase, as shown in **Scheme 7.9**.[148]
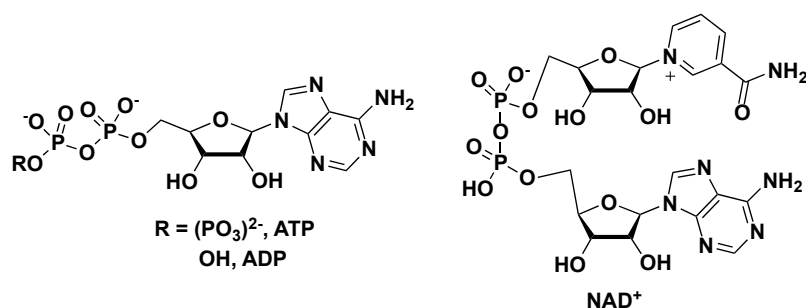
Figure 7.25: ATP, ADP and NAD$^+$ structures.
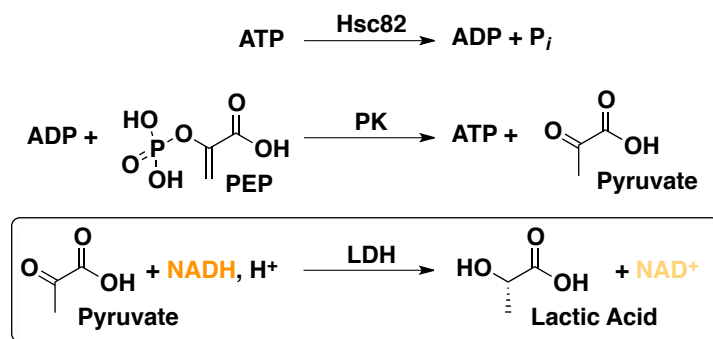
Scheme 7.9: Enzymatic cascade reactions to evaluate by spectrophotometer the ATPase activity of Hsc82.

The ADP produced by the ATPase hydrolysis cycle of Hsc82, reacts with PEP (phosphoenaolpyruvate) to form pyruvate in a reaction catalyzed by the enzyme pyruvate kinase (PK), whereby ATP is regenerated. Pyruvate then continues the cascade process and is reduced to lactic acid by action of lactate dehydrogenase (LDH), whereby NADH is oxidized to NAD$^+$. As NADH has a maximum of absorbance in the Vis-light at 340 nm, the Hsc82-dynamics and ATPase cycle can be easily monitored by following the continuous decrease in absorbance at the listed wavelength (A_{340}).[159]

Entry	Compound	ATPase Normalize Activity	STD
1	DMSO	1.00	0.07
2	7.15	1.10	0.07
3	7.16	0.70	0.05
4	7.17	0.80	0.10
5	7.18	1.10	0.10
6	7.19	1.00	0.14
7	7.26	1.40	0.14
8	7.27	0.90	0.05
9	7.28	0.90	0.02
10	7.20	0.90	0.10
11	7.21	1.00	0.05
12	7.22	1.20	0.05
13	7.23	2.50	0.10
14	7.24	0.90	0.05
15	7.25	1.00	0.09

Table 7.3: Results of the ATPase assays for compounds **7.15**-**7.28** and standard deviations.
All compounds were tested three times and standard deviations were calculated accordingly.

At first, the 'native' ATPase activity of Hsc82 was tested in presence of DMSO (the solvent used to dissolve compounds **7.15**-**7.27**) to set a standard value to be used to normalize all the forthcoming experiments. After that, all the synthetized potential modulators were tested

by preparing an HEPES (20 mM, pH 7.5) solution containing KCl (100 mM), MgCl$_2$ (1 mM), PEP (1 mM), NADH (0.18 mM), LK (2.5 U ml^{-1}), LDH (4 U ml^{-1}), Hsc82 (2 µM) and the desired dihydrodimer **7.x** (50 µM). The enzymatic cascade was initiated by addition of ATP (final concentration of 1 mM).

The results obtained with the *in vitro* screening of **7.15**-**7.27** are summarized in table **Table 7.3**. As shown, only compound **7.23** (entry 13) could promote a relevant increasing (2.5 times) in the normalized ATPase activity, maybe due to its remarkable H-bonding capacity.
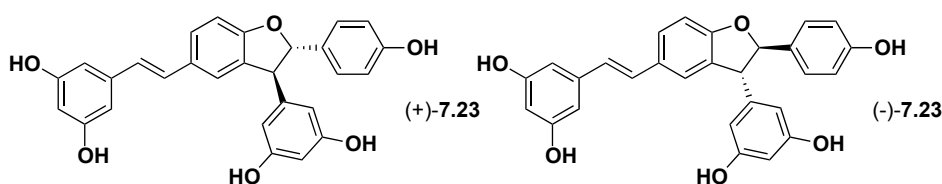
Figure 7.26: Enantiomers of **7.23**.

Entry	Compound	ATPase Normalize Activity	STD
1	DMSO	1.00	0.07
2	(±)-7.23	2.50	0.10
3	(-)-7.23	2.40	0.11
4	(+)-7.23	2.30	0.10

Table 7.4: Normalized ATPase activity of the two enantiomers of compound **7.23** and its isolated enantiomers.

Since all the tested dimers were a racemic form of trans enantiomers, it was of interest to verify whether their single enantiomers could give different results. The two enantiomers of the **7.23** were already available in our laboratory as they had been synthetized during previous studies.[141] The isolated compounds (-)-**7.23** and (+)-**7.23** (**Figure 7.26**) were also tested and the results compared with the one obtained with the racemic mixture of the same compound (**7.23**). The Hsc82's ATPase modulation efficiency of racemic **7.23** turned out to be comparable with the *in vitro* activity of the two isolated enantiomers, as shown in **Table 7.4**.

Therefore, the isolation of the enantiomers of the other dimers has been considered unnecessary.

During their studies Bernardi, Colombo *et al*[148] found that the alkylation with amine-containing chains of the 4-hydroxyl group of the 2-(4-hydroxy-phenyl)-3-methylbenzofuran scaffold (second and third generation ligands) led to an increase in their ability to stimulate ATPase process. Accordingly, it was decided to investigate this possibilities with a small selection of compounds **7.15**-**7.28**, to couple a *N,N*-dimethylethanamine side chain whose beneficial effects on the stimulation activity had already been reported.[148] Specifically, the alkylations of the 4-phenolic group of compound **7.15**, **7.24** and **7.25** were successfully accomplished according to published protocols, producing compounds **7.29**, **7.30** and **7.31** (**Figure 7.27**).

(**7.29**): $R_1 = R_3 = R_1' = R_3' = H$;
(**7.30**): $R_1 = R_3 = R_1' = R_3' = OCH_3$
(**7.31**): $R_1 = R_3 = R_1' = R_3' = CH_3$
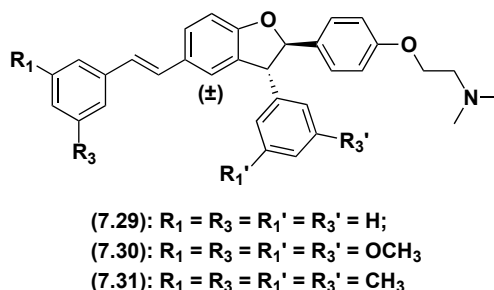
Figure 7.27: Compounds **7.29**, **7.30** and **7.31**.
Reagents and conditions: 2-chloro-*N,N*-dimethylethylamine hydrochloride, tetrabutylamonium hydrogen sulfate and K_2CO_3 , $CHCl_3$, H_2O, 50 °C, 24 h. Isolated yields: 35 % (**7.29**), 60 % (**7.30**) and 21 % (**7.31**).

At first, compound **7.29** was synthetized to demonstrates the activation effects reported from tertiary amines on 2,3-dihydrobenzoduran moieties using the 'nude' skeleton of **7.15**. Then, to investigate the possibility of activating potential Hs82's ATPase modulators sharing structural similarities with compound **7.23** (*i.e.* compounds **7.24** and **7.25**) were produced and tested as well. Despite its promising Hsc82's ATPase modulation activity, compound **7.23** was not further alkylated. The presence of five phenolic groups, in fact, could have led to an unselective poly-alkylation, producing a poly-amine compound. The presence of more than one charged residue could indeed affect the pharmacodynamics and kinetics of the

obtained compound. Moreover, the alkylation of the 4-(*E*)-styrylphenols OH group would have irremediably affected their laccase-mediated oxidative couplings.

Entry	Compound	ATPase Normalize Activity	STD
1	DMSO	1.00	0.07
2	7.15	1.10	0.07
	7.29	2.30	0.24
3	7.24	0.90	0.05
	7.30	0.90	0.02
4	7.25	1.00	0.09
	7.31	1.00	0.02

Table 7.5: Normalized ATPase activity of the alkylated compounds
7.29, **7.30** and **7.31**.

The *in vitro* testing of the alkylated compounds **7.29**, **7.30** and **7.31** demonstrated the ability of the *N,N*-dimethylethanamine side chain to promote the modulation activity of the 2,3-dihydrobenzofuran scaffolds, as the incubation of compound **7.29** with Hsc82 showed a 2.3 increasing in the ATPase activity. Unfortunately, the same was not true for the alkylation of the more sterically-demanding compounds **7.24** and **7.25**, as shown in the data collected in (**Table 7.5**). This might mean that steric hindrance could have affected the right orientation of the tertiary amine in the allosteric pocket of the protein, thus impairing its activation effects. Computational studies to confirm these hypotheses and evaluate the binding efficiencies of all the tested compounds are now in progress.

Docking studies

To assess at molecular level which are the binding properties that guide the efficiency in modulating Hsp90 ATPase activity of the active compounds, protein-ligand docking calculations are being performed (Colombo, D'Annessa *et al,* ICRM-CNR). The preliminary obtained results were well in agreement with experimental assays. Indeed, compound **7.23** was the strongest binder with a predicted binding energy of -10.024 kcal mol^{-1} calculated for the best pose obtained (**Figure 7.28**).
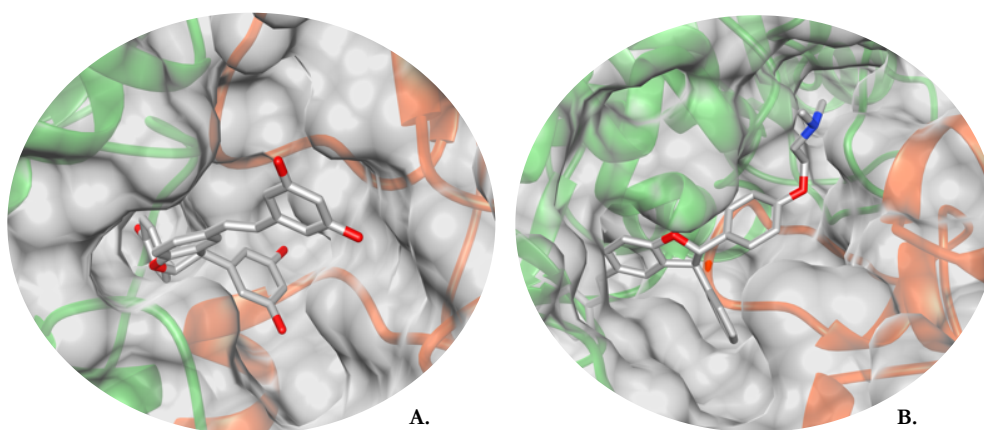

Figure 7.28: Docking of **2*S*,3*S*-7.23** (**A**) and **2*S*,3*S*-7.29** (**B**).

Thanks to the presence of the hydroxyl substituents in positions R_1, R_3, R_4 and R_6 thus compound established a series of hydrogen bonds with residues L502, D503, R591 and L658 all belonging to protomer B, thus strongly stabilizing the closed and activated structure of the target protein, which supports the high modulatory activity observed for **7.23**. This behavior was also in line with previous results on a series of the different, yet related, benzofuran-based compounds.[148, 150] Indeed, elimination of such substituents able to form hydrogen bonds strongly decreased the binding affinity, as in the case of compounds **7.5, 7.24, 7.25, 7.30** and **7.31.** Interestingly, neither the addition of a methylamine substituent in position R_7 as for **7.30** and **7.31**, potentially favoring the formation of hydrogen bonds or salt bridges, restored the binding efficiency. This was not the case however with compound **7.29**, the R_7-dimethylamine derivative of **7.5**. While **7.5** was inactive, an effect in promoting ATPase activity by **7.29** was observed, at similar extent when compared to **7.23** (2.30 ± 0.14

vs 2.50 ± 0.10). **7.29** formed a hydrogen bond and a salt bridge, both with D503 from protomer B.

It is possible to argue that the introduction of a dimethylamine substituent in position R_7 is beneficial only when the other phenyl rings are not substituted. Indeed, the presence of larger groups in positions R_1-R_6 increases the steric hindrance of the compounds that adopt a less suitable conformation into the binding pocket, thus affecting the stability of the binding. Furthermore, the presence of a dimethylamine at the terminal of a flexible carbon chain was previously observed to correlate with Hsp90 ATPase activation, consistent with what observed here.
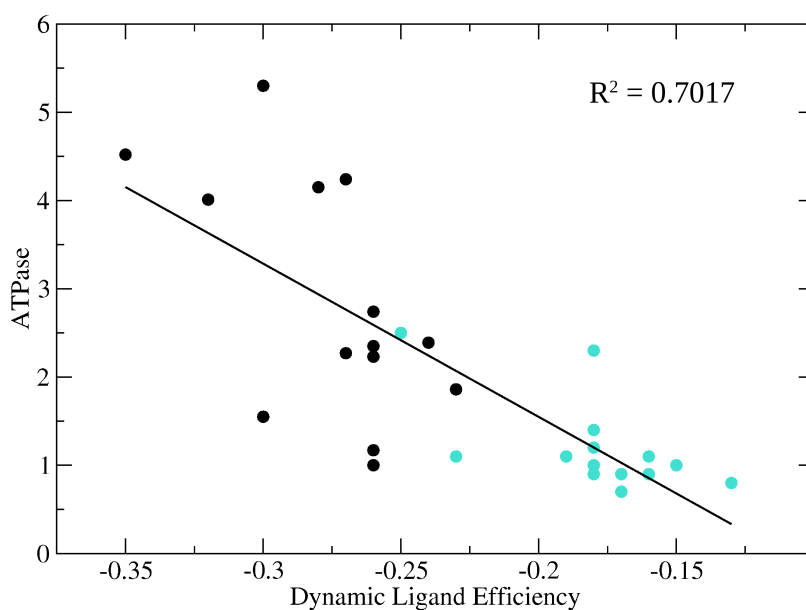
Figure 7.29: Correlation between the DLE parameter and the measured ATPase activities. The blue spots represent the compounds synthetized in this study.

It's noteworthy that **7.23** and **7.29**, compounds exerting the same degree of stimulation of ATPase activity, share an asymmetric binding mode, both exclusively establishing direct interaction with residues from only one protomer. Hsp90 is characterized by a closed nucleotide-bound state in which ATP hydrolysis happens in a sequential mode, with the most reactive protomer being significantly distorted. The active conformation of the protein, *i.e.* the one possessing kinase activity, can be described as a family of asymmetric ensembles in which one of the two protomers is conformationally perturbed. It was therefore hypnotized

that the by binding of **7.23** and **7.29** could be able to stabilize these activated ensembles, thus resulting in the promotion of the hydrolysis of ATP hydrolysis and the acceleration of the chaperone cycle.

Finally, it is interesting to underline that a significant correlation could be found between the Dynamic Ligand Efficiency (DLE), a calculated parameter associating the predicted docking scores in a multiconformational protein to simulated ATPase stimulations, and the ATPase activities experimentally measured in the presence of the designed potential allosteric ligands (**Figure 7.29**). Interestingly, the correlation between the DLE of the set of newly designed compounds together with the ones previously described in the previously works done by Colombo *et al.* and the measured ATPase stimulations, turns out to provide an interesting linear correlation coefficient of -0.80 (-0.61 on the new series alone). This finding supports the validity of the Quantitative Structure Dynamics Activity Relationship model for the design of allosteric activators of Hsp90.

Conclusions

A chemo-enzymatic synthesis of (±)-2,3-*trans*-dihydrobenzofurans was successfully proposed and validated by the preparation of a small library of oxygenated heterocyclic compounds. Moreover, the outstanding selectivity of the laccase-mediated oxidation for the regio-selective production of compounds **7.15**-**7.25** with the respect to use of stoichiometric chemical oxidants has been also demonstrated.
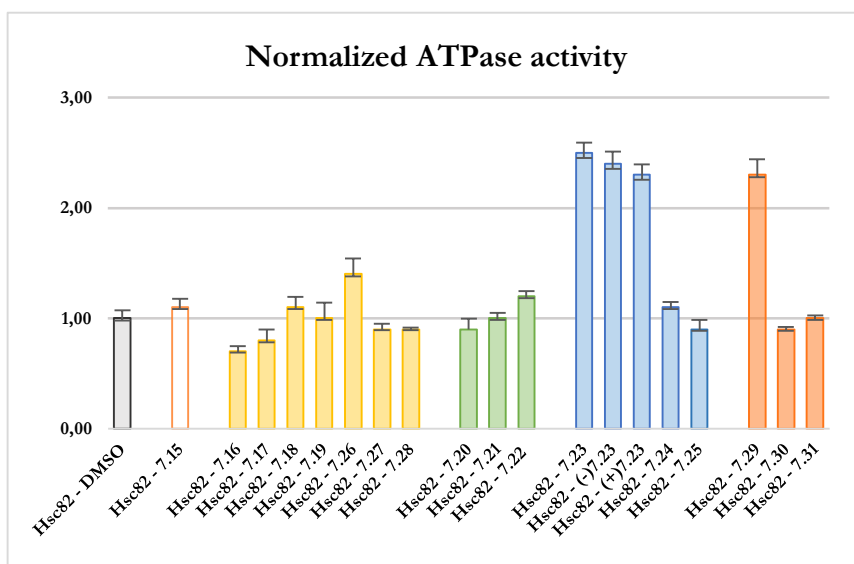

Figure 7.30: Normalized Hsc82-ATPase activity in the presence of un-substituted (**white**), *p*-bisubstituted (**yellow**), *m*-bisubstituted (**green**), *m, m'*-tetrasubstituted (**blue**) and amine-modified (**red**) (±)-2,3-dihydrobenzofurans.

A structure relation activity (SAR) study has been conducted on the R and C_3-position of the scaffolds previously proposed by Colombo *et. al*, by integrating experimental data and computational analysis. It has been demonstrated that, in general, a bulky substitution at the mentioned portion of the molecules affected negatively the modulation of the Hsp90's kinase activity of the parental reported scaffolds, unless H-bonding interactions could be provided (as in the case of compound **7.23**)

The conjugation with an alkyl chain bearing a tertiary amine promoted, as expected, an increased modulation activity toward the Hsp90's ATPase cycle but only in the case of the less sterically demanding compound **7.29** which did not possess decorations on the aromatic rings. Molecular dynamics are now being run to further investigate the binding event between the small family of amine-containing compounds **7.29-7.31** and verify this hypothesis.

Compounds **7.23** and **7.29** have both demonstrated a high ability to activate the Hsp90 ATPase cycle, thus potentially impairing its chaperone functions (as shown in **Figure 7.30**). Docking studies have shown how compounds **7.23** and **7.29** are capable to interact with specific aminoacidic residues of protomer B of Hsp90 *via* a set of hydrogen bonding and, in the case of **7.19**, charge interactions.

Moreover, thanks to these results, the efficiency in predicting the Hsp90's ATPase cycle modulation activity of small molecules of the Quantitative Structure Dynamics Activity Relationship model for the design of allosteric activators of Hsp90 proposed by Colombo *et al.* (**Figure 7.29**) was underlined (linear correlation coefficient of -0.80).

The aromatization of compounds **7.23** and **7.29**, to restore the reported benzofuran moiety of the compounds proposed by Colombo, Bernardi, Sattin *et al.* is now being investigated.

7.5 Experimental

7.5.1: Glucoside chemical synthesis

(*i*) Peracetylated glucose (1 equiv, final concentration 0.1 M) was added at room temperature to a solution of glacial acetic acid (3.0 equiv.) and ethylenediamine (2.5 equiv.) in tetrahydrofuran. The resulting mixture was stirred for 3 hours in a round bottom flask cupped with a calcium chloride valve. The conversion of the starting material was checked by TLC (mobile phase petroleum ether : AcOEt; 4 : 6). Once the peracetylated glucose was fully consumed, the reaction mixture was diluted with two volumes with water and extracted twice with DCM. The combined organic layers were washed with of a 5 % aqueous solution of hydrochloric acid, a saturated aqueous solution of sodium bicarbonate and water, until pH 7 was reached. After drying over sodium sulfate, the solvent was concentrated *in vacuo* affording the desired product used without any further purifications.
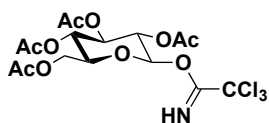
(*ii*) 1,5-diazabicyclo(5.4.0)undec-5-ene (0.4 equiv.) and trichloroacetonitrile (1.1 equiv.) were added at room temperature and under nitrogen atmosphere to a solution of 2,3,4,6-tetraacetylglucopyranose (1 equiv.) in dry DCM (0.2 M). The resulting mixture was stirred for 45 min. After checking the complete conversion of the starting material by TLC (mobile phase petroleum ether : AcOEt; 6 : 4), the crude product was concentrated *in vacuo* and purified by flash column chromatography (mobile phase petroleum ether : AcOEt; 7 : 3), affording the desired compound.

 (*iii*) Under nitrogen atmosphere, glucose trichloroacetimidate (5 eq) and crushed 4 Å molecular sieves were added to a stirring solution of TBSM-protected phenylpropanoid alcohol (1 equiv.) in dry DCM (0.1 M). After cooling to -15 °C, trimethylsilyl trifluoromethanesulfonate (0.03 equiv.), dissolved in dry DCM, was added dropwise. The resulting mixture was stirred for 30 minutes at -15 °C. The reaction was subsequently quenched with triethylamine (0.5 equiv.), filtered through a Celite®545 pad and the solvent concentrated *in vacuo*. The desired fully-protected product was purified by flash column chromatography (mobile phase petroleum ether : AcOEt; 8 : 2).

(iv) Under nitrogen atmosphere and at 0 °C, the fully-protected phenylpropanoid glucoside (1 equiv.) was dissolved in dry THF (0.03 M). A 1 M solution in THF of tetra-*n*-butylammonium fluoride (1 equiv.) in THF was then added and the reaction stirred for 20 min. After checking the conversion of the starting material by TLC (mobile phase petroleum ether : AcOEt, 1 : 1), the mixture was diluted with diethyl ether, washed with water, brine and water again, dried over sodium sulfate and concentrated *in vacuo*, affording the desired product that was used without any further purifications.

(v) Phenol-deprotected phenylpropanoid glucoside (1 equiv.) was suspended in MeOH (0.03 M) and, under vigorous stirring, a 0.5 M solution of MeONa in MeOH (2 eq) was added slowly and dropwise. The resulting mixture was stirred for 30 min. After that, the reaction was diluted three times with MeOH and a Dowex® 50WX8 hydrogen form resin was added. The mixture was than stirred until the pH 7 was reached. The resin was then filtered and the solvent concentrated *in vacuo*, affording the desired product that was used without any further purifications.

Peracetylated (L)-glucose trichloroacetimidate. According to general procedure ***7.5.1 i-ii***, L-glucose trichloroacetimidate (8.0 g, 16.39 mmol, yellow solid, isolated yield: 64 %) was obtained from L-glucose penta-acetate (10.0 g, 25.62 mmol). **^{1}H-NMR** (400 MHz; CDCl$_3$): δ 5.61-5.55 (m, 1H: H-1), 5.22-5.07 (m, 2H: H-6), 4.31-4.11 (m, 4H: H-2, H-3, H-4, H-5), 2.09 (s, 3H: H-7), 2.06 (s, 3H: H-7), 2.05 (s, 3H: H-7), 2.03 (s, 3H: H-7).

Compound (L)-4.7a. According to general procedure ***7.5.1 iii-v***, fully deprotected **(L)-4.7a** (280 mg, 1.13 mmol, oil, isolated yield: 20 %) was obtained from phenol-protected coniferyl alcohol (1.6 g, 5.44 mmol) and L-glucosetrichloroacetimidate (3.7 g, 7.62 mmol). The NMR data were in accordance to the values listed for the **(D)-4.7a** described in chapter 4.
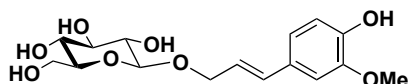
7.5.2: Laccase-mediated dimerization of phenolic glycosides

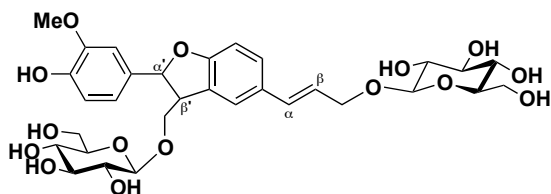To a solution of phenylpropanoid glycoside (0.05 M) in acetate buffer (20 mM pH 5), the needed amount of a 1 mg ml^{-1} laccase solution prepared in the same buffer (4.6 U ml^{-1}), was added to achieve the value of 0.005 U mmol$_{substrate}$$^{-1}$. The resulting mixture was incubated at 30 °C and 300 rpm and monitored by TLC (mobile phase MeOH : chloroform : H$_2$O; 6:4:0.5 or MeOH : AcOEt : H$_2$O; 6:4:0.5). Once the starting glycoside was consumed, the pH of the media was changed to 7 and the mixture was lyophilized. The crude product was purified by flash column chromatography (mobile phase MeOH : chloroform : H$_2$O; 7:3:0.3 or MeOH : AcOEt : H$_2$O; 7:3:0.3), affording the desired dimers as a mixtures of *trans*-diastereoisomers.

Compound 7.1. According to general procedure **7.5.2**, **7.2** (31 mg, 0.07 mmol, oil, isolated

yield: 35 %) was obtained from compound (**D**)-**4.5a** (63 mg, 0.20 mmol) and laccase (0.32 U). **^{1}H-NMR** (400 MHz; MeOD, mixture of diastereoisomers), δ: 7.54 (s, 0.5H), 7.47 (s, 0.5H), 7.25-7.23 (m, 2H), 6.79-6.74 (m, 3H), 6.64 (d, *J* = 15.9 Hz, 1H: Hα), 6.29-6.20 (m, 1H: Hβ), 5.57 (d, *J* = 6.0 Hz, 0.5H: Hα'$_A$), 5.53 (d, *J* = 6.5 Hz, 0.5H: Hα'$_B$), 4.54-4.48 (m, 1H), 4.40-4.37 (m, 2H: H-anomer$_{A+B}$), 4.36-4.30 (m, 1H), 4.23-4.15 (m, 1H), 3.92-3.79 (m, 3H), 3.72-3.60 (m, 4H), 3.42-3.22 (m, 14H). **^{13}C-NMR** (101 MHz; MeOD, mixture of diastereoisomers): δ 181.9, 179.3, 159.6, 157.07, 156.99, 132.86, 132.80, 132.59, 132.39, 130.0, 128.3, 127.06, 126.94, 122.8, 122.4, 114.83, 114.81, 108.6, 103.0, 101.69, 101.64, 87.38, 87.22, 76.74, 76.63, 76.59, 73.7, 70.34, 70.24, 69.6, 61.4. **MS**, *m/z* ESI = 645.3[M+Na]$^+$.
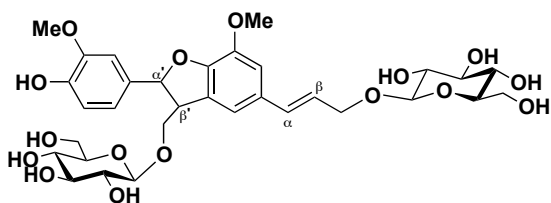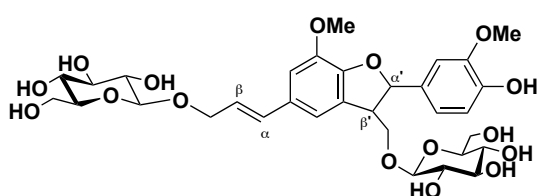
Compound 7.2. According to general procedure **7.5.2**, **7.2** (150 mg, 0.22 mmol, oil, isolated

yield: 34 %) was obtained from compound (**D**)-**4.7a** (470 mg, 1.4 mmol) and laccase (2.35 U). **¹H-NMR** (400 MHz; DMSO-d_6, mixture of diastereoisomers A and B), δ: 7.12 (s, 0.5H), 7.03 (s, 0.5H), 6.97-6.94 (m, 2H), 6.81-6.74 (m, 2H), 6.57 (d, J = 15.8 Hz, 1H: Hα), 6.26-6.17 (m, 1H: Hβ), 5.55 (d, J = 6.1 Hz, 0.5H: Hα'$_A$), 5.50 (d, J = 7.2 Hz, 0.5H: Hα'$_B$), 4.40 (dd, J = 12.8, 5.7 Hz, 1H: H-7), 4.26 (d, J = 7.8, 0.5H: H-anomer$_A$), 4.25 (d, J = 7.7, 0.5H: H-anomer$_B$), 4.22 (d, J = 7.8 Hz, 1H: H-anomer$_{A+B}$), 4.17 (dd, J = 12.7, 5.8 Hz, 1H: H-7), 4.06 (dd, J = 9.5, 5.8 Hz, 1H), 3.98 (dd, J = 9.8, 7.0 Hz), 3.81 (s, 2H: OCH$_{3A}$), 3.80 (s, 1H: OCH$_{3B}$), 3.75 (s, 1H: OCH$_{3A}$), 3.74 (s, 2H: OCH$_{3B}$), 3.72-3.56 (m, 4H), 3.50-3.42 (m, 2H), 3.20-2.98 (m, 9H). **¹³C-NMR** (101 MHz; DMSO-d_6, mixture of diastereoisomers): δ 147.95, 147.91, 147.80, 147.72, 144.21, 144.14, 132.7, 132.34, 132.27, 132.18, 130.79, 130.71, 129.8, 129.2, 124.1, 119.1, 118.8, 116.10, 116.00, 115.7, 111.10, 111.08, 111.04, 110.85, 103.4, 102.3, 87.5, 77.33, 77.24, 77.07, 77.01, 73.9, 70.9, 70.47, 70.40, 69.26, 69.20, 61.5, 56.20, 56.17, 56.10, 51.1, 50.8. **MS**, m/z ESI = 705.3 Da [M+Na]$^+$.

Compound 7.3. According to general procedure **7.5.2**, the desired dimers **7.3** (109 mg, 0.16

mmol, oil, isolated yield: 37 %) was obtained from compound (**L**)-**4.7a** (380 mg, 0.89 mmol) and laccase (1.90 U). **¹H-NMR** (400 MHz; DMSO-d_6): δ 7.14 (s, 0.5H), 7.04 (s, 0.5H), 6.98-6.95 (m, 2H), 6.81-6.74 (m, 2H), 6.58 (d, J = 15.9 Hz, 1H: Hα), 6.27-6.18 (m, 1H: Hβ), 5.55 (d, J = 6.1 Hz, 0.5H: Hα'$_A$), 5.50 (d, J = 7.3 Hz, 0.5H:Hα'$_B$), 4.41 (dd, J = 12.8, 5.5 Hz, 1H: H-7), 4.26 (dd, J = 7.8, 2.7 Hz, 0.5H: H-anomer$_A$), 4.25 (dd, J = 7.8, 2.7 Hz, 0.5H: H-anomer$_B$), 4.22 (d, J = 7.8 Hz, 1H: H-anomoer$_{A+B}$), 4.19-4.16 (m, 1H: 7), 4.07 (dd, J = 9.5, 5.9 Hz, 1H), 3.99 (dd, J = 9.6, 7.0 Hz, 1H), 3.82 (s, 1.5H: OCH$_{3A}$), 3.81 (s, 1.5H: OCH$_{3B}$), 3.76 (s, 1.5H: OCH$_{3A}$), 3.75 (s, 1.5H: OCH$_{3B}$), 3.72-3.60 (m, 4H), 3.46 (dq, J = 12.0,

6.0 Hz, 3H), 3.21-2.98 (m, 8H). **¹C-NMR** (101 MHz; DMSO-d_6): δ 148.02, 147.97, 147.84, 147.75, 146.93, 146.80, 144.22, 144.15, 132.6, 132.33, 132.27, 132.11, 130.78, 130.70, 129.8, 129.2, 124.08, 124.06, 119.2, 118.8, 116.14, 116.05, 115.77, 115.72, 111.16, 111.07, 110.9, 103.45, 103.31, 102.4, 87.57, 87.56, 77.45, 77.39, 77.36, 77.32, 77.26, 74.00, 73.94, 70.61, 70.54, 69.26, 69.20, 61.60, 61.57, 61.54, 56.22, 56.19, 56.11, 51.1, 50.8. **MS**, m/z ESI = 705.3 Da [M+Na]$^+$.

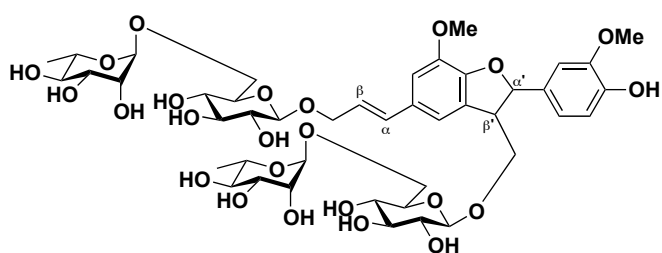**Compound 7.4.** According to general procedure **7.5.2**, the desired dimer **7.4** (74 mg, 0.07 mmol, oil, isolated yield: 33 %) was obtained from compound **4.7b** (225 mg, 0.46 mmol) and laccase (1.12 U). **¹H-NMR** (400 MHz; D$_2$O, mixture of diastereoisomers): δ 7.01 (d, J = 2.6 Hz, 1H), 6.96 (dd, J = 8.5, 1.4 Hz, 1H), 6.86-6.80 (m, 2H), 6.58 (d, J = 15.8 Hz, 1H: Hα), 6.24-6.17 (m, 1H: Hβ), 5.60 (d, J = 6.2 Hz, 0.5H: Hα'$_A$), 5.55 (d, J = 6.7 Hz, 0.5H: Hα'$_B$), 4.49 (d, J = 7.9 Hz, 1H: H-anomer$_A$), 4.45 (dd, J = 12.4, 6.2 Hz, 1H: H-7), 4.37 (d, J = 7.9 Hz, 1H: H-anomer$_A$), 4.32 (dd, J = 12.7, 6.8 Hz, 1H: H-7), 4.08-4.01 (m, 1H), 3.96-3.91 (m, 3H), 3.89-3.83 (m, 5H), 3.80-3.76 (m, 4H), 3.73-3.56 (m, 7H), 3.53-3.23 (m, 11H), 1.25-1.15 (m, 6H). **¹³C-NMR** (101 MHz; D$_2$O, mixture of diastereoisomers): δ 147.6, 147.2, 143.8, 133.7, 131.1, 128.4, 123.1, 119.0, 115.86, 115.78, 115.6, 110.9, 110.3, 102.9, 101.4, 100.61, 100.45, 96.1, 88.0, 75.8, 74.7, 73.2, 72.1, 70.28, 70.10, 69.6, 68.7, 66.7, 56.12, 55.97, 50.7, 48.9, 16.7. **MS**, m/z ESI = 997.3 Da [M+Na]$^+$.

7.5.3: *E*-stilbenes chemical synthesis

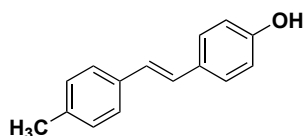A solution of *p*-hydroxybenzaldehyde (0.5 M, 1 eq) and of the desired substituted phenylacetic acid (1.2-2.4 eq) was prepared in CH_2Cl_2 at rt. Piperidine (2.5 eq) was added and the resulting mixture was gradually heated to 130 °C, distilling the solvent. The resulting neat mixture was left reacting at 130 °C for 24-48 h. After that, the crude residue was dissolved in MeOH, analyzed by TLC and purified by flash chromatography (ETP : AcOEt = 7 : 3), obtaining the target *E*-stilbene.

Compound 7.5 According to general procedure **7.5.3**, the desired stilbene **7.5** (250 mg, 1.27 mmol, white solid, isolated yield: 56 %) was obtained after 24 h from phenylacetic acid (803 mg, 5.90 mmol), *p*-hydroxybenzaldehyde (300 mg, 2.46 mmol) and piperidine (608 μl, 6.15 mmol). **¹H-NMR** (400 MHz; CDCl₃, r.t.): 7.50-7.48 (m, 2H), 7.42-7.38 (AA'BB' system, 2H), 7.36-7.32 (m, 2H), 7.25-7.21 (m, 1H), 7.05 (d, J = 16.3 Hz, 1H), 6.96 (d, J = 16.3 Hz, 1H), 6.87-6.84 (AA'BB' system, 2H), 6.44 (s, 1H). Data in agreements with those reported in literature.[160]

Compound 7.6 According to general procedure **7.5.3**, the desired stilbene **7.6** (113 mg, 0.54 mmol, white solid, isolated yield: 44 %) was obtained after 48 h from 4-methyl phenylacetic acid (443 mg, 2.95 mmol), *p*-hydroxybenzaldehyde (150 mg, 1.23 mmol) and piperidine (304 μl, 3.07 mmol). **¹H-NMR** (400 MHz; MeOD, r.t.): δ 7.40-7.37 (m, 4H), 7.40-7.37 (m, 4H), 7.18-7.12 (AA'BB' system, 2H), 7.03 (d, J = 16.4 Hz, 1H), 6.94 (d, J = 16.4 Hz, 1H), 6.80-6.77 (AA'BB' system, 2H), 2.34 (s, 3H). Data in agreements with those reported in literature.[160]
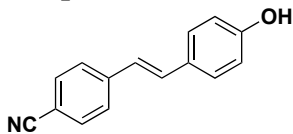
Compound 7.7 According to general procedure **7.5.3**, the desired stilbene **7.7** (58 mg, 0.26 mmol, white solid, isolated yield: 64 %) was obtained after 44 h from 4-cyano phenylacetic acid (148 mg, 0.98 mmol), *p*-hydroxybenzaldehyde (50 mg, 0.41 mmol) and piperidine (101 μl, 1.02 mmol). **^{1}H-NMR** (400 MHz; MeOD, r.t.): δ 7.71-7.65 (m, 4H), 7.48-7.45 (AA'BB' system, 2H), 7.29 (d, J = 16.4 Hz, 1H), 7.04 (d, J = 16.3 Hz, 1H), 6.83-6.81 (AA'BB' system, 2H). Data in agreements with those reported in literature.[161]

Compound 7.8 According to general procedure **7.5.3**, the desired stilbene **7.8** (0.63 g, 2.61 mmol, yellow solid, isolated yield: 64 %) was obtained after 18 h from 4-nitro phenylacetic acid (2.27 g, 12.52 mmol), *p*-hydroxybenzaldehyde (0.50 g, 4.09 mmol) and piperidine (1.01 ml, 10.24 mmol). **^{1}H-NMR** (400 MHz; MeOD, r.t.): δ 8.22-8.19 (AA'BB' system, 2H), 7.74-7.71 (AA'BB' system, 2H), 7.49-7.47 (AA'BB' system, 2H), 7.34 (d, J = 16.4 Hz, 1H), 7.10 (d, J = 16.4 Hz, 1H), 6.84-6.81 (AA'BB' system, 2H). Data in agreements with the one reported in literature.[162]

Compound 7.9 According to general procedure **7.5.3**, the desired stilbene **7.9** (140 mg, 0.62 mmol, oil, isolated yield: 38 %) was obtained after 48 h from 4-hydroxy phenylacetic acid (654 mg, 3.93 mmol), *p*-hydroxybenzaldehyde (200 mg, 1.64 mmol) and piperidine (406 μl, 4.10 mmol). **^{1}H-NMR** (500 MHz; DMSO-*d_6*, r.t.): δ 7.48 (AA'BB' system, 2H), 7.38 (AA'BB' system, 2H), 7.01-6.92 (m, 4H), 6.76 (AA'BB' system, 2H), 3.77 (s, 3H). Data in agreements with those reported in literature.[163]
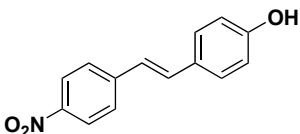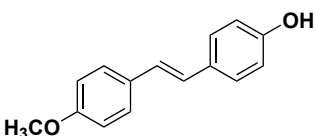
Compound 7.10 According to general procedure **7.5.3**, the desired stilbene **7.10** (147 mg, 0.7 mmol, white solid, isolated yield: 28 %) was obtained after 24 h from 3-methyl phenylacetic acid (886 mg, 5.90 mmol), *p*-hydroxybenzaldehyde (300 mg, 2.46 mmol) and piperidine (608 μl, 6.15 mmol). **^{1}H-NMR** (400 MHz; MeOD, r.t.): δ 7.40-7.38 (m, 2H), 7.32-7.29 (AA'BB' system, 2H), 7.20 (t, J = 7.6 Hz, 1H), 7.09-7.02 (m, 2H), 6.96-6.92 (m, 1H), 6.80-6.78 (m, 2H), 2.36 (s, 3H). Data in agreements with those reported in literature.[164]

Compound 7.11 According to general procedure **7.5.3**, the desired stilbene **7.11** (52 mg, 0.49 mmol, white solid, isolated yield: 60 %) was obtained after 24 h from 3-cyano phenylacetic acid (317 mg, 1.97 mmol), *p*-hydroxybenzaldehyde (100 mg, 0.82 mmol) and piperidine (204 μl, 2.05 mmol). **^{1}H-NMR** (400 MHz; MeOD, r.t.): δ 7.87-7.81 (m, 2H), 7.56-7.44 (m, 4H), 7.23 (d, J = 16.4 Hz, 1H), 7.01 (d, J = 16.4 Hz, 1H), 6.82-6.80 (AA'BB' system, 2H). Data in agreements with those reported in literature.[165]

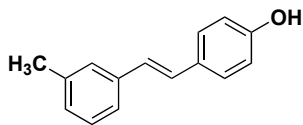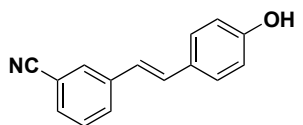**Compound 7.12** According to general procedure **7.5.3**, the desired stilbene **7.12** (113 mg, 0.26 mmol, white solid, isolated yield: 57 %) was obtained after 48 h from 3-methylthio phenylacetic acid (358 mg, 1.97 mmol), *p*-hydroxybenzaldehyde (100 mg, 0.82 mmol) and piperidine (204 μl, 2.05 mmol). **^{1}H-NMR** (400 MHz; CDCl$_3$, r.t.): δ 7.43-7.39 (m, 3H), 7.31-7.24 (m, 2H), 7.14-7.08 (m, 2H), 6.95 (d, J = 16.3 Hz, 1H), 6.81-6.78 (AA'BB' system, 2H), 2.51 (s, 3H); **^{13}C-NMR** (101 MHz; CDCl$_3$, r.t.): δ 156.8, 136.5, 135.1, 129.3, 128.8, 127.27, 127.19, 125.7, 125.3, 115.1, 19.8; **MS**, *m/z* ESI = 241.3 Da [M-H]$^-$.
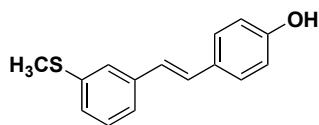
Compound 7.13 According to general procedure **7.5.3**, the desired stilbene **7.13** (55 mg, 0.22 mmol, oil, isolated yield: 28 %) was obtained after 48 h from 3,5-dimethoxy phenylacetic acid (386 mg, 1.97 mmol), *p*-hydroxybenzaldehyde (100 mg, 0.82 mmol) and piperidine (204 μl, 2.05 mmol). **^{1}H-NMR** (400 MHz; MeOD, r.t.): δ 7.42-7.38 (AA'BB' system, 2H), 7.07 (d, J = 16.3 Hz, 1H), 6.92 (d, J = 16.3 Hz, 1H), 6.81-6.77 (AA'BB' system, 2H), 6.68 (d, J = 2.2 Hz, 2H), 6.38 (t, J = 2.2 Hz, 1H), 3.82 (s, 6H). Data in agreements with those reported in literature.[166]
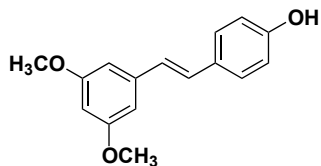
Compound 7.14 According to general procedure **7.5.3**, the desired stilbene **7.14** (72 mg, 0.32 mmol, white solid, isolated yield: 39 %) was obtained after 48 h from 3,5-dimethyl phenylacetic acid (323 mg, 1.97 mmol), *p*-hydroxybenzaldehyde (100 mg, 0.82 mmol) and piperidine (204 μl, 2.05 mmol). **^{1}H-NMR** (400 MHz; CDCl$_3$, r.t.): δ 7.39-7.37 (AA'BB' system, 2H), 7.12 (bs, 2H), 7.04 (d, J = 16.3 Hz, 1H), 6.91 (d, J = 16.4 Hz, 1H), 6.87 (bs, 1H), 6.80-6.77 (AA'BB' system, 2H), 2.17 (s, 6H). **^{13}C NMR** (101 MHz; CD$_3$OD), δ 208.6, 156.9, 137.76, 137.63, 129.2, 128.2, 127.7, 127.3, 125.6, 123.6, 115.1, 29.2, 20.0. **MS**, *m/z* ESI 222.9 [M-H]$^-$.

7.5.4: Laccase-mediated dimerization of substituted stilbenes

A solution (1 mg/mL in acetate buffer pH 4.5) of laccase from *T. versicolor* (average activity: 4 U mg^{-1}) was added (42.2 U mmol$_{substrate}$$^{-1}$) to a solution of *E*-stilbene (0,078 M in acetone). Buffer acetate was added to the reaction mixture to reach a 1 : 1 ratio acetone/buffer. The reaction mixture was shaken (160 rpm) at 27 °C and monitored by TLC (CHCl$_3$: acetone, 9 : 1) till the complete disappearance of the starting stilbene substrate. After 24 h, the reaction was quenched by extraction with AcOEt, the organic solvent evaporated *in vacuo* and the crude residue purified by flash chromatography (ETP : AcOEt, 7 : 3) to give a racemic mixture of *trans*-diastereoisomers.
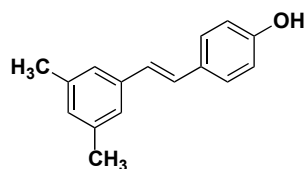
Compound 7.15 According to general procedure **7.5.4**, the desired (±)-2,3-*trans*-dihybenzofuran **7.15** (62 mg, 0.16 mmol, white solid, isolated yield: 76 %) was obtained from compound **7.5** (83 mg, 0.41 mmol), and laccases (17.7 U). **^{1}H-NMR** (400 MHz; CDCl$_3$, r.t.): δ 7.74-7.50 (d, J = 7.8 Hz, 2H), 7.42-7.32 (m, 6H), 7.26-7.21 (m, 6H), 7.06 (d, J = 16.3 Hz, 1H), 6.97-6.90 (m, 2H), 6.86-6.83 (AA'BB' system, 2H), 5.53 (d, J = 8.5 Hz, 1H), 4.87 (s, 1H), 4.59 (d, J = 8.4 Hz, 1H). **^{13}C-NMR** (101 MHz; CDCl$_3$): δ 159.6, 155.6, 141.5, 137.7, 132.7, 131.0, 128.9, 128.6, 128.5, 128.4, 127.9, 127.6, 127.3, 127.1, 126.3, 126.2, 122.9, 115.5, 109.7, 93.3, 57.6. **MS-ESI, *m/z*** 389.0 [M-H]$^{-}$.

Compound 7.16 According to general procedure **7.5.4**, the desired (±)-2,3-*trans*-dihybenzofuran **7.16** (60 mg, 0.14 mmol, white solid, isolated yield: 60 %) was obtained from compound **7.6** (95 mg, 0.45 mmol), and laccases (19.0 U). **^{1}H-NMR** (400 MHz; CDCl$_3$, r.t.): δ 7.39-7.34 (m, 2H), 7.26-7.22 (AA'BB' system, 2H), 7.19-7.10 (m, 6H), 7.00 (d, J = 16.3 Hz, 1H), 6.94 (d, J = 8.3 Hz, 1H), 6.89 (d, J = 16.3 Hz, 1H), 6.86-6.82 (AA'BB' system, 2H), 5.49 (d, J = 8.6 Hz, 1H),

4.85 (s, 1H), 4.55 (d, J = 8.5 Hz, 1H), 2.39 (s, 3H), 2.36 (s, 3H). **¹³C-NMR** (101 MHz; CDCl₃): δ 206.9, 159.5, 155.5, 138.5, 136.9, 136.9, 134.9, 132.8, 131.2, 129.6, 129.3, 128.3, 127.6, 127.6, 127.5, 126.2, 126.1, 122.8, 115.5, 109.6, 93.4, 57.3, 21.2, 21.1. **MS-ESI, *m/z*** 417.0 [M-H]⁻.

Compound 7.17 According to general procedure **7.5.4**, the desired (±)-2,3-*trans*-dihybenzofuran **7.17** (37 mg, 0.08 mmol, white solid, isolated yield: 74 %) was obtained from compound **7.7** (50 mg, 0.27 mmol), and laccases (9.5 U). **¹H-NMR** (400 MHz; CDCl₃, r.t.): δ δ 7.69-7.67 (AA'BB' system, 2H), 7.63-7.06 (AA'BB' system, 2H), 7.53-7.51 (AA'BB' system, 2H), 7.46 (dd, J = 8.4, 1.5 Hz, 1H), 7.35-7.33 (AA'BB' system, 2H), 7.22-7.20 (AA'BB' system, 2H), 7.17-7.12 (m, 2H), 7.00 (d, J = 8.3 Hz, 1H), 6.92-6.86 (m, 3H), 5.48 (d, J = 8.3 Hz, 1H), 5.17 (s, 1H), 4.66 (d, J = 8.3 Hz, 1H). **¹³C-NMR** (101 MHz; CDCl₃): δ 160.4, 156.2, 156.1, 146.7, 142.0, 132.8, 132.5, 131.8, 131.6, 130.4, 130.0, 129.1, 129.1, 127.6, 126.5, 124.7, 124.7, 123.2, 119.0, 118.5, 115.7, 115.7, 111.5, 110.3, 110.3, 110.1, 93.1, 57.7. **MS-ESI, *m/z*** 463.2 [M+Na]⁺.
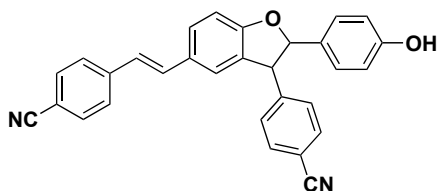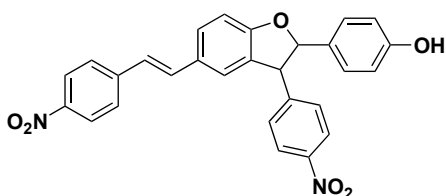
Compound 7.18 According to general procedure **7.5.4**, the desired (±)-2,3-*trans*-dihybenzofuran **7.18** (68 mg, 0.14 mmol, white solid, isolated yield: 68 %) was obtained from compound **7.8** (100 mg, 0.45 mmol), and laccases (17.4 U). **¹H-NMR** (400 MHz; CDCl₃, r.t.): δ 8.24-8.22 (AA'BB' system, 2H), 8.17-8.15 (AA'BB' system, 2H), 7.68-7.66 (AA'BB' system, 2H), 7.54 (dd, J = 8.3, 1.8 Hz, 1H), 7.46-7.44 (AA'BB' system, 2H), 7.32 (d, J = 16.3 Hz, 1H), 7.27 (bs, 1H), 7.19-7.17 (AA'BB' system, 2H), 7.06 (d, J = 16.4 Hz, 1H), 6.96 (d, J = 8.3 Hz, 1H), 6.81-6.79 (AA'BB' system, 2H), 5.52 (d, J = 8.4 Hz, 1H), 4.79 (d, J = 8.3 Hz, 1H). **¹³C-NMR** (101 MHz; CDCl₃): δ 208.6, 160.5, 157.7, 149.1, 147.3, 146.3, 144.5, 132.7, 130.6, 130.5, 130.3,

129.1, 128.9, 127.3, 126.4, 123.8, 123.6, 123.5, 123.2, 115.1, 109.6, 99.9, 93.3, 56.9. **MS-ESI, m/z** 479.0 [M-H]⁻.

Compound 7.19 According to general procedure **7.5.4**, the desired (±)-2,3-*trans*-dihybenzofuran **7.19** (33 mg, 0.07 mmol, white solid, isolated yield: 55 %) was obtained from compound **7.9** (60 mg, 0.27 mmol), and laccases (9.3 U). **¹H-NMR** (400 MHz; CDCl₃, r.t.): δ 7.41-7.39 (AA'BB' system, 2H), 7.36 (dd, J = 8.3, 1.0 Hz, 1H), 7.29-7.26 (m, 3H), 7.18-7.17 (m, 3H), 6.94-6.88 (m, 7H), 6.69-6.20 (AA'BB' system, J = 6.9 Hz, 2H), 5.46 (d, J = 8.7 Hz, 1H), 4.54 (d, J = 8.7 Hz, 1H), 3.84 (s, 3H), 3.84 (s, 3H). **¹³C-NMR** (101 MHz; CDCl₃): δ 159.3, 159.9, 158.8, 155.6, 133.4, 132.6, 131.3, 131.6, 130.5, 129.4, 127.6, 127.5, 127.3, 126.5, 125.9, 122.6, 115.5, 114.3, 114.1, 109.6, 93.5, 56.9, 55.3, 55.3. **MS-ESI, m/z** 449.0 [M-H]⁻.

Compound 7.20 According to general procedure **7.5.4**, the desired (±)-2,3-*trans*-dihybenzofuran **7.20** (66 mg, 0.16 mmol, white solid, isolated yield: 66 %) was obtained from compound **7.10** (100 mg, 0.45 mmol), and laccases (20.0 U). **¹H-NMR** (400 MHz; CDCl₃, r.t.): δ 7.40 (dd, J = 8.3, 1.8 Hz, 1H), 7.26-7.19 (m, J = 4.2 Hz, 6H), 7.14 (bd, J = 7.6 Hz, 1H), 7.06-7.00 (m, 4H), 6.95 (d, J = 8.3 Hz, 1H), 6.90 (d, J = 16.3 Hz, 1H), 6.87-6.82 (AA'BB' system, 2H), 5.53 (d, J = 8.4 Hz, 1H), 4.82 (s, 1H), 4.54 (d, J = 8.4 Hz, 1H), 2.37 (s, 3H), 2.36 (s, 3H). **¹³C-NMR** (400 MHz; CDCl₃): δ 159.6, 155.6, 141.5, 138.6, 138.1, 137.8, 132.9, 131.2, 131.1, 128.9, 128.7, 128.5, 128.3, 128.1, 127.9, 127.7, 127.6, 126.8, 126.4, 125.5, 123.4, 122.9, 115.6, 109.6, 97.3, 57.6, 30.9, 214.5, 21.4. **MS-ESI, m/z** 417.0 [M-H]⁻.
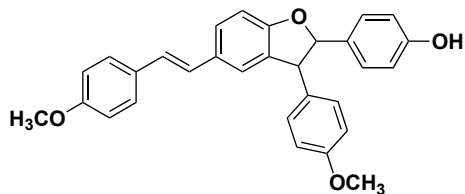
Compound 7.21 According to general procedure **7.5.4**, the desired (±)-2,3-*trans*-dihybenzofuran **7.21** (23 mg, 0.06 mmol, white solid, isolated yield: 49 %) was obtained from compound **7.11** (50 mg, 0.23 mmol), and laccases (9.5 U). **¹H-NMR** (400 MHz; CDCl₃, r.t.): δ 7.73-7.70 (m, 1H), 7.69-7.63 (m, J = 1.5 Hz, 2H), 7.52-7.42 (m, 6H), 7.23-7.21 (AA'BB' system, 2H), 7.16 (s, 1H). 7.10 (d, J = 16.3 Hz, 1H), 7.00 (d, J = 8.3 Hz, 1H), 6.90-6.86 (m, 3H), 5.47 (d, J = 8.2 Hz, 1H), 4.64 (d, J = 8.2 Hz, 1H). **¹³C-NMR** (101 MHz; CDCl₃): δ 160.2, 156.1, 143.0, 138.8, 132.8, 131.8, 131.6, 131.2, 130.8, 130.5, 130.3, 130.2, 129.8, 129.6, 129.4, 128.8, 127.5, 124.2, 123.1, 118.8, 118.5, 115.8, 113.2, 112.9, 110.3, 93.1, 57.2. **MS-ESI, *m/z*** 438.9 [M-H]⁻.
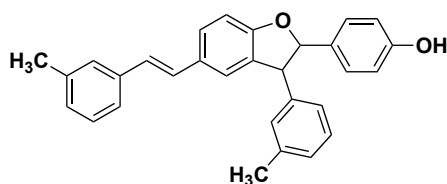
Compound 7.22 According to general procedure **7.5.4**, the desired (±)-2,3-*trans*-dihybenzofuran **7.22** (23 mg, 0.05 mmol, white solid, isolated yield: 46 %) was obtained from compound **7.12** (50 mg, 0.21 mmol), and laccases (8.7 U). **¹H-NMR** (400 MHz; CDCl₃, r.t.): δ 7.40 (dd, J = 8.3, 1.7 Hz, 1H), 7.35 (b, 1H), 7.32-7.19 (m, 9H), 7.14 (dt, J = 6.7, 2.0 Hz, 1H), 7.10 (t, J = 1.7 Hz, 1H), 7.05 (d, J = 16.3 Hz, 1H), 6.99 (dt, J = 7.6, 1.3 Hz, 1H), 6.96 (d, J = 8.3 Hz, 1H), 6.90-6.83 (m, 3H), 5.52 (d, J = 8.4 Hz, 1H), 4.54 (d, J = 8.4 Hz, 1H), 2.52 (s, 3H), 2.48 (s, 3H). **¹³C-NMR** (101 MHz; CDCl₃): δ 159.7, 155.7, 142.2, 139.3, 138.7, 138.3, 132.6, 130.90, 130.74, 129.4, 129.06, 128.99, 128.1, 127.6, 126.3, 125.8, 125.39, 125.24, 125.04, 124.4, 123.06, 123.02, 115.5, 109.8, 93.1, 57.6, 15.9, 15.7. **MS-ESI, *m/z*** 481.1 [M-H]⁻.
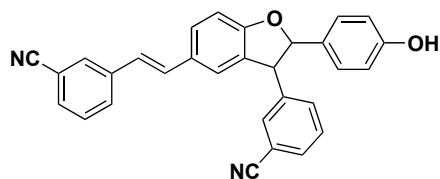
Compound 7.23 According to general procedure **7.5.4**, the desired (±)-2,3-*trans*-dihybenzofuran **7.23** (17 mg, 0.04 mmol, white sol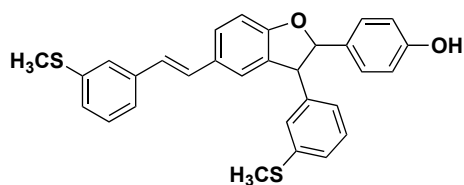id, isolated yield: 33 %) was obtained from compound **iii** (50 mg, 0.22 mmol), and laccases (9.2 U). **¹H-NMR** (400 MHz; CDCl₃, r.t.): δ 7.43 (dd, J= 8.3, 1.6 Hz, 1H), 7.26 (b.s. 1H), 7.24 (m, 2H), 7.06 (d, J= 16.3 Hz, 1H), 6.90 (d, J= 16.3 Hz, 1H), 6.87 (d, J= 8.3 Hz, 1H), 6.85 (m, 2H), 6.54 (d, J= 2.1 Hz, 2H), 6.29 (t, J= 2.2 Hz, 1H), 6.26 (t, J= 2.1 Hz, 1H), 6.20 (d, J= 2.2 Hz, 2H), 5.45 (d, J=8 Hz, 1H), 4.47 (d, J= 8 Hz, 1H). **¹³C-NMR** (101 MHz; CDCl₃): δ 161.30, 160.44, 160.22, 159.10, 145.91, 141.46, 133.28, 132.81, 132.43, 129.80, 129.29, 129.23, 127.92, 124.62, 116.85, 110.81, 108.11, 106.42, 103.43, 103.08, 94.72, 58.52. **MS-ESI, *m/z*** 453.5 [M-H]⁻.

Compound 7.24 According to general procedure **7.5.4**, the desired (±)-2,3-*trans*-dihybenzofuran **7.24** (29 mg, 0.06 mmol, white solid, isolated yield: 58 %) was obtained from compound **7.13** (50 mg, 0.20 mmol), and laccases (8.2 U). **¹H-NMR** (400 MHz; CDCl₃, r.t.): δ 7.39 (dd, J = 8.3, 1.7 Hz, 1H), 7.26-7.22 (m, 4H), 7.03 (d, J = 16.2 Hz, 1H), 6.94 (d, J = 8.3 Hz, 1H), 6.88-6.81 (m, 3H), 6.64 (d, J = 2.2 Hz, 2H), 6.43 (t, J = 2.3 Hz, 1H), 6.39 (t, J = 2.2 Hz, 1H), 6.37 (d, J = 2.3 Hz, 2H), 5.54 (d, J = 8.3 Hz, 1H), 4.50 (d, J = 8.3 Hz, 1H), 3.83 (s, 6H), 3.78 (s, 6H). **¹³C-NMR** (101 MHz; CDCl₃): δ 161.13, 160.94, 159.7, 155.8, 143.9, 139.7, 132.7, 130.82, 130.70, 129.0, 128.0, 127.6, 126.3, 123.1, 115.5, 109.7, 106.5, 104.3, 99.7, 99.1, 93.0, 57.8, 55.37, 55.34. **MS-ESI, *m/z*** 509.3 [M-H]⁻.

Compound 7.25 According to general procedure **7.5.4**, the desired (±)-2,3-*trans*-dihybenzofuran **7.25** (34 mg, 0.08 mmol, white solid, isolated yield: 58 %) was obtained from compound **7.14** (50 mg, 0.22 mmol), and laccases (9.4 U). **¹H-NMR** (400 MHz; CDCl₃, r.t.): δ 7.39 (dd, J = 8.3, 1.7 Hz, 1H), 7.27-7.23 (AA'BB' system, 2H), 7.18 (bs, 1H), 7.09 (bs, 2H), 7.03 (d, J = 16.3 Hz, 1H), 6.96-6.89 (m, 4H), 68.30-6.86 (m, 4H), 5.54 (d, J = 8.2 Hz, 1H), 4.50 (d, J = 8.2 Hz, 1H), 2.33 (s, 6H), 2.32 (s, 6H). **¹³C-NMR** (101 MHz; CDCl₃): δ 160.6, 157.6, 143.5, 139.6, 137.1, 137.6, 134.9, 133.10, 129.16, 129.0, 128.7, 128.4, 128.3, 128.1, 127.9, 127.8, 127.6, 126.8, 126.5, 125.5, 123.3, 122.9, 114.5, 108.6, 94.3, 55.6, 33.9, 21.45, 21.41, 20.45, 19.41. **MS-ESI, *m/z*** 445.0 [M-H]⁻.
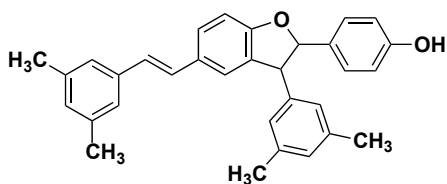
7.5.6: Reduction of compound 7.18

Compound **7.18** (0.14 M) and DIPEA (20 eq.) were dissolved in CH_2Cl_2 under magnetic stirring and nitrogen atmosphere. A solution of $HSiCl_3$ (7.14 equiv.) in dry CH_2Cl_2 (1.25M) was prepared apart, and it was added drop-wise to the first solution over 10 minutes at 0 °C, following the reaction with TLC analysis. As the reduction was not completed after 22 and 28 h, 10 equivalents of DIPEA and 3.5 equivalents of $HSiCl_3$ (1.25 M in dry CH_2Cl_2) were added to the reacting mixture, which was stirred for additional 24 h. After that, a saturated solution of $NaHCO_3$ was added drop-wise and the biphasic mixture allowed to stir for 30 min. The crude mixture was extracted with ethyl acetate, dried over Na_2SO_4, filtered and then the solvent was removed under reduced pressure to afford the crude product. The crude amine was then purified by flash chromatography ($CHCl_3$: acetone, 9.75 : 0.25) to give the main di-amine product **7.26** and the two reaction intermediates **7.27** and **7.28**.

Compound 7.26 13.7 mg, 0.033 mmol, yield: 21%; **^{1}H-NMR** (400 MHz; CD_3OD, r.t.): δ 7.47-7.24 (m, 3H), 7.16-6.94 (m, 6H), 6.84-6.70 (m, 8H), 5.36-5.34 (m, 1H), 4.43 (d, J = 8.9 Hz, 1H); **^{13}C-NMR** (101 MHz; CD_3OD): δ 159.0, 157.2, 145.9, 145.6, 131.68, 131.63, 131.44, 131.32, 128.8, 128.5, 127.3, 126.9, 126.7, 126.0, 124.6, 122.0, 116.0, 115.5, 114.9, 108.9, 93.8, 78.2, 77.8, 77.5, 56.9, 29.3; **MS-ESI, *m/z*** 419.0 [M-H]⁻.
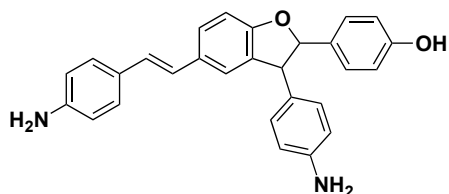
Compound 7.26 1.8 mg, 0.004 mmol, yield: 3%; **^{1}H-NMR** (400 MHz; $CDCl_3$, r.t.): δ 8.25-8.23 (AA'BB' system, 2H), 7.41-7.38 (m, 3H), 7.30-7.26 (AA'BB' system, J = 8.5 Hz, 2H), 7.24-7.20 (AA'BB' system, J = 8.5 Hz, 2H), 7.10 (bs, 1H), 6.96 (d, J = 8.4 Hz, 1H), 6.87-6.84 (m, 4H), 6.68-6.65 (AA'BB' system, 2H), 5.46 (d, J = 8.4 Hz, 1H), 4.70 (d, J = 8.4 Hz, 1H); **^{13}C-NMR** (101
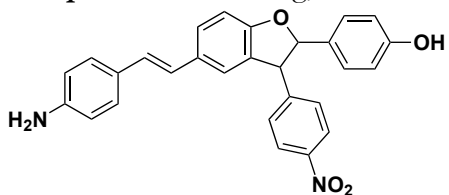
MHz; CDCl$_3$): δ 1159.0, 156.0, 149.0, 145.9, 132.1, 131.9, 129.5, 129.2, 127.9, 127.61, 127.44, 126.9, 124.6, 124.2, 122.3, 115.7, 115.2, 110.1, 92.8, 57.7, 29.7; **MS-ESI, *m/z*** 449.0 [M-H]$^-$.

Compound 7.27 5.6 mg, 0.012 mmol, yield: 8 %; **^{1}H-NMR** (400 MHz; CD$_3$OD, r.t.): δ 8.25-8.19 (AA'BB' system, 2H), 7.57-7.55 (AA'BB' system, 2H), 7.43-7.40 (m, 1H), 7.25-7.19 (m, 4H), 7.01-6.93 (m, 4H), 6.85-6.83 (AA'BB' system, 2H), 6.71-6.69 (AA'BB' system, 2H), 5.48 (d, J = 8.8 Hz, 1H), 4.49 (d, J = 8.8 Hz, 1H); **^{13}C-NMR** (101 MHz; CD$_3$OD), δ 160.6, 155.7, 146.4, 145.7, 144.4, 133.2, 130.9, 129.8, 129.3, 128.7, 127.6, 126.4, 124.1, 123.7, 123.4, 115.52, 115.47, 109.9, 93.8, 56.8, 29.7; **MS-ESI, *m/z*** 449.0 [M-H]$^-$.
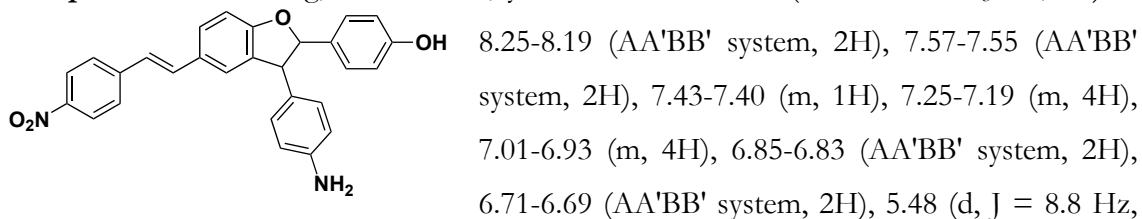
7.5.7: Alkylation of Phenols

Phenolic compound (0.05 M, 1 equiv.) and 2-chloro-*N,N*-dimethylamine hydrochloride (3 equiv.) were suspended in chloroform. Tetrabutylammonium hydrogensulfate (0.05 equiv.), potassium carbonate (8 equiv.) and water (H_2O : $CHCl_3$ = 2: 100) were then added and the reaction stirred at 50 °C. After that, the mixture was diluted with chloroform, the organic phase washed with water and dried over sodium sulfate. The solvent was evaporated at reduced pressure and the crude residue purified by flash chromatography ($CHCl_3$: MeOH = 9 : 1) to give desired alkylated product.

Compound 7.29 According to general procedure **7.5.7**, the desired alkylated (±)-2,3-*trans*-

dihybenzofuran **7.29** (19 mg, 0.03 mmol, oil, isolated yield: 60 %) was obtained from compound **7.15** (21 mg, 0.05 mmol), 2-chloro-*N,N*-dimethylamine hydrochloride (35 mg, 0.16 mmol), TBAHSO$_4$ (9 mg, 0.03) (9.4 U). **^{1}H-NMR** (400 MHz; CDCl$_3$, r.t.): δ 7.47-7.45 (m, 2H), 7.42-7.32 (m, 6H), 7.30-7.26 (m, 3H), 7.25-7.20 (m, 4H), 7.05 (d, J = 16.3 Hz, 1H), 6.97-6.90 (m, 4H), 5.53 (d, J = 8.4 Hz, 1H), 4.60 (d, J = 8.4 Hz, 1H), 4.14 (t, J = 5.7 Hz, 2H), 2.83 (t, J = 5.6 Hz, 2H), 2.42 (s, 7H). **^{13}C-NMR** (101 MHz; CDCl$_3$): δ 160.3, 159.4, 142.1, 138.3, 133.3, 131.6, 129.5, 129.21, 129.10, 129.00, 128.5, 127.99, 127.93, 127.7, 126.94, 126.78, 123.6, 115.3, 110.3, 94.0, 66.3, 58.6, 58.2, 46.2, 30.30, 30.2; **MS-ESI, *m/z*** 462.3 [M+1]$^+$.
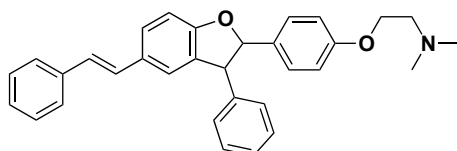
Compound 7.30 According to general procedure **7.5.7**, the desired alkylated (±)-2,3-*trans*-

dihybenzofuran **7.30** (19 mg, 0.03 mmol, oil, isolated yield: 60 %) was obtained from compound **7.24** (27 mg, 0.05 mmol), 2-chloro-*N,N*-dimethylamine hydrochloride (35 mg, 0.24 mmol), TBAHSO$_4$ (9 mg, 0.03). **^{1}H-NMR** (400 MHz; CDCl$_3$, r.t.): δ 7.39 (dd, J = 8.3,

1.7 Hz, 1H), 7.27-7.23 (AA'BB' system, 2H), 7.18 (bs, 1H), 7.09 (bs, 2H), 7.03 (d, J = 16.3 Hz, 1H), 6.96-6.89 (m, 4H), 68.30-6.86 (m, 4H), 5.54 (d, J = 8.2 Hz, 1H), 4.50 (d, J = 8.2 Hz, 1H), 2.33 (s, 6H), 2.32 (s, 6H). **^{13}C-NMR** (101 MHz; CD$_3$OD): δ 161.1, 160.9, 159.7, 158.5, 158.2, 143.9, 139.7, 133.0, 130.81, 130.71, 130.3, 129.0, 128.0, 127.55, 127.36, 126.3, 123.1, 115.7, 114.7, 114.1, 113.8, 109.7, 106.5, 104.3, 99.7, 99.0, 92.9, 65.15, 65.10, 57.8, 57.4, 55.4, 44.96, 44.91, 44.2. **MS-ESI, *m/z*** 582.4 [M+1]$^+$.
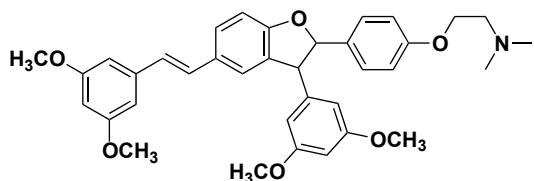
Compound 7.31 According to general procedure **7.5.7**, the desired alkylated (±)-2,3-*trans*-

dihybenzofuran **7.31** (19 mg, 0.03 mmol, oil, isolated yield: 60 %) was obtained from compound **7.25** (30 mg, 0.07 mmol), 2-chloro-*N,N*-dimethylamine hydrochloride (44 mg, 0.30
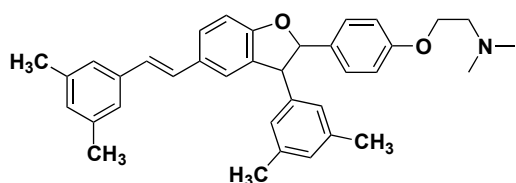
mmol), TBAHSO$_4$ (12 mg, 0.04). **^{1}H-NMR** (400 MHz; CDCl$_3$, r.t.): δ 7.40-38 (m, 1H), 7.28-7.20 (m, 3H), 7.01 (d, J = 16.5 Hz, 1H), 6.93-6.83 (m, 5H), 6.62 (s, 2H), 6.41-6.35 (m, 3H), 5.53 (d, J = 8.3 Hz, 1H), 4.48 (d, J = 8.5 Hz, 1H), 4.14 (s, 2H), 3.81 (s, 6H), 3.76 (s, 6H), 2.97 (s, 3H), 2.46 (s, 6H). **^{13}C-NMR** (101 MHz; CDCl$_3$): δ 159.5, 158.7, 141.6, 138.4, 138.0, 137.6, 133.1, 131.31, 131.11, 128.98, 128.92, 128.2, 127.6, 127.3, 126.4, 126.1, 124.1, 123.0, 114.7, 109.6, 93.2, 65.7, 58.0, 57.5, 45.6, 29.7, 21.31, 21.28. **MS-ESI, *m/z*** 518.2 [M+1]$^+$.

7.5.8: HPLC methods

a) Compounds **7.1**-**7.4**

- *Column* = Kinetex C18 HPLC 5μm EVO C18 100Å, 150x4.6 mm

- *Flow* = 0.7 mL/min; - *Loop* = 20 μL; - *Detection Lambda* =: 270 nm; - *Injection* = 10 μL

- *Gradient* of CH_3CN and H_2O (0.1 ppm TFA, pH 3)

0–1 min 90% H_2O, 10% CH_3CN; 1–20 min 80% H_2O, 20% CH_3CN; 20–22 min 80% H_2O, 20% CH_3CN; 22–23 90% H_2O, 10% CH_3CN

b) Oxidations of **7.5** to **7.15**

- *Column* = Kinetex C18 HPLC 5μm EVO C18 100Å, 150x4.6 mm

- *Flow* = 0.3 mL/min; - *Loop* = 20 μL; - *Detection Lambda* =: 270 nm; - *Injection* = 10 μL

- *Gradient* of CH_3CN and H_2O (0.1 ppm TFA, pH 3)

0 min 80% H_2O, 20% CH_3CN; 0–60 min 15% H_2O, 85% CH_3CN; 61-70 min 80% H_2O, 20% CH_3CN

7.5.9: ATPase assay

Hsc82 (2 μM) was added to a solution prepared in HEPES buffer (20 mm, pH 7.5) containing KCl (100 mM), $MgCl_2$ (1 mM), NADH (0.18 μM), L-lactate dehydrogenase (4 U ml^{-1}), phosphoenolpyruvate (1 mM), pyruvate kinase (2.5 U ml^{-1}) and the desired compound (dissolved in DMSO to a final concentration of 50 μm). The reaction was initiated by the addition of ATP (1 mM) and was 30 °C for 30 minutes collecting the absorbance data at 360 nm.

8. REFERENCES

(1)   Carrea, G.; Riva, S. *Organic Synthesis with Enzymes in Non-Aqueous Media*; Wiley-VCH: Weinheim, Germany, 2008.

(2)   Klibanov, A. M.; Koskinen, A. M. P. *Enzymatic Reations in Organic Media*; Chapman & Hall: Glasgow, U.K., 1996.

(3)   Klibanov, A. M. *Nature* **2001**, *409* (6817), 241–246.

(4)   Harwood, J. *Trends Biochem. Sci.* **1989**, *14* (4), 125–126.

(5)   Kumar, A.; Dhar, K.; Kanwar, S. S.; Arora, P. K. *Biol. Proced. Online* **2016**, *18*, 2.

(6)   Park, S.; Kazlauskas, R. J. *Curr. Opin. Biotechnol.* **2003**, *14* (4), 432–437.

(7)   Carrea, G.; Riva, S. *Angew. Chem. Int. Ed. Engl.* **2000**, *39*, 2226–2254.

(8)   Stergiou, P.-Y.; Foukis, A.; Filippou, M.; Koukouritaki, M.; Parapouli, M.; Theodorou, L. G.; Hatziloukas, E.; Afendra, A.; Pandey, A.; Papamichael, E. M. *Biotechnol. Adv.* **2013**, *31*, 1846–1859.

(9)   Plou, F. J.; Cruces, M. A.; Ferrer, M.; Fuentes, G.; Pastor, E.; Bernabé, M.; Christensen, M.; Comelles, F.; Parra, J. L.; Ballesteros, A. *J. Biotechnol.* **2002**, *96* (1), 55–66.

(10)   Therisod, M.; Klibanov, A. M. *J. Am. Chem. Soc.* **1986**, *108* (18), 5638–5640.

(11)   Silva, M. C.; Carvalho, J.; Riva, S.; Maria Luisa, S. e M. *Curr. Org. Chem.* **2011**, *15* (6), 928–941.

(12)   Michels, P. C.; Khmelnitsky, Y. L.; Dordick, J. S.; Clark, D. S. *Trends Biotechnol.* **1998**, *16* (5), 210–215.

(13)   Akbar, U.; Shin, D. S.; Schneider, E.; Dordick, J. S.; Clark, D. S. *Tetrahedron Lett.* **2010**, *51* (8), 1220–1225.

(14)   Secundo, F.; Carrea, G.; De Amici, M.; Di Ventimiglia, S. J.; Dordick, J. S. *Biotechnol. Bioeng.* **2003**, *81* (4), 391–396.

(15)   Krejzová, J.; Šimon, P.; Vavříková, E.; Slámová, K.; Pelantová, H.; Riva, S.; Spiwok, V.; Křen, V. *J. Mol. Catal. B Enzym.* **2013**, *87*, 128–134.

(16)   Khmelnitsky, Y. L.; Budde, C.; Arnold, J. M.; Usyatinsky, A.; Clark, D. S.; Dordick, J. S. *J. Am. Chem. Soc.* **1997**, *119* (47), 11554–11555.

(17)   Magrone, P.; Cavallo, F.; Panzeri, W.; Passarella, D.; Riva, S. *Org. Biomol. Chem.* **2010**, *8* (24), 5583–5590.

(18)   Bassanini, I.; Gavezzotti, P.; Riva, S. *Unpublished Results*; 2015.

(19)   Xing, R.; Liu, K.; Jiao, T.; Zhang, N.; Ma, K.; Zhang, R.; Zou, Q.; Ma, G.; Yan, X. *Adv. Mater.* **2016**, *28* (19), 3669–3676.

(20)   Liu, K.; Xing, R.; Zou, Q.; Ma, G.; Möhwald, H.; Yan, X. *Angew. Chemie - Int. Ed.* **2016**, *55* (9), 3036–3039.

(21)   Zhang, N.; Zhao, F.; Zou, Q.; Li, Y.; Ma, G.; Yan, X. *Small* **2016**, *12* (43), 5936–5943.

(22)   Mura, S.; Bui, D. T.; Couvreur, P.; Nicolas, J. *J. Control. Release* **2015**, *208*, 25–41.

(23)   Trung Bui, D.; Maksimenko, A.; Desmaële, D.; Harrisson, S.; Vauthier, C.; Couvreur, P.; Nicolas, J. *Biomacromolecules* **2013**, *14* (8), 2837–2847.

(24)   Christodoulou, M. S.; Fokialakis, N.; Passarella, D.; García-Argáez, A. N.; Gia, O. M.; Pongratz, I.; Dalla Via, L.; Haroutounian, S. A. *Bioorg. Med. Chem.* **2013**, *21* (14), 4120–4131.

(25)   Christodoulou, M. S.; Zarate, M.; Ricci, F.; Damia, G.; Pieraccini, S.; Dapiaggi, F.; Sironi, M.; Lo Presti, L.; García-Argáez, A. N.; Dalla Via, L.; Passarella, D. *Eur. J. Med. Chem.* **2016**, *118*, 79–89.

(26)   Zhang, J.; Liu, A.; Hou, R.; Zhang, J.; Jia, X.; Jiang, W.; Chen, J. *Eur. J. Pharmacol.* **2009**, *607* (1–3), 6–14.

(27)   Sun, C.; Wang, Z.; Zheng, Q.; Zhang, H. *Phytomedicine* **2012**, *19* (3–4), 355–363.

(28)   Zhang, L.; Yu, H.; Zhao, X.; Lin, X.; Tan, C.; Cao, G.; Wang, Z. *Neurochem. Int.* **2010**, *57* (5), 547–555.

(29)   Kurkin, V. A. *Sect. Title Pharmacol.* **2013**, *3* (1), 26–28.

(30)   Kurkin, V. A.; Dubishchev, A. V.; Ezhkov, V. N.; Titova, I. N.; Avdeeva, E. V. *Pharm. Chem. J.* **2006**, *40* (11), 614–619.

(31)   Matsubara, Y.; Yusa, T.; Sawabe, A.; Iizuka, Y.; Okamoto, K. *Agric. Biol. Chem.* **1991**, *55* (February 2015), 647–650.

(32)   Williams, G. J.; Thorson, J. S. In *Advances in Enzymology and Related Areas of Molecular Biology*; John Wiley & Sons, Inc.; pp 55–119.

(33)   Schuman, B.; Evans, S. V.; Fyles, T. M.; Rose, D.; Lau, K. *PLoS One* **2013**, *8* (8), e71077.

(34)   Ruddock, L. W.; Molinari, M. *J. Cell Sci.* **2006**, *119* (21).

(35)   Schmölzer, K.; Gutmann, A.; Diricks, M.; Desmet, T.; Nidetzky, B. *Biotechnol. Adv.* **2016**, *34* (2), 88–111.

(36)   Liang, D.-M.; Liu, J.-H.; Wu, H.; Wang, B.-B.; Zhu, H.-J.; Qiao, J.-J. *Chem. Soc. Rev.* **2015**, *44* (22), 8350–8374.

(37)   Aerts, D.; Verhaeghe, T. F.; Roman, B. I.; Stevens, C. V.; Desmet, T.; Soetaert, W. *Carbohydr. Res.* **2011**, *346* (13), 1860–1867.

(38)   Bojarová, P.; Křen, V. *Trends Biotechnol.* **2009**, *27* (4), 199–209.

(39)   Desmet, T.; Soetaert, W.; Bojarová, P.; Křen, V.; Dijkhuizen, L.; Eastwick-Field, V.; Schiller, A. *Chem. - A Eur. J.* **2012**, *18* (35), 10786–10801.

(40)   Monsan, P.; Paul, F.; P., M.; F., P.; V., P.; P., M.; O., S.; B.E., F.; H.M., T.; C.E., R. *FEMS Microbiol. Rev.* **1995**, *16* (2–3), 187–192.

(41)   Jahn, M.; Stoll, D.; Warren, R. A. J.; Szabó, L.; Singh, P.; Gilbert, H. J.; Ducros, V. M.-A.; Davies, G. J.; Withers, S. G. *Chem. Commun.* **2003**, *D50* (12), 1327–1329.

(42)   Mayer, C.; Jakeman, D. L.; Mah, M.; Karjala, G.; Gal, L.; Warren, R. A. .; Withers, S. G. *Chem. Biol.* **2001**, *8* (5), 437–443.

(43)   Akita, H.; Kawahara, E.; Kishida, M.; Kato, K. *J. Mol. Catal. B Enzym.* **2006**, *40* (1–2), 8–15.

(44)   Harborne, J. B.; Williams, C. A. In *The Flavonoids*; Mabry, T. J., Mabry, H., Eds.; Chapman and Hall Ltd: 11 New Fetter Lane London EC4P 4EE, 1975; pp 420–427.

(45)   Mazzaferro, L. S.; Breccia, J. D. *Biocatal. Biotransform.* **2011**, *29*, 103–109.

(46)   Šimčíková, D.; Kotik, M.; Weignerová, L.; Halada, P.; Pelantová, H.; Adamcová, K.; Křen, V. *Adv. Synth. Catal.* **2015**, *357* (1), 107–117.

(47)   Gerstorferová, D.; Fliedrová, B.; Halada, P.; Marhol, P.; Křen, V.; Weignerová, L. *Process Biochem.* **2012**, *47* (5), 828–835.

(48)   Weignerová, L.; Marhol, P.; Gerstorferová, D.; Křen, V. *Bioresour. Technol.* **2012**, *115*, 222–227.

(49)   Tomas-Barberan, F. A.; Blazquezt, M. A.; Garcia-Viguera, C.; Ferreres, F.; Francisco, T.-L. *Phytochem. Anal.* **1992**, *3*, 178–181.

(50)   Kishida, M.; Akita, H. *Tetrahedron* **2005**, *61* (44), 10559–10568.

(51)   Bassanini, I.; Gavezzotti, P.; Monti, D.; Krejzová, J.; Křen, V.; Riva, S. *J. Mol. Catal. B Enzym.* **2016**, *134*.

(52)   Koszelewski, D.; Tauber, K.; Faber, K.; Kroutil, W. *Trends in Biotechnology*. 2010, pp 324–332.

(53)   Mathew, S.; Yun, H. *ACS Catal.* **2012**, *2* (6), 993–1001.

(54)   Fuchs, M.; Farnberger, J. E.; Kroutil, W. *European J. Org. Chem.* **2015**, *2015* (32), 6965–6982.

(55)   Nugent, T. C.; El-Shazly, M. *Adv. Synth. Catal.* **2010**, *352* (5), 753–819.

(56)   Monti, D.; Forchin, M. C.; Crotti, M.; Parmeggiani, F.; Gatti, F. G.; Brenna, E.; Riva, S. *ChemCatChem* **2015**, *7* (19), 3106–3109.

(57)   Steffen-Munsberg, F.; Vickers, C.; Kohls, H.; Land, H.; Mallin, H.; Nobili, A.; Skalden, L.; van den Bergh, T.; Joosten, H. J.; Berglund, P.; Höhne, M.; Bornscheuer, U. T. *Biotechnology Advances*. Elsevier September 1, 2015, pp 566–604.

(58)   Koszelewski, D.; Clay, D.; Rozzell, D.; Kroutil, W. *European J. Org. Chem.* **2009**, *2009* (14), 2289–2292.

(59)   Koszelewski, D.; Lavandera, I.; Clay, D.; Guebitz, G. M.; Rozzell, D.; Kroutil, W. *Angew. Chemie - Int. Ed.* **2008**, *47* (48), 9337–9340.

(60)   Koszelewski, D.; Lavandera, I.; Clay, D.; Rozzell, D.; Kroutil, W. *Adv. Synth. Catal.* **2008**, *350* (17), 2761–2766.

(61)   Sayer, C.; Martinez-Torres, R. J.; Richter, N.; Isupov, M. N.; Hailes, H. C.; Littlechild, J. A.; Ward, J. M. *FEBS J.* **2014**, *281* (9), 2240–2253.

(62)   Savile, C. K.; Janey, J. M.; Mundorff, E. C.; Moore, J. C.; Tam, S.; Jarvis, W. R.; Colbeck, J. C.; Krebber, A.; Fleitz, F. J.; Brands, J.; Devine, P. N.; Huisman, G. W.; Hughes, G. J. *Science (80-.).* **2010**, *329* (5989), 305–309.

(63)   Martin, A. R.; DiSanto, R.; Plotnikov, I.; Kamat, S.; Shonnard, D.; Pannuri, S. *Biochem. Eng. J.* **2007**, *37* (3), 246–255.

(64)   de Miguel Bouzas, T.; Barros-Velázquez, J.; Villa, T. G. *Protein Pept. Lett.* **2006**, *13* (7), 645–651.

(65) Littlechild, J. A. *Front. Bioeng. Biotechnol.* **2015**, *3* (October), 161.

(66) Chen, Y.; Yi, D.; Jiang, S.; Wei, D. *Appl. Microbiol. Biotechnol.* **2016**, *100* (7), 3101–3111.

(67) Mathew, S.; Deepankumar, K.; Shin, G.; Hong, E. Y.; Kim, B.-G.; Chung, T.; Yun, H. *RSC Adv.* **2016**, *6* (73), 69257–69260.

(68) Mathew, S.; Nadarajan, S. P.; Chung, T.; Park, H. H.; Yun, H. *Enzyme Microb. Technol.* **2016**, *87–88*, 52–60.

(69) Lorenz, P.; Schleper, C. In *Journal of Molecular Catalysis B: Enzymatic*; Elsevier, 2002; Vol. 19–20, pp 13–19.

(70) Ferrer, M.; Martínez-Martínez, M.; Bargiela, R.; Streit, W. R.; Golyshina, O. V.; Golyshin, P. N. *Microbial Biotechnology*. January 1, 2016, pp 22–34.

(71) Ferrandi, E. E.; Sayer, C.; Isupov, M. N.; Annovazzi, C.; Marchesi, C.; Iacobone, G.; Peng, X.; Bonch-Osmolovskaya, E.; Wohlgemuth, R.; Littlechild, J. A.; Monti, D. *FEBS J.* **2015**, *282* (15), 2879–2894.

(72) Wilson, M. C.; Piel, J. *Chemistry and Biology*. Cell Press May 23, 2013, pp 636–647.

(73) Zarafeta, D.; Kissas, D.; Sayer, C.; Gudbergsdottir, S. R.; Ladoukakis, E.; Isupov, M. N.; Chatziioannou, A.; Peng, X.; Littlechild, J. A.; Skretas, G.; Kolisis, F. N. *PLoS One* **2016**, *11* (1), e0146454.

(74) Menzel, P.; Gudbergsdóttir, S. R.; Rike, A. G.; Lin, L.; Zhang, Q.; Contursi, P.; Moracci, M.; Kristjansson, J. K.; Bolduc, B.; Gavrilov, S.; Ravin, N.; Mardanov, A.; Bonch-Osmolovskaya, E.; Young, M.; Krogh, A.; Peng, X. *Microb. Ecol.* **2015**, *70* (2), 411–424.

(75) Kielbasa, S. M.; Wan, R.; Sato, K.; Horton, P.; Frith, M. C. *Genome Res.* **2011**, *21* (3), 487–493.

(76) Ferrandi, E. E.; Previdi, A.; Bassanini, I.; Riva, S.; Peng, X.; Monti, D. *Appl. Microbiol. Biotechnol.* **2017**.

(77) Park, E. S.; Kim, M.; Shin, J. S. *Appl. Microbiol. Biotechnol.* **2012**, *93* (6), 2425–2435.

(78) Shin, J. S.; Kim, B. G. *J. Org. Chem.* **2002**, *67* (9), 2848–2853.

(79) Nobili, A.; Steffen-Munsberg, F.; Kohls, H.; Trentin, I.; Schulzke, C.; Höhne, M.; Bornscheuer, U. T. *ChemCatChem* **2015**, *7* (5), 757–760.

(80) Bormann, S.; Gomez Baraibar, A.; Ni, Y.; Holtmann, D.; Hollmann, F. *Catal. Sci. Technol.* **2015**, *5* (4), 2038–2052.

(81) Hofrichter, M.; Ullrich, R. *Curr. Opin. Chem. Biol.* **2014**, *19* (1), 116–125.

(82) Wang, Y.; Lan, D.; Durrani, R.; Hollmann, F.; Hauer, B.; Lutz, S. *Curr. Opin. Chem. Biol.* **2017**, *37*, 1–9.

(83) Martínez, A. T.; Ruiz-Dueñas, F. J.; Camarero, S.; Serrano, A.; Linde, D.; Lund, H.; Vind, J.; Tovborg, M.; Herold-Majumdar, O. M.; Hofrichter, M.; Liers, C.; Ullrich, R.; Scheibner, K.; Sannia, G.; Piscitelli, A.; Pezzella, C.; Sener, M. E.; Kiliç, S.; van Berkel, W. J.; Guallar, V.; Lucas, M. F.; Zuhse, R.; Ludwig, R.; Hollmann, F.; Fernández-Fueyo, E.; Record, E.; Faulds, C. B.; Tortajada, M.; Winckelmann, I.; Rasmussen, J. A.; Gelo-Pujic, M.; Gutiérrez, A.; del Río, J. C.; Rencoret, J.; Alcalde, M. *Biotechnol. Adv.* **2017**, *35*, 815–831.

(84)   Ullrich, R.; Nüske, J.; Scheibner, K.; Spantzel, J.; Hofrichter, M. *Appl. Environ. Microbiol.* **2004**, *70* (8), 4575–4581.

(85)   Pecyna, M. J.; Ullrich, R.; Bittner, B.; Clemens, A.; Scheibner, K.; Schubert, R.; Hofrichter, M. *Appl. Microbiol. Biotechnol.* **2009**, *84* (5), 885–897.

(86)   Piontek, K.; Strittmatter, E.; Ullrich, R.; Gröbe, G.; Pecyna, M. J.; Kluge, M.; Scheibner, K.; Hofrichter, M.; Plattner, D. A. *J. Biol. Chem.* **2013**, *288* (48), 34767–34776.

(87)   Kluge, M.; Ullrich, R.; Scheibner, K.; Hofrichter, M. *Green Chem.* **2012**, *14* (2), 440.

(88)   Wang, X.; Ullrich, R.; Hofrichter, M.; Groves, J. T. *Proc. Natl. Acad. Sci. U. S. A.* **2015**, *112* (12), 3686–3691.

(89)   Peter, S.; Kinne, M.; Wang, X.; Ullrich, R.; Kayser, G.; Groves, J. T.; Hofrichter, M. *FEBS J.* **2011**, *278* (19), 3667–3675.

(90)   Molina-Espeja, P.; Garcia-Ruiz, E.; Gonzalez-Perez, D.; Ullrich, R.; Hofrichter, M.; Alcalde, M. *Appl. Environ. Microbiol.* **2014**, *80* (11), 3496–3507.

(91)   Molina-Espeja, P.; Ma, S.; Mate, D. M.; Ludwig, R.; Alcalde, M. *Enzyme Microb. Technol.* **2015**, *73–74*, 29–33.

(92)   Ni, Y.; Fernández-Fueyo, E.; Baraibar, A. G.; Ullrich, R.; Hofrichter, M.; Yanase, H.; Alcalde, M.; VanBerkel, W. J. H.; Hollmann, F. *Angew. Chemie - Int. Ed.* **2016**, *55* (2), 798–801.

(93)   Fernández-Fueyo, E.; Ni, Y.; Gomez Baraibar, A.; Alcalde, M.; van Langen, L. M.; Hollmann, F. *J. Mol. Catal. B Enzym.* **2016**, *134*, 347–352.

(94)   Poraj-Kobielska, M.; Peter, S.; Leonhardt, S.; Ullrich, R.; Scheibner, K.; Hofrichter, M. *Biochem. Eng. J.* **2015**, *98*, 144–150.

(95)   Fernández, I.; Khiar, N. *Chem. Rev.* **2003**, *103* (9), 3651–3705.

(96)   Wojaczyńska, E.; Wojaczyński, J. *Chem. Rev.* **2010**, *110* (7), 4303–4356.

(97)   Matsui, T.; Dekishima, Y.; Ueda, M. *Appl. Microbiol. Biotechnol.* **2014**, *98* (18), 7699–7706.

(98)   Velde, F. van de; Rantwijk, F. van; Sheldon, R. A. *Trends Biotechnol.* **2001**, *19* (2), 73–80.

(99)   Colonna, S.; Gaggero, N.; Manfredi, A.; Casella, L.; Gullotti, M.; Carrea, G.; Pasta, P. *Biochemistry* **1990**, *29* (46), 10465–10468.

(100)   Colonna, S.; Gaggero, N.; Casella, L.; Carrea, G.; Pasta, P. *Tetrahedron: Asymmetry* **1992**, *3* (1), 95–106.

(101)   Colonna, S.; Sordo, S. Del; Gaggero, N.; Carrea, G.; Pasta, P. *Heteroat. Chem.* **2002**, *13* (5), 467–473.

(102)   Colonna, S.; Gaggero, N.; Pasta, P.; Ottolina, G. *Chem. Commun.* **1996**, No. 20, 2303.

(103)   Colonna, S.; Gaggero, N.; Carrea, G.; Pasta, P. *Chem. Commun.* **1997**, No. 5, 439–440.

(104)   De Gonzalo, G.; Torres Pazmiño, D. E.; Ottolina, G.; Fraaije, M. W.; Carrea, G. *Tetrahedron Asymmetry* **2005**, *16* (18), 3077–3083.

(105)   De Gonzalo, G.; Torres Pazmiño, D. E.; Ottolina, G.; Fraaije, M. W.; Carrea, G. *Tetrahedron Asymmetry* **2006**, *17* (1), 130–135.

(106) Aranda, E.; Kinne, M.; Kluge, M.; Ullrich, R.; Hofrichter, M. *Appl. Microbiol. Biotechnol.* **2009**, *82* (6), 1057–1066.

(107) Karich, A.; Scheibner, K.; Ullrich, R.; Hofrichter, M. *J. Mol. Catal. B Enzym.* **2016**, *134*, 238–246.

(108) Pasta, P.; Carrea, G.; Monzani, E.; Gaggero, N.; Colonna, S. *Biotechnol. Bioeng.* **1999**, *62* (4), 489–493.

(109) Dai, W.; Li, G.; Wang, L.; Chen, B.; Shang, S.; Lv, Y.; Gao, S. *RSC Adv.* **2014**, *4* (87), 46545–46554.

(110) Zhang, J.; Li, Z.; Gong, W.; Han, X.; Liu, Y.; Cui, Y. *Inorg. Chem.* **2016**, *55* (15), 7229–7232.

(111) Jalba, A.; Régnier, N.; Ollevier, T. *European J. Org. Chem.* **2017**, *2017* (12), 1628–1637.

(112) Riva, S. *Trends Biotechnol.* **2006**, *24* (5), 219–226.

(113) Giardina, P.; Faraco, V.; Pezzella, C.; Piscitelli, A.; Vanhulle, S.; Sannia, G. *Cell. Mol. Life Sci.* **2010**, *67* (3), 369–385.

(114) Quintanar, L.; Stoj, C.; Taylor, A. B.; Hart, P. J.; Kosman, D. J.; Solomon, E. I. *Acc. Chem. Res.* **2007**, *40* (6), 445–452.

(115) Jones, S. M.; Solomon, E. I. *Cell. Mol. Life Sci.* **2015**, *72* (5), 869–883.

(116) Niedermeyer, T. H. J.; Mikolasch, A.; Lalk, M. *J. Org. Chem.* **2005**, *70* (6), 2002–2008.

(117) Mikolasch, A.; Niedermeyer, T. H. J.; Lalk, M.; Witt, S.; Seefeldt, S.; Hammer, E.; Schauer, F.; Gesell, M.; Hessel, S.; Jülich, W.-D.; Lindequist, U. *Chem. Pharm. Bull. (Tokyo).* **2006**, *54* (5), 632–638.

(118) Mikolasch, A.; Hessel, S.; Salazar, M. G.; Neumann, H.; Manda, K.; Gõrdes, D.; Schmidt, E.; Thurow, K.; Hammer, E.; Lindequist, U.; Beller, M.; Schauer, F. *Chem. Pharm. Bull. (Tokyo).* **2008**, *56* (6), 781–786.

(119) Mikolasch, A.; Hildebrandt, O.; Schlüter, R.; Hammer, E.; Witt, S.; Lindequist, U. *Appl. Microbiol. Biotechnol.* **2016**, 1–15.

(120) Hahn, V.; Mikolasch, A.; Wende, K.; Bartrow, H.; Lindequist, U.; Schauer, F. *Biotechnol. Appl. Biochem.* **2009**, *54* (4), 187–195.

(121) Hahn, V.; Mikolasch, A.; Schauer, F. *Appl. Microbiol. Biotechnol.* **2014**, *98* (4), 1609–1620.

(122) Wellington, K. W.; Bokako, R.; Raseroka, N.; Steenkamp, P. *Green Chem.* **2012**, *14* (9), 2567–2576.

(123) Ciecholewski, S.; Hammer, E.; Manda, K.; Bose, G.; Nguyen, V. T. H.; Langer, P.; Schauer, F. *Tetrahedron* **2005**, *61* (19), 4615–4619.

(124) Constantin, M. A.; Conrad, J.; Beifuss, U. *Tetrahedron Lett.* **2012**, *53* (26), 3254–3258.

(125) Abdel-Mohsen, H. T.; Sudheendran, K.; Conrad, J.; Beifuss, U. *Green Chem.* **2013**, *15*, 1490.

(126) Cannatelli, M. D.; Ragauskas, A. J. *Chem. Eng. Res. Des.* **2015**, *97* (September), 128–134.

(127) Leutbecher, H.; Conrad, J.; Klaiber, I.; Beifuss, U. *Synlett* **2005**, No. 20, 3126–3130.

(128) Hajdok, S.; Conrad, J.; Leutbecher, H.; Strobel, S.; Schleid, T.; Beifuss, U. *J Org Chem* **2009**, *74* (19), 7230–7237.

(129) Hajdok, S.; Leutbecher, H.; Greiner, G.; Conrad, J.; Beifuss, U. *Tetrahedron Lett.* **2007**, *48* (29), 5073–5076.

(130) Leutbecher, H.; Hajdok, S.; Braunberger, C.; Neumann, M.; Mika, S.; Beifuss, U.; Conrad, J. *Green Chem.* **2009**, *11* (5), 676–679.

(131) Wellington, K. W.; Qwebani-Ogunleye, T.; Kolesnikova, N. I.; Brady, D.; De Koning, C. B. *Arch. Pharm. (Weinheim).* **2013**, *346* (4), 266–277.

(132) Abdel-Mohsen, H. T.; Conrad, J.; Beifuss, U. *J. Org. Chem.* **2013**, *78* (16), 7986–8003.

(133) Navarra, C.; Goodwin, C.; Burton, S.; Danieli, B.; Riva, S. *J. Mol. Catal. B Enzym.* **2010**, *65* (1–4), 52–57.

(134) Ponzoni, C.; Beneventi, E.; Cramarossa, M. R.; Raimondi, S.; Trevisi, G.; Pagnoni, U. M.; Riva, S.; Forti, L. *Adv. Synth. Catal.* **2007**, *349* (8–9), 1497–1506.

(135) Beneventi, E.; Conte, S.; Cramarossa, M. R.; Riva, S.; Forti, L. *Tetrahedron* **2015**, *71* (20), 3052–3058.

(136) Chirivì, C.; Fontana, G.; Monti, D.; Ottolina, G.; Riva, S.; Danieli, B. *Chem. - A Eur. J.* **2012**, *18* (33), 10355–10361.

(137) Davin, L. B. *Science (80-.).* **1997**, *275* (5298), 362–367.

(138) Pickel, B.; Constantin, M. A.; Pfannstiel, J.; Conrad, J.; Beifuss, U.; Schaller, A. *Angew. Chemie - Int. Ed.* **2010**, *49* (1), 202–204.

(139) Gavezzotti, P.; Navarra, C.; Caufin, S.; Danieli, B.; Magrone, P.; Monti, D.; Riva, S. **2011**, *4*, 2421–2430.

(140) Navarra, C.; Gavezzotti, P.; Monti, D.; Panzeri, W.; Riva, S. *"Journal Mol. Catal. B, Enzym.* **2012**, *84*, 115–120.

(141) Gavezzotti, P.; Bertacchi, F.; Fronza, G.; K??en, V.; Monti, D.; Riva, S. *Adv. Synth. Catal.* **2015**, *357* (8), 1831–1839.

(142) Forneris, F.; Ricklin, D.; Wu, J.; Tzekou, A.; Wallace, R. S.; Lambris, J. D.; Gros, P. *Science (80-.).* **2010**.

(143) Shah, V.; Wiest, R.; Garcia-Cardena, G.; Cadelina, G.; Groszmann, R. J.; Sessa, W. C. *Am. J. Physiol.* **1999**, *277* (2 Pt 1), G463-8.

(144) Luo, W.; Sun, W.; Taldone, T.; Rodina, A.; Chiosis, G. *Mol. Neurodegener.* **2010**, *5* (1), 24.

(145) Whitesell, L.; Lindquist, S. L. *Nat. Rev. cancer* **2005**, *5* (10), 761–772.

(146) Pennisi, R.; Ascenzi, P.; di Masi, A. *Biomolecules* **2015**, *5* (4), 2589–2618.

(147) Richter, K.; Haslbeck, M.; Buchner, J. *Molecular Cell.* Cell Press October 22, 2010, pp 253–266.

(148) Sattin, S.; Tao, J.; Vettoretti, G.; Moroni, E.; Pennati, M.; Lopergolo, A.; Morelli, L.; Bugatti, A.; Zuehlke, A.; Moses, M.; Prince, T.; Kijima, T.; Beebe, K.; Rusnati, M.; Neckers, L.; Zaffaroni, N.; Agard, D. A.; Bernardi, A.; Colombo, G. *Chem. - A Eur. J.* **2015**, *21* (39), 13598–13608.

(149) Sattin, S.; Panza, M.; Vasile, F.; Berni, F.; Goti, G.; Tao, J.; Moroni, E.; Agard, D.; Colombo, G.; Bernardi, A. *European J. Org. Chem.* **2016**, *2016* (20), 3349–3364.

(150) D'Annessa, I.; Sattin, S.; Tao, J.; Pennati, M.; Sànchez-Martìn, C.; Moroni, E.; Rasola, A.; Zaffaroni, N.; Agard, D. A.; Bernardi, A.; Colombo, G. *Chem. - A Eur. J.* **2017**, *23* (22).

(151) Martina, K.; Baricco, F.; Caporaso, M.; Berlier, G.; Cravotto, G. *ChemCatChem* **2016**, *8* (6), 1176–1184.

(152)   Coccia, F.; Tonucci, L.; D'Alessandro, N.; D'Ambrosio, P.; Bressan, M. *Inorganica Chim. Acta* **2013**, *399* (September 2015), 12–18.

(153)   Richmond, E.; Moran, J. *J. Org. Chem.* **2015**, *80* (13), 6922–6929.

(154)   Neumann, K. T.; Klimczyk, S.; Burhardt, M. N.; Bang-Andersen, B.; Skrydstrup, T.; Lindhardt, A. T. *ACS Catal.* **2016**, *6* (7), 4710–4714.

(155)   Sinha, A. K.; Kumar, V.; Sharma, A.; Sharma, A.; Kumar, R. *Tetrahedron* **2007**, *63* (45), 11070–11077.

(156)   De Filippis, B.; Agamennone, M.; Ammazzalorso, A.; Bruno, I.; D'Angelo, A.; Di Matteo, M.; Fantacuzzi, M.; Giampietro, L.; Giancristofaro, A.; MacCallini, C.; Amoroso, R. *Medchemcomm* **2015**, *6* (8), 1513–1517.

(157)   Nicotra, S.; Cramarossa, M. R.; Mucci, A.; Pagnoni, U. M.; Riva, S.; Forti, L. *Tetrahedron* **2004**, *60* (3), 595–600.

(158)   Orlandi, M.; Tosi, F.; Bonsignore, M.; Benaglia, M. *Org. Lett.* **2015**, *17* (16), 3941–3943.

(159)   Buchner, J.; Kiefhaber, T. *Protein Folding Handbook Part I*; WILEY-VCH Verlag GmbH & Co. KGaA: Weinheim, 2005.

(160)   Chou, C.-H.; Chu, L.-T.; Yu, P.-C.; Wu, B.-J.; Liao, Y.-C. *Heterocycles* **2007**, *71* (1), 165.

(161)   Chidichimo, G.; Salerno, G.; Veltri, L.; Gabriele, B.; Nicoletta, F. P. *Liq. Cryst.* **2004**, *31* (5), 733–737.

(162)   Diemer, V.; Chaumeil, H.; Defoin, A.; Carré, C. *Synthesis (Stuttg).* **2007**, *2007* (21), 3333–3338.

(163)   Lion, C. J.; Matthews, C. S.; Stevens, M. F. G.; Westwell, A. D. *J. Med. Chem.* **2005**, *48* (4), 1292–1295.

(164)   Schmidt, B.; Elizarov, N.; Berger, R.; Hölter, F. *Org. Biomol. Chem.* **2013**, *11* (22), 3674.

(165)   Lewis, F. D.; Sinks, L. E.; Weigel, W.; Sajimon, M. C.; Crompton, E. M. *J. Phys. Chem. A* **2005**, *109* (11), 2443–2451.

(166)   Jo, G.; Hyun, J.; Hwang, D.; Lee, Y. H.; Koh, D.; Lim, Y. *Magn. Reson. Chem.* **2011**, *49* (6), 374–377.